Università degli Studi di Napoli Federico II

Doctoral degree in

Model Organisms in Biomedical and Veterinary Research

Dissertation

Central regulation of food intake peptides during ageing in the teleost model *Nothobranchius furzeri.*

Advisor

Prof. Paolo de Girolamo

Author

Alessia Montesano

2013-2016

CONTENTS

Abstract

In course of ageing, significant modifications occur to energy homeostasis in elderly subjects, representing often risk factors for morbidity and mortality. The mechanisms deputed to energetic control have been selected by ancestral diets, resulting from nutrient disposal during evolution. To better understand the regulation behind changes of appetite drive, we focus our study on the age-related expression of peptides specifically involved in the food intake process in the Central Nervous System (CNS). In fact, the appetite is modulated by a network of molecules balancing metabolic needs and caloric income. Specifically, we analyse the mRNA and protein expression levels of neuropeptide Y (NPY) and orexin (HCRT/ORX), both appetite stimulators, and nesfatin-1 (NUCB2), a hunger inhibitor. To evaluate the changes during ageing, we use the teleost fish *Nothobranchius furzeri*, that is an established model for ageing research, besides being the vertebrate with shortest lifespan described in captivity. We study starvation-induced neuropeptide regulation in the MZM-0410 and GRZ strains, at different ageing time-points (MZM: 5-27; GRZ: 5-12 weeks old), after food deprivation for 96 hours. We apply a multidisciplinary approach: the presence of the peptides in *N. furzeri* is confirmed by Western blot, gene expression is quantified by qPCR and the cells expressing mRNAs and neuropeptides are identified on brain sections. Further, the neuronal activation pattern after starvation is described by immunohistochemistry for phospho-S6 ribosomal protein. We show that during ageing NPY and NUCB2 are upregulated, whereas HCRT is downregulated; some differences exist between the two strains. Starvation determinates upregulation of NPY and HCRT, but just in young age. Fasting doesn't cause variation of NUCB2 expression. Whereas, neurons expressing all three molecules are localised in neuroendocrine areas, where neuronal activation occurs. In conclusion, we present the first characterisation of NPY, HCRT and NUCB2 in *N. furzeri*, underlining their role as central modulator of food intake, as described in other vertebrates, but also highlighting some peculiarity of the two strains. Moreover, at present, this is the first analysis of food intake neuropeptides regulation upon ageing in a fish model.

Abbreviations

A	anterior thalamic nucleus
aa	amino acid
AgRP	Agouti-related peptide
AMPK	5' adenosine monophosphate-activated protein kinase
ARC	hypothalamic arcuate nucleus
BBB	brain-blood barrier
Cans	commissure ansulata
CART	cocaine- and amphetamine-regulated transcript
CN	cortical nucleus
CNS	central nervous system
CP	central posterior thalamic nucleus
Cpost	posterior commessura
D	dorsal telencephalon
DAO	dorsal accessory optic nucleus
DIL	inferior diffuse lobe of hypothalamus
DIO	diet-induced-obese
dot	dorsal optic tract
DRS	differential stress resistance
ECL	external cell layer
FR	retroflex fascicle
GL	glomerular layer of olphactory bulbs
GRZ	short-lived *N. furzeri* strain from Gona Re Zhou, Zimbabwe
Ha	habenular nucleus
Hc	caudal hypothalamus
HC	commissural horizontal
HCRT	hypocretin/orexin
Hd	dorsal hypothalamus
Hv	ventral hypothalamus
I	intermediate thalamic nucleus
ICL	internal cell layer
ICV	intra-cerebroventricular
IF	immunofluorescence
IHC	immunohistochemistry

IP	intraperitoneal
ISH	*In situ* hybridisation
lfb	lateral forebrain bundle
LHA	hypothalamic area
llf	lateral longitudinal fascicle
LV	lateral nucleus of cerebellar valvula
mca	anterior mesencephalo-cerebellar tract
mfb	medial forebrain bundle
mlf	medial longitudinal fascicle
mTOR	mechanistic target of rapamycin
MZM	long-lived *N. furzeri* strain from Mozambique
NG	glomerular nucleus
NG	glomerular nucleus
NIlf	nucleus of longitudinal fascicle
nIII	nerve III
NPY	neuropeptide Y
NPY	neuropeptide Y
NRP	posterior recess nucleus
nt	nucelotides
NTS	nucleus tractus solitarius
NUCB2	nucleobindin-2
OB	olfactory bulbs
ON	(in atlas) optic nerve
ON	overnight
ORX	orexin/hypocretin
OT	optic tectum
PAGE	polyacrylamide gel electrophoresis
PG	preglomerular nucleus
PGZ	periglomerular grey zone
PKA	Ras-protein kinase A
PM	magnocellular preoptic nucleus
POMC	peptides proopiomelanocortin
PP	(in atlas) preoptic nucleus
PP	pancreatic polypeptide

PT	posterior thalamic nucleus
PVN	paraventricular nucleus
PVO	paraventricular organ
PY	peptide Y
PYY	peptide YY
rec	hypothalamic recess
RT	room temperature
S6RP	S6 ribosomal protein
SC	suprachiasmatic nucleus
SDS	sodium dodecyl sulfate
sgt	secondary gustatory tract
SPN	superficial pretectal nucleus
TBP	TATA box binding protein
TI	longitudinal tori
TN	tuberal nucleus
TPp	periventricular nucleus of posterior tuberculum
TS	semicircular tori
V	ventral telencephalon
Va	valvula of cerebellum
VAO	ventral accessory optic nucleus
VL	ventrolateral thalamic nucleus
VM	ventromedial thalamic nucleus
VMN	ventromedial hypothalamic nucleus
WB	Western blot

INDEX OF FIGURES

INDEX OF TABLES

1. INTRODUCTION

1.1. Central regulation of food intake

The “glucostatic theory” of regulation of food intake was based on the activity of two functional hypothalamic “feeding” centres: the first, “hunger centre”, located in the lateral hypothalamic area (LHA), that perceives the inter-meal decrease of hematic glucose, stimulating food consumption; the second, “satiety centre”, in the ventromedial hypothalamic nucleus (VMN), that is directly activated by post-prandial hyperglycemia and has a hunger inhibiting role (Mayer and Thoma, 1967). In recent decades, further investigations have advanced knowledge about the topic surpassing this simplistic theory to reveal a complex regulatory mechanism only partly explained by endocrine signalling. Numerous neuropeptides and their respective receptors, are involved in the control of food intake, showing first that, beside VMN and LHA, other hypothalamic nuclei are involved in the control of appetite and that the activities of neural circuits controlling energy homeostasis rely on the delicate balance of factors, which finish or stimulate food consumption. At present, more than 50 factors are known to play a key role in the Central Nervous System (CNS), either with an inhibitory (anorexigenic) or stimulating (orexigenic) action (Tab. 1). For example, during the last 20 years the importance of the hypothalamic arcuate nucleus (ARC), was demonstrated to embody two populations of neurons: the first expressing the powerfully orexigenic peptides, neuropeptide Y (NPY) and Agouti- related peptide (AgRP); the second expressing the anorexigenic peptides proopiomelanocortin (POMC) and cocaine- and amphetamine-regulated transcript (CART). Both coexisting populations are directly stimulated by peripheral hormones, as well as circulating metabolites and amino acids (Levitsky, 2005). These convey information to the CNS either indirectly, via the vagus nerve, or by crossing the brain- blood barrier (BBB) and directly reaching brain areas (Brightman and Broadwell, 1976). In particular, signals from adipose body status, carried by leptin (secreted by adipocytes) and insulin (secreted by the endocrine pancreas in proportion to adiposity), interact with the central autonomic circuits. This stimulate the catabolic pathways (POMC/CART neurons) and inhibiting the anabolic pathways (NPY/AgRP neurons) in the ARC. These neurons, present in the ARC, and acting under direct control of peripheral stimuli, are called first-order neurons. The subsequent pathways project to other key neuronal populations into paraventricular

nucleus (PVN) and LHA: these second-order neurons are responsible for the transmission of the autonomic output to other brain sites and the spinal cord by neuropeptide-expression, including orexin/ hypocretin (ORX/HCRT), melanin concentrating hormone, neurotensin, and histamine. They make connections with central autonomic pathways that project to hindbrain autonomic centres that process satiety signals (Fig. 1). Communication occurs due to these downstream neurons that project to third- and higher-order neurons located in many areas of the brain. The second step of neuronal messaging is as important as the activity of the first order neurons, because PVN and LHA show incredible functional plasticity. In addition to metabolic information, the LHA also receives information from brain areas associated with reward, motivation, learning and memory, and from brainstem areas associated with vagal and visceral sensory input, sensorimotor coordination, and arousal. In turn, second-order LHA neurons project widely through the entire brain from the cortex to the spinal cord (Berthoud, 2002). Moreover, because many neurons of the PVN, PFA and LHA project to the ARC, neuronal traffic flows bidirectionally, meaning that the second-order neurons are not passive recipient of information from the ARC, but also actively modify the message. The hypothalamus is probably not directly involved in the process of satiety signalling. Information about meals is mostly conveyed to the hindbrain by vagal fibres of the gastrointestinal tract. The message arrives to the nucleus tractus solitarius (NTS) in the caudal brainstem. That integrates sensory information from stomach, duodenum and abdominal organs, as well as taste information from the oral cavity (Travers and Norgren, 1987). Such transmission occurs due to mechanical and chemical stimulation (Fig. 1).

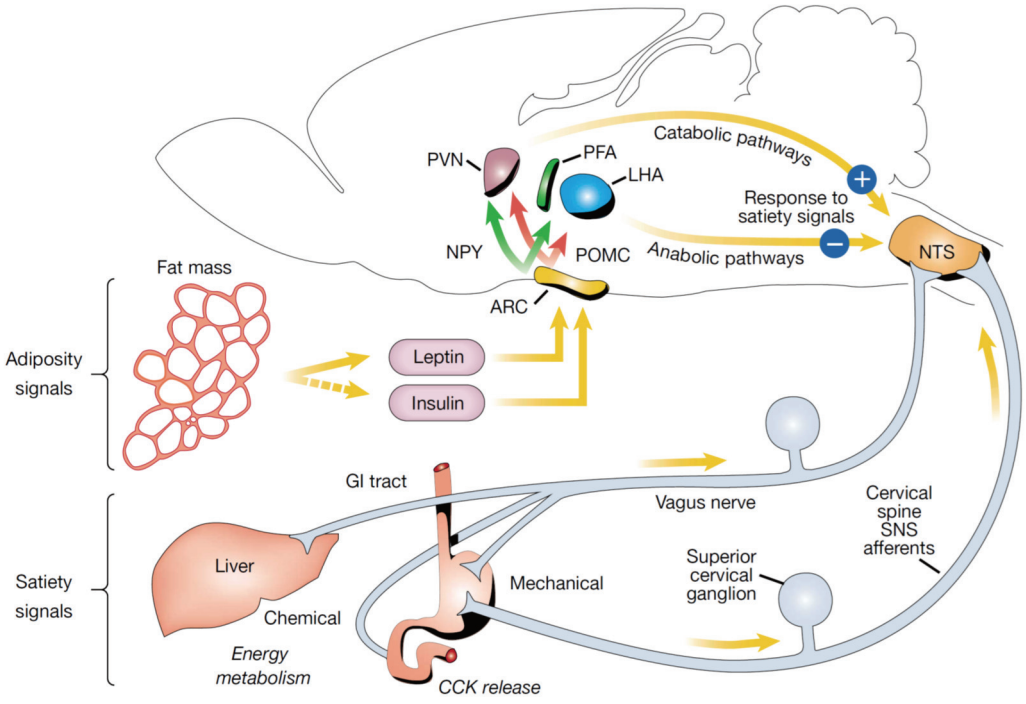

Figure 1. Neuroanatomical representation of different pathways in the CNS and peripheral stimuli. Not shown are ascending projections from hindbrain to forebrain that may also contribute to adaptive changes in food intake. Abbreviations: PVN (paraventricular nucleus); PFA (perifornical area); LHA (lateral hypothalamic area); NTS (nucleus tractus solitaris); NPY (neuropeptide Y); POMC (pro-opiomelanocortin); ARC (arcuate nucleus); CCK (cholecystokinin). Picture from Schwartz *et al.*, 2000.

Table 1. Neuropeptides and hormones involved in food intake regulation in CNS. Modified from Kmiec, 2011.

Central orexigenic factors	Central anorexigenic factors
Neuropeptide Y (NPY)	α-Melanocyte-stimulating hormone (α-MSH)
Agouti-related peptide (AgRP)	Cocaine- and amphetamine-regulated transcript (CART)
Orexin A/B (ORX-A/B)	Corticotropin-releasing hormone (CRH)
Melanin-concentrating hormone (MCH)	Thyrotropin-releasing hormone (TRH)
Galanin (GAL)	Neurotensin (NTS)
Growth hormone- releasing hormone (GHRH)	Galanin- like peptide (GALP)
ß- Endorphin (ß-END)	Oxitocin (Oxt)
Dynorphins (Dyn)	Glucagon- like peptide 1 (GLP-1)
γ-Aminobutyric acid (GABA)	Serotonin (5HT)
Noradrenaline (NA)	Prolactin (PRL)
	Neuromedin (NmU)
	Nesfatin-1 (NUCB2)

1.2. Variation of appetite during ageing

Ageing often results in a decline in energy consumption (de Boer *et al*., 2013). Consequently, depending on energy expenditure and balance, elderly people may lose weight. Ageing-associated changes in regulation of appetite and the lack of hunger have been called anorexia of ageing. While overweight and obesity remain serious and growing problems in adult population; the main concern in those of very advanced age is food intake reduction. This occurs in healthy adults even in conditions of adequate food availability. The phenomenon was first described in 1988 (Morley and Silver, 1988) and seems to be due to a decreased drive to eat (hunger feeling), resulting from a lower energy and faster or prolonged anorexic signalling (alias, satiety). Imbalances between nutrient intake and energy expenditure change may lead to transition from “physiological” to “pathological” conditions, exhibiting weight loss, impaired muscle function (sarcopenia), decreased bone mass, immune dysfunction, and exponential increase of secondary diseases incidence. Such symptoms characterise frailty syndrome (Martone *et al*., 2013; for review, see Landi *et al*., 2015), morbidity and mortality (MacIntosh *et al*., 2000). The regulation of appetite, particularly when deficient, is the key to understanding the pathologic trigger of anorexia of ageing. Food intake is controlled through highly complex processes, with fail-safe mechanisms in place to guarantee that the feeding drive remains unimpaired. Complex mechanisms are involved in age-related deterioration of activities in the brain regions, especially in the hypothalamus, in response to supplementary feedback from peripheral systems, specific nutrients and circulating hormones. The complexity of the mechanism is based on the dynamic homeostasis of the energy balance, which, as previously mentioned, becomes displaced during ageing. It is clear that diet and genetics play important roles in the regulation of metabolism, health span, and lifespan (Yec and Curran, 2016). However, there is a limited knowledge about these interactions. For example, dietary restriction is one of the most effective and well-studied environmental manipulations that influence the rate of ageing and health span. The genetics underlying the effects of dietary restriction are multifaceted (Lakowski and Hekimi, 1998). Nevertheless, it is described in many models, including yeast, worms, flies and rodents, that caloric restriction attenuates the incidence and progression of many age-dependent pathologies.

1.3. Model design, evolutionary conserved mechanisms and neuropeptides

The majority of the studies about the regulation of food intake, use rodents as models for investigation. Nevertheless, in rodents, in spite to the human evolutionary proximity, there are evident differences between individuals and stains, which seem to have a significant influence on the control of energy homeostasis during ageing. Two rat strains are most frequently used to identify body mass changes upon ageing: the first includes specimens that usually gain weight modestly, such as Wistar or Brown-Norway; the second includes animals that increase in body mass (e.g. Sprague-Dawley or Fisher 344). Some mutants, such as Zucker rat, *db/db* (leptin receptor activity is deficient) or *ob/ob* (leptin is missing) mice could not be considered as good model, since they show high variance in ageing phenotype (for review, see Kmiec, 2011). As confirmation of close correlation between energy metabolism and ageing, the effect of that dietary restriction or certain drugs, like metformin or rotenone (Baumgart *et al.*, 2016), which mimic caloric restriction is also know extending the lifespan. This is also shown in many different organisms: yeast, invertebrate (worms), non-mammalian (fly and fish) and mammalian (rodents and non-human primates) vertebrates. In all vertebrates, energy homeostasis is regulated through complicated inter-related pathways, that inhibit or stimulate food consumption. Numerous studies confirm that the structure and function of appetite-regulating hormones in fish are well conserved and show similarities with higher vertebrates (for review see Shahjahan *et al.*, 2014). Moreover, many specific pathways that are modulated during ageing, such as the 5' adenosine monophosphate-activated protein kinase (AMPK) and consequently the mechanistic target of rapamycin (mTOR), are also in common with the energy metabolism maintenance and most of them are evolutionary conserved in fish models (Seiliez *et al*., 2005; Fuentes *et al*., 2013; Librán-Pérez *et al*., 2015; Volkoff, 2014a). Furthermore, in spite of the differences related to the fact that the endocrine functions could specifically differ between ectothermic fish and homoeothermic mammals (Gorrisen *et al*., 2006; Volkoff *et al*., 2005; Volkoff *et al*., 2009), it was possible to identify and characterise many common neuropeptides. The structure of the appetite regulators is somewhat conserved among vertebrates, with regards to gene structures, amino acids composition or 3D protein configuration. Some peptides are better conserved than others, but in many cases the tertiary structure

stays unchanged (Copeland *et al*., 2011). Also, actinoptegyan fish, which include most of the teleost in use as biomedical study models have undergone, in addition to the double tetraploidisation (whole genome duplication, 2R theory), an extra round of duplication, called 3D event (Meyer and Van de Peer, 2005). This leads to multiple isoforms/variants of the regulators. As experimental models, fish are valuable because it is possible to perform surgical procedures (e.g. intraperitoneal and intra-cerebroventricular injections, IP, ICV) and repeated sampling with easy environmental manipulation in short time. In this sense, fish models can improve understanding of fundamental changes of food intake regulation and adaptation to different conditions, such as response to an energetic failure (fasting or caloric restriction), or during ageing. As mentioned previously, certain neuropeptides are highly conserved regarding their structure and/or function in both mammals and fish. Some, like NPY and HCRT/ORX, are well studied in the different species; others, such as nesfatin-1 (NUCB2) were found more recently. NPY is part of the homonymous neuropeptide Y family, composed of 36-amino acid exhibiting carboxy terminal (C-terminal) amidation. This also includes peptide YY (PYY), common in all the vertebrates, pancreatic polypeptide (PP), found only in the pancreas of tetrapods and peptide Y (PY) found only in some teleost. NPY and PYY were found in many fish species, but few produce PY (Cerdá-Reverter *et al*., 2000). NPY was originally isolated and characterised in porcine brain (Takemoto, 1982) and since then it has been considered the most potent orexigenic peptide. It acts mainly in the first-order neurons of the hypothalamus. The gene and the peptide structures are highly conserved among vertebrates (Fig. 2, 3.); in fact, it is identified also in fish, (Halford *et al*., 2004) and it is distributed in many regions of CNS of *C. auratus* (Pontet *et al*., 1989), *O. mykiss* (Danger *et al*., 1991), and *C. gariepinus* (Zandbergen *et al*., 1994). Dietary restriction and ICV injections of NPY (Narnaware *et al*., 2000; Kojima *et al*., 2010) in different fish species, such as goldfish, influence its regulation. These data indicate that the brain NPY-ergic system is dynamically involved in the regulation of daily food intake with a strong appetite stimulating action. Numerous studies show that NPY is involved in the regulation of feeding in fish and both central and peripheral injections of NPY increase food intake in goldfish (López-Patiño *et al*., 1999), channel catfish (*I. punctatus*) (Silverstein and Plisetskaya, 2000) and tilapia (*O. mossambicus*) (Kiris *et al*., 2007). Fasting induces an increase of NPY expression in the hypothalamus of goldfish (Narnaware and Peter, 2001) and snout bream (*M. amblycephala*) (Ji *et al.,* 2015) and refeeding can reverse these effects.

Nevertheless, there was no significant difference in NPY expression after fasting in Atlantic cod (*G. morhua*) and Atlantic salmon (*S. salar*) (Kehoe and Volkoff, 2007; Murashita *et al*., 2009). In winter skate, NPY mRNA expression increased in the telencephalon, but not the hypothalamus after 2 weeks of fasting (MacDonald and Volkoff, 2009). As reported for mammals, NPY also in fish interacts with a number of central appetite regulators, including either orexigenic, such as orexins (Mercer *et al*., 2011; Volkoff, 2006), or anorexigenic, like nesfatin-1 (Sedbazar *et al*., 2014). NPY mRNA and peptide is not just expressed in the brain. In Brazilian flounder (*P. orbignyanus*)*,* for example, it is also described in liver, spleen, gill, intestine, heart and kidney (Campos *et al*., 2010). Among its orexigenic function, NPY also affects the blood pressure and circadian rhythmicity (Zimanyi *et al.*, 1998). In fish, as well as in mammals, NPY co-modulation in gonadotropin (Chabot *et al.*, 1988), growth hormone, adrenocorticotropic and thyrotropin secretions (Mc Donald *et al.*,1985) are shown. NPY gene regulation during ageing has been evaluated in mammals, studying also the correlation between fed and fasted animals and evidencing a downregulation in old rats fed *ad libitum* and an increase in subjects after food deprivation (Hakansson *et al*., 1996; Blanton *et al*., 2001; Sohn *et al*., 2002). This modulation is lost in diet-induced-obese model (DIO) (Beck, 2006). In different organisms (from yeast to rodents), NPY interferes in seven of the nine cellular hallmarks of ageing: loss of proteostasis (Minor *et al*. 2009; Aveleira *et al*., 2015) deregulated nutrient sensing (Hong *et al*., 2012), mitochondrial dysfunction (Kaipio and Pesonen, 2009; Kir *et al*., 2013), cellular senescence (De la Fuente *et al*., 2000; Bedoui *et al*., 2008), stem cell exhaustion (Son *et al*., 2011; Park *et al*., 2015), altered intercellular communication (Roa and Herbison, 2012) and reduced inflammation (Li *et al*., 2015). There are no reports relating NPY to the other hallmarks of ageing, that are genomic instability, epigenetic alterations, and telomere attrition (for a review, see Botelho and Cavadas, 2015). Orexin, alias hypocretin (ORX/HCRT) is a neuropeptide described in many vertebrates (Sakurai *et al*., 1998; Deyer *et al*., 1999; Hungs *et al*., 2001) and is active in second-order neuronal population of the hypothalamus. It was initially characterised as orphan-receptor ligands involved in food regulation (Sakurai *et al*., 1998). Orexin exists in two molecular forms derived from the same precursor: the first is a peptide know as orexin A (ORX-A), which has variable number of residue between the species, e.g. *M. musculus* 33 aa*, N. furzeri* 43 aa, *C. auratus* 49 aa (Fig. 3); the second a 28-residue peptide, named orexin B (ORX-B) (Fig. 3). The gene responsible for the

precursor (prepro-orexin) coding is characterised in several fish species such as *D. rerio, T. rubripes, G. morhua, C. auratus, O. latipes, P. americanus and L. acellata* (Alvarez and Sutcliffe, 2002; Kaslin *et al*., 2004; Nakamaki *et al*., 2006; Faraco *et al*., 2006; Xu and Volkoff, 2007; Burkley *et al*., 2010; MacDonald and Volkoff, 2010). The gene and the primary structure of the precursor are well conserved in the vertebrate (Fig. 2, 3). Instead, as indicated before, the structure of the released peptides, especially the orexin A, is conserved less than other neuropeptides (Wong *et al.*, 2011. Liu *et al*., 2015). During fasting, prepro-orexin mRNA expression is upregulated. This means that orexin is involved in the response reaction of the regulative maintenance mechanism to energy failure. This modulation is further supported by the observed dose-dependent increase in food intake after ICV injection directly of the peptides ORX-A or ORX-B (Sakurai *et al.* 1998; Volkoff *et al.*,1999; Nakamaki *et al.*, 2005; Levitas-Djerbi *et al*., 2015). Of the two orexins, ORX-A's effects on the food regulation are more potent, both in mammal and fish (Haynes et.al 2000; Rodger *et al.*, 2001; Novak *et al*., 2005). Moreover, the hypocretin system regulates neural activity responsible for daily functions, such as sleep/wake homeostasis and long-term behavioural changes (Hungs *et al.*, 2001, Nisembaum *et al*., 2014; Gao and Hermes, 2015). Animal models of DIO consistently display attenuated levels of orexin signalling molecules in both the CNS and peripheral tissues (Kotz *et al*., 2005; Zhang *et al*., 2005a-b; Sellayah and Sikder, 2014). The downregulation of orexin during ageing is described in mammals, including human (for review, see Wysokínsk *et al*., 2015). In elderly people, under a variety of conditions in which symptom onset and severity are strongly tied to ageing, not always the loss of neurons corresponds to a decrease of total body orexin level (Drouot *et al.*, 2003; Baumann *et al*., 2005; Fronczek *et al*., 2012). Rodents exhibit clear age-related reductions in the orexin system in the hypothalamus and other brain regions (Brownell and Conti, 2010; Sawai *et al*., 2010; Kessler *et al*., 2011). At present, no data about ORX regulation in ageing are described in fish models. Nesfatin-1 (nucleobindin-2 Encoded Satiety and Fat influencingprotein-1) is an 82 amino acid anorexigenic peptide (81 in fish, Fig. 3) encoded in the N-terminal of its translated precursor, nucleobindin-2 (NUCB2) (Oh-I *et al.*, 2006; Mohan and Unniappan, 2013). Translation of NUCB2 results in protein consisting in 396 amino acids highly conserved between mammalian and no-mammalian species (Oh-I *et al*., 2006). Post-translation it is cleaved by prohormone convertases results in the N-terminal fragment, nesfatin-1 (residues 1-82) and two

C-terminal peptides, nesfatin-2 (residues 85-163) and nesfatin-3 (residues 166-396) (Oh-I *et al*., 2006; Gonzalez *et al*., 2010, 2012b). The mid-segment of nesfatin-1 is considered to be its bioactive core, known to reduce food intake and fat mass (Oh-I *et al*., 2006) in rodents and goldfish (Kerbel and Unniappan, 2012). Interestingly, while several biological effects have been described for nesfatin-1 (Stengel *et al*., 2013), so far no function has been ascribed to nesfatin-2 and nesfatin-3 (for review see Stengel, 2015). In fish, two isoforms of NUCB2 (NUCB2A and NUCB2B) exist. Nesfatin-1 has been identified in goldfish, *C. auratus*, (Gonzalez *et al*., 2010), Ya fish, *S. prenanti*, (Lin *et a*l., 2014) rainbow trout, *O. mykiss*, (Caldwell *et al*., 2014), zebrafish, *D. rerio*. (Hatef et al., 2015). Fish NUCB2A and NUCB2B sequences were compared with mammalian NUCB2 sequence: tissue distribution of both mRNAs was also observed in pituitary, liver, hepatopancreas, intestine and gonads. Their local expression also changed upon food deprivation (Gonzalez *et al*., 2010; Hatef *et al*., 2015). In mammals, nesfatin-1 inhibits huger and body weight gaining in mice and rats, while injection of an antibody neutralising nesfatin-1 stimulates appetite (Oh-I *et al*., 2006; Goebel-Stengel *et al*., 2011; Stengel *et al*., 2009; Atsuchi *et al*., 2010; Gonzalez *et al*., 2011). These results provide supporting evidence of the metabolic role of NUCB2 in both mammals and fish. Extensive distribution of NUCB2A and NUCB2B in fish organs demonstrates the presence of nesfatin-1 in peripheral tissues, and suggests that nesfatin-1 has pleiotropic action in both mammals and fish. It is important to specify that previous studies did not distinguish between full length of NUCB2 and processed nesfatin-1, considering that also the full length of NUCB2 exerts a biological effect on food intake (Stengel, 2015). Nesfatin-1 is also a multi-functional peptide (Mohan and Unniappan, 2012; Gonzales *et al.,* 2012a) involved in reproductive (Gonzales *et al.* 2012b), cardiac (Feijoo-Bandin *et al*., 2013) and endocrine functions (Mortazavi *et al*., 2015). At the present, there are no findings about the regulation or distribution changes during ageing, in either mammals or other vertebrates.

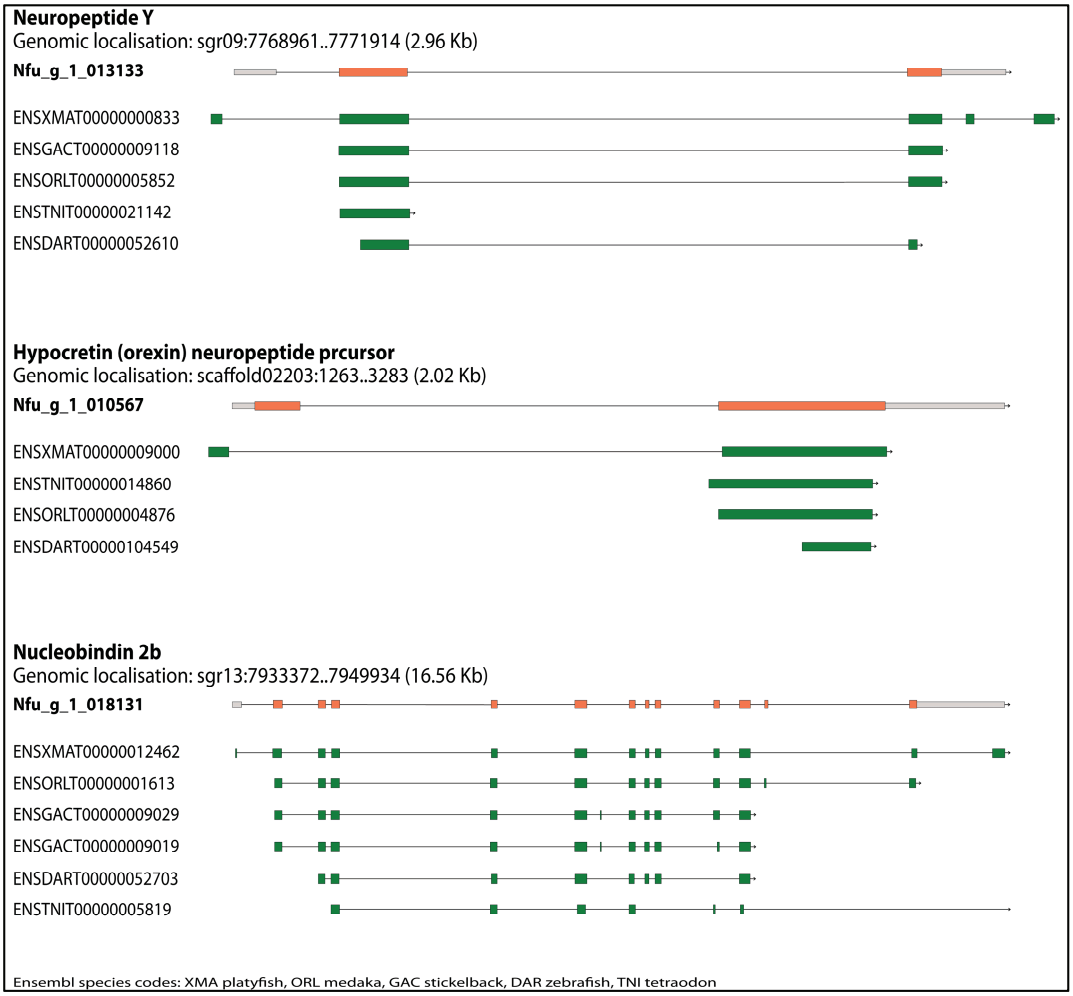

Figure 2. NPY, HCRT and NUCB2 intron/exon gene structure of *N. furzeri* and alignment of transcripts from other fish species (downloaded and modified from http://nfingb.leibniz-fli.de/, transcript information for the other fish species can be found at http://www.ensembl.org/). The structure of the two paralogues NUCB2A e NUCB2B were higher similar. In the image NUCB2B is shown as template.

a.

b.

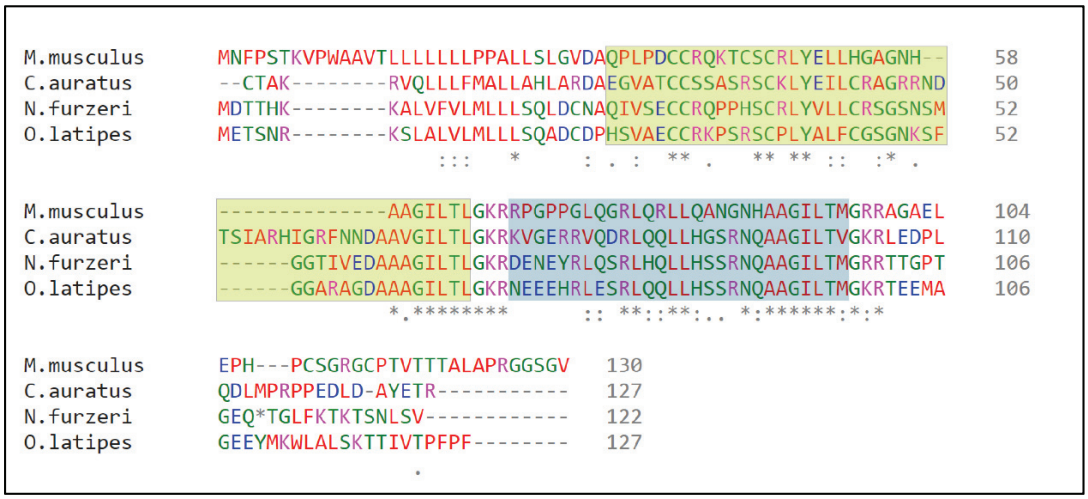

Figure 3. (continued)

c.

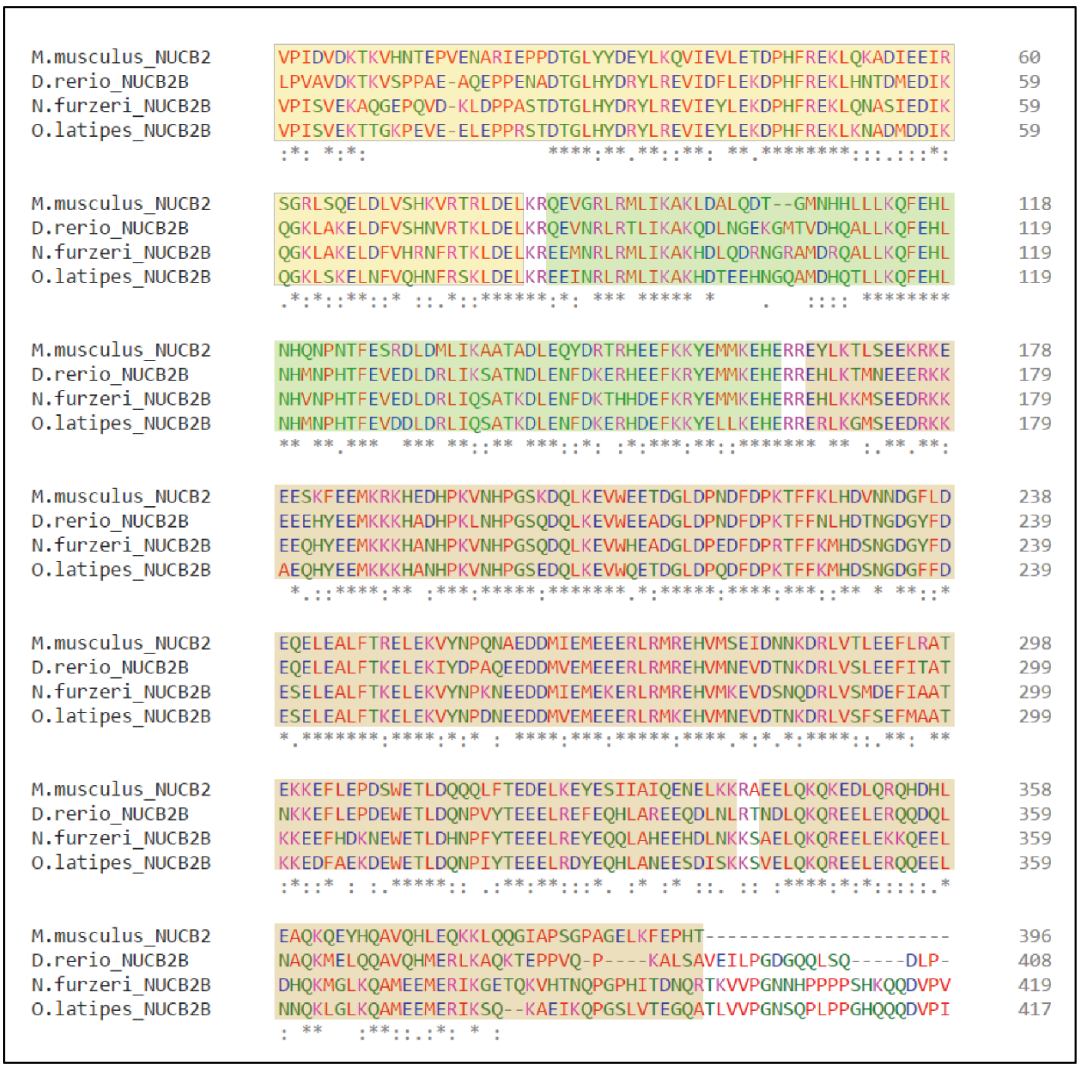

Figure 3. Peptide sequence alignments in different species: **a)** neuropeptide Y; **b)** hypocretin; **c)** nucleobindin-2. *Nothobranchus furzeri*; *Oryzias latipes* (medaka); *Carassius auratus* (goldfish) and *Mus musculus*. Asterisks mark conserved amino acids. (alignment was done with Clustal Omega http://www.ebi.ac.uk/Tools/msa/clustalo/).

1.4. The teleost model *Nothobranchius furzeri*

Fish constitute the largest group of vertebrates (Paxton *et al*. 1998) and as early as 1978 (Woodhead, 1978), the use of fish in research showed great potential as experimental models by fulfilling the requirements of research methodologies, established in The Three Rs (3Rs) by M. S. Russell and R. L. Burch in 1959. For example, zebrafish (*Danio rerio*) is an excellent experimental model in many fields of research, and it is currently one of the best characterised animals at the genetic level (Gerhard *at al*., 2003). In spite of this, the employment of *D. rerio* in ageing research has been refuted (Yu *et al*., 2006) mainly because of the long lifespan in laboratory conditions (~5 years, Gerhard *et al*., 2002). Nevertheless, other fish provide a good balance between phylogenetic distance and lifespan. For example, annual killifish of the genus *Nothobranchius*, a small piscine group of teleost (body size ≤ 7 cm) from the cyprinodont clade (order Cyprinodontiformes). Particularly, *Nothobranchius furzeri* is the shortest-lived vertebrate that can be bred in captivity (Valdesalici and Cellerino, 2003) and is the most recently established non-mammalian model for ageing research (for review see Lucas- Sánchez *et al*., 2014a). Life expectancy is variable, not just between the different *Nothobranchius* species, but also between strains. Recent studies describe median lifespan in captivity of 40 weeks and a maximum lifespan of ~60 weeks (Baumgart *et al*., 2016). Strains from more humid regions in Mozambique (e.g., MZM-0410) have a longer maximum lifespan of ~1 year (Terzibasi *et al*., 2008, 2013), whereas other strains coming from a semiarid habitat of Zimbawe as GRZ, have a maximum lifespan of 4–6 months. In particular, this latter strain is highly inbred (Reichwald *et al*., 2009 and 2015). Differences in rearing and maintenance, as such as dietary regime (Terzibasi *et al*. 2009) and temperature (Valenzano *et al*., 2006; Lu and Hsu, 2015), which could be easily manipulated in laboratory, are conditioning factors of life expectancy. In the wild, *N. furzeri* occupies marginal inhospitable habitats, such as puddles in savannahs that desiccate during dry seasons and refill with water during rainy seasons (Bartákova *et al*., 2013). In particular, *N. furzeri* habitat is geographically narrowed to small natural pools in Mozambique and at the Zimbawe border, between the Save river, in the north, and the Lembobo ridge, in the south (Reichard *et al*., 2009, 2014). The water environment is turbid, due to fauna's excreta and marsh flora, and the substrate is typically composed of soft mud. The diet is mostly based on small crustaceans (Cladocera, Copepoda, Ostracoda and Conchostraca),

preferably their *nauplii*, and mosquito larvae or hemipteran nymphs (for review see Cellerino *et al.*, 2015). This environmental peculiarity represents an advantage for fish maintenance in captivity, because it allows escape from high water parameters profiling in terms of contamination and water characteristics. Adult subjects are sexual dimorphic and dichromatic (Valdesalici and Cellerino, 2003). Males show multi-colour livery and be identified, according to the caudal fin pigmentation, in yellow and red morphs. Females have an iridescent body colour with transparent fins (Fig. 4a). The life cycle is extraordinary adapted to the seasonal availability of water. The average duration of water pools is only 75 days in a season (Terzibasi Tozzini *et al.*, 2013). The animals evolved to develop quickly enough to reproduce and depose a large amount of eggs in a short time, to preserve the species survival. Sexual maturity is reached 3-4 weeks (Valdesalici and Cellerino, 2009), once adulthood is reached, eggs release is constant (Lucas-Sánchez *et al*., 2011). To survive the dry season, embryos show extreme plasticity in development by building desiccation-resistant chorion and interrupting the morphogenesis and metabolism at three distinct developmental stages (diapause I, II, and III). Each stage has a variable time interval, from 2 days to 3 years (Fig. 4b). This peculiar phenomenon has many unexplored regulatory mechanisms which are topic of investigation for many embryologists and developmental biologists. Moreover, in *N. furzeri*, the rapid age-dependent decline of cellular functions (Wendler *et al*., 2015) follows the same molecular rules as higher vertebrates (Genade *et al.,* 2005, Lucas-Sánchez *et al*., 2014b). N. furzeri has an explosive growth (Blazek *et al*., 2013) and rapid expression of ageing phenotypes at the behavioural, histological and molecular level (Valezano *et al*., 2006; Di Cicco *et a*l., 2011; Hartmann *et al*., 2011) including age-dependent gliosis and rapid decay of adult neurogenesis (Terzibasi *et al*., 2012). Also several metabolic and degenerative disorders are described (Lucas- Sánchez *et al*. 2015) as well as immune system deterioration (Cooper *et al*., 1983), heart dysfunction and tumour development (Di Cicco *et al.,* 2011). Moreover, the complete genome has recently been assembled (Reichwald *et al*., 2015, Valenzano *et al.*, 2015) and protocols for transgenesis (Hartmann and Englert, 2012; Valenzano *et al*., 2011) and CRISPR/Cas9-mediated mutagenesis have been established (Harel *et al.*, 2015). This knowledge further increases the versatility of a model which could be used to address several scientific questions.

a.

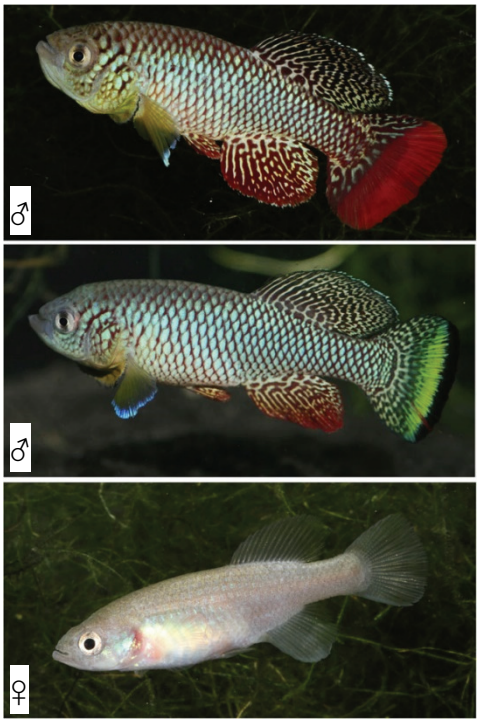

b.

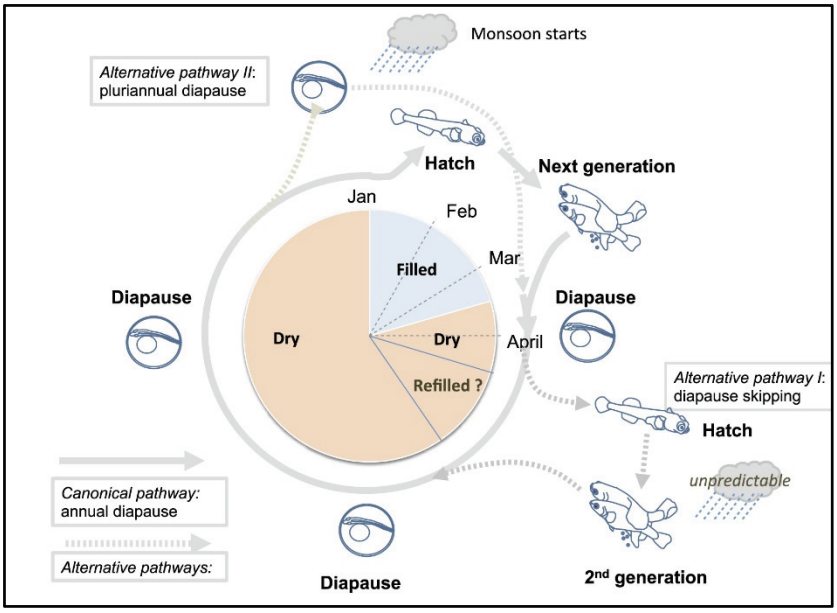

Figure 4. *Nothobranchius furzeri* phenotypes and life cycle: **a)** two different phenotypes of male (♂): red and yellow fin; on the bottom a female (♀); **b)** graphic representation of the life cycle and different possible pathways. Pictures granted and modified from Cellerino *et al.*, 2015.

1.5. Teleost brain and cytoarchitecture of the main neuroendocrine territories

The teleost brain is composed of three macroscopic regions: forebrain (prosoencephalon), midbrain (mesencephalon), and hindbrain (rhombencephalon). The forebrain is subdivided into telencephalon and diencephalon. The midbrain is subdivided into a dorsal part, consisting of lobes of optic tectum, and the tegmentum in the ventral part. The hindbrain encompasses cerebellum and pons cranially, respectively dorsal and ventral positioned, and medulla oblongata, caudally. The following describes briefly described the different part of the brain, focusing in particular on the areas which play a principal role in neuroendocrine activity.

Forebrain

Telencephalon

In teleost fish, during initial steps of embryonic life, the telencephalic vesicle develops through an evagination process, and the roof of the neuronal tube extend laterally so that the paired dorsal part rolls out lateroventrally. This developmental variance mainly differentiates the piscine and mammalian structures. The telencephalon includes the olfactory bulbs and hemispheres, distinguished in dorsal (pallium) and ventral (subpallium) areas. The olfactory bulbs are sessile, interconnected via the medial olfactory tract and organised in layers. Neuronal circuitry patterns and distribution of chemical transmitters and peptides suggest that the telencephalon, in *sensu strictu*, is functionally distinguished in a dorsal part, an important source of olfactory bulbs, and afferents consisting mainly of fibres, and a ventral area, containing neurons which project to the pituitary gland, and so involved in neuroendocrine cerebral system.

Diencephalon

The diencephalon is located between the telencephalon and mesencephalon. The rostral boundary is the preoptic area and the caudal boundary is the pretectal region. The diencephalon is subdivided into epithalamus, thalamus, and hypothalamus. The preoptic region, regarded as the most rostral diencephalic subdivision, surrounds the preoptic periventricular recess and is located between anterior commissure and the optic chiasm. It forms a functional continuum with the most caudal tuberal hypothalamus. In fact, these two structures form a single

complex and from endocrinological point of view the preoptic area is considered as pertinence of hypothalamus. In this area there are two important nuclei: the preoptic nucleus and the suprachiasmatic nucleus. The first is located dorsally in the periventricular zone and split into a magnocellular, with large neurosecretory cells, and parvocellular portions; the second is located in the superior part of the periventricular zone. The epithalamus represents the rostrodorsal part of diencephalon and comprises the habenular nuclei, the epiphysis and the dorsal saccus. These structures are mostly involved in the synchronisation of movement and in circadian rhythm cycle. The thalamus is divided into a dorsal and ventral region. Here are kept all the major sensory stimuli (except olfaction). The hypothalamus, is located below the thalamus and represents the most ventral diencephalic region, caudally to the preoptic area. It is easily distinguished from the preoptic area by its densely packed and stained cells surrounding the nascent infundibular recess. It is connected via the pituitary stalk, containing hypothalamic and preoptic neuroendocrine fibres, to the hypophysis. In teleost, the hypothalamus can be divided into three main regions: the periventricular region, the medially located tuberal region and the paired inferior lobes, formed from the expansion ventro-caudal of the posterior recess. The subdivision of the hypothalamic regions, based on the cell disposition, comprises a dorsal, ventral, lateral and caudal hypothalamus. All of them show a periventricular cells distribution, bordered by laterally migrated nuclei. The cells belonging to the dorsal area are big and form a lamina, indeed, the ventral zone contains smaller cells disposed in a thick layer. The cells of the inferior diffuse lobe are presumably migrated from the dorsal hypothalamus. Thus these may be considered as part of the dorsal hypothalamus, which expands laterally, recognisable around the recess. The pretectal region, is located in front of the rostral margin of the optic tectum and includes both diencephalic and mesencephalic structures. Functionally, the pretectum may be characterised as a primarily visual region, receiving both retinal and tectal visual inputs.

Midbrain

Mesencephalon

The mesencephalon is distinguished in the dorsally located optic tectum, the tegmentum in ventromedial part, and semicircular tori in ventrolateral side. This subdivision has also a functional meaning: optic tectum is involved in sensory functions and integration of messages from the optic tract with sensory information, with the combination and translation in coordination outputs. The longitudinal tori play role in perception of visual message from optic tectum, the tegmentum encloses motor structures, such as the oculomotor nuclei, and continues into the medulla oblongata (rhombencephalon).

Hindbrain

Rhombencephalon

The rhombencephalon is composed of the cerebellum, pons and medulla oblongata. The cerebellum is composed of three main areas: the valvula, protruding in rostral direction into the mesencephalic ventricle, the centrally-located corpus, and the caudal lobe with granular eminentiae. The cerebellum is mainly responsible for coordinated movements. The medulla and the midbrain, often referred to as “brainstem”, are characterised by miscellaneous of cells that together form the reticular formation, functionally responsible for respiration, circulation, and wakefulness.

2. AIMS AND PIPELINE OF THE STUDY

The major goal of this study is to achieve deeper knowledge about how elderly organism change food intake regulation during ageing. We selected *N. furzeri* as model; the latest established non mammalian vertebrate for studying age-related changes. Up to date, there is a big gap of information about how the energy metabolism is regulated in a vertebrate organism with such short life span. We aim to lay the basis of this investigation with multidisciplinary approach; in fact, we combine detailed anatomical description with analysis of expression of three important central food intake regulators: neuropeptide Y, orexin and nesfatin-1. Each neuromodulator is singularly analysed in young adult subjects of two strains of the same species, MZM and GRZ, respectively long and short lived, to identify intraspecific differences. Then, the patterns between young and old are compared to elicit a preliminary evaluation of age-dependent regulation. Also, to evaluate how and if the central regulation adjusts itself to different energy income, young adult subjects are starved for 96 hours and compared with regularly fed animals of same age. Caloric restriction (30-60% below *ad libitum*) is the most effective and reproducible intervention to regulate ageing in several model organisms (yeast, flies, fish, rodents and primates), described for the first time by Crowell and McCay, already in 1936. Although the molecular mechanisms that mediate the effect of caloric restriction are still being investigated and debated, there is a shared hypothesis that caloric restriction and lifespan extension involve the downregulation of insulin and insulin- like signalling (IIS), as well as of the amino signalling target of rapamycin (mTOR)- S6 kinase pathway and the glucose signalling Ras-protein kinase A (PKA) pathway (Fabrizio *et al*., 2001; Kapahi *et al*., 2004; Slack *et al*., 2015). Moreover, fasting is a dietary regimen that has proven to trigger similar biological pathways as caloric restriction. It has gained popularity over the years due to easier application than dietary restriction, especially in experiment carried out using fish models. Fasting for short time or intermittent range, causes an extreme environment that induces protective changes in normal cells, this phenomenon is called differential stress resistance (DRS). Based on this knowledge, to evidence the activation of the conserved mTOR mechanism (Seiliez *et al*., 2008) and its modification in *N. furzeri*, according with energy status, the phosphorylation of ribosomal protein S6 is also evaluated and considered as functional marker of neuronal activation (Knight *et al*., 2012).

3. MATERIAL AND METHODS

3.1. Husbandry and experiment onset

Fish housing and care followed a specific protocol valid for both strains, MZM and GRZ, but was adjusted depending on the age of the fish and on the experimental conditions. Animals were kept constantly at 26°C and 12 h of light/dark cycles. At the age of 3 weeks post hatching, young fish were moved from 7.5 l group tanks to single housed tanks with low water flow. Salinity was maintained always between 2.5 - 3 mS and parameters as pH, and mineral content were periodically checked to avoid discrepancies between experimental groups. Fish were fed manually and, within 2 h, uneaten food was removed from the tank to avoid water contamination. Young fry up to an age of 3 weeks was fed only with *Artemia salina* twice per day. Older fish received twice per day bloodworm larvae (*Chironomus plumosus*) and once per day *A. salina*. At time points (MZM: 5-27 weeks old; GRZ: 5-12 weeks old) experimental groups were selected and the animals in study were starved for 96 h before sacrifice. Contemporary also tissues from control animals of the same hatching were dissected.

Equipment

General lab equipment was used for the molecular and cell biology techniques, including balances, centrifuges, electrophoresis equipment, heating blocks and plates, hybridisation and incubation ovens, micropipettes, PCR and gradient thermocyclers, pH-meter, shakers, UV-transilluminator, vortexes and waterbaths. Fixed frozen sections were obtained using the Cryostat CM 1900, Leica (Leica, Solms, Germany) and for paraffin sectioning Leica RM2155 microtome was used. Zeiss ApoTome.2 microscopes (Carl Zeiss, Jena, Germany) and Zeiss Zen 2 Blue software were used to acquire fluorescent images. Leica microscope DM RA2 (Leica Camera AG) attached to a Leica DC300 F camera for light microscopic images.

Specimens

Fish were euthanised using 250 mg l^{-1} Tricaine methane-sulfonate (MS-222, Tricane-S®, Western Chemical Inc.) as suggested by AVMA (Euthanasia of amphibian and fish, American Veterinary Medical Association 2007) in buffered solution (for review see Topic Popovic *et al*., 2011), according to ethical standards. Total number of 136 specimens (MZM and GRZ; different age; different diet) was employed in this study: 64 for gene regulation, 24 for protein expression and 48 for morphological study.

3.2. Quantitative real-time polymerase chain reaction

Sample preparation, RNA extraction and reverse transcription of cDNA synthesis

After euthanasia, fish were dissected on ice and whole brains were explanted and transferred to 2 ml Eppendorf safe-lock tubes. Tissue were homogenised in 1 ml of phenol/guanidine-based QIAzol Lysis Reagent (Qiagen, cat. 79306) with a 7 mm stainless steel bead (Qiagen, cat. 69990) by use of Qiagen Tissue Lyser II for 3x 1 min at 30 Hz. After 5 min incubation at room temperature (RT), 200 ml Chloroform was added and the samples were mixed carefully (Tissue Lyser II, 30 seconds, 20 Hz). After incubation of 3 min at RT samples were centrifuged at 20,000 x g for 20 min at 4°C. The aqueous phase was transferred into a new tube and mixed with 1 µl Glycoblue (Ambion), 1.1x isopropanol and 0.16x sodium acetate (NaAc 2M, pH 4.0), incubated for 10 min at RT and centrifuged at 20,000 x g for 30 min at 4°C to allow RNA precipitation. After removing the supernatant, the pellet was washed two times with 80% ethanol and air dried. The pellet was diluted in 20 µl RNAse free H_2O and the RNA concentration was measured with a spectrophotometer (NanoDrop 1000, Thermo Scientific). 500 ng of purified RNA were used as template for reverse transcription, using QuantiTect Reverse Transcription Kit (Qiagen, cat. 205313) according to the manufacturer´s instruction. Elimination of genomic DNA was achieved by use of gDNA wipe-out buffer and incubation at 42°C for 5 min. The reverse transcription reaction was performed for 15 min at 42°C and deactivated for 3 min at 95°C. After cDNA synthesis samples were diluted 1:10 to a final volume of 200 µl with ultra-pure water. cDNA samples were stored at -20°C.

Primer test and qPCR

Real-time PCR reactions were performed in 10 µl volume with 1 µl diluted cDNA using the Quantitect SYBR Green PCR kit (Qiagen). Forward and reverse primers were always located in two different exons (Tab. 2, Fig. 5). The correct amplicon size was verified by 1% Agarose-gel electrophoresis. A cDNA pool was serially diluted (from 80 to 2.5 ng per reaction) and used to create standard as well as melting curves and to calculate amplification efficiencies for each primer pair prior use for quantification. All reactions were performed in triplicates and negative (water) as well as genomic (without reverse transcriptase) controls were always included. Expression was normalised to TBP (TATA box binding protein) by deltaCT method and fold changes are calculated relative to 5 week old controls. Statistical analysis of real-time data was done by unpaired two-tailed t-test (GraphPad Prism 5).

Table 2. qPCR primer pair sequences (Eurofin genomics).

Gene	qPCR primer sequence
NPY_fw (21 nt)	CAG CCC TGA GAC ACT ACA TCA
NPY_rv (19 nt):	CTG CTC TCC TTC AGC AGC A
HCRT_fw (20nt)	TGA CTG CCC TCC ATA AAA GC
HCRT_rv (20nt)	GCT GAG ACA GCA GCA ACA TC
NUCB2_fw (20 nt)	ACT GTG GGC TGG TCC TAC TG
NUCB2_rv (20 nt)	CTT CCC TGA GGT AAC GGT CA
TBP_fw (20 nt)	CGG TTG GAG GGT TTA GTC CT
TBP_rv (20 nt)	GCA AGA CGA TTC TGG GTT TG

3.3 Western blot

Sample preparation

Brain was dissected on ice and treated with 200 µl of lysis buffer, homogenised by ceramic (zirconium oxide) beads 5x for 1 min in the Tissue Lyser II at 30 Hz. The homogenate was centrifuged at 13,500 x g for 15 min and the supernatant was retained. The protein concentration was determined using BCA (bicinchoninic acid) Protein Assay (ThermoFischer Scientific Pierce BCA Protein Assay Kit, cat. 23227) and the absorbance spectrum (GloMax®-Multi+ Microplate Multimode Reader with Instinct®) at 560 nm. Protein aliquots were diluted in loading buffer in order to have 1 mg/ml of protein and then heated at 95°C for 10 min.

Electrophoresis - SDS PAGE

Proteins and the molecular weight markers (Biotinylated Protein Ladder #7727 Cell Signaling; PageRuler™ Prestained Protein Ladder 10 to 180 kDa, #26616 Fisher Scientific) were loaded in 5% stacking and 15% resolving acrylamide gel (30% Acylamide Sigma-Aldrich®, cat. A3699). The gel was casted in Mini-Protean II chambers (Biorad®), filled with the migration buffer, and run 30 min at 80 V first, followed by 1 h at 120 V.

Transfer of protein and staining

Wet blotting was performed using nitrocellulose membranes (0.2 µm pore size, Biorad®) for 30 min at 100 V, immersed in transfer buffer. To check for success of the transfer, membranes were stained with Ponceau Red. The membranes were blocked with 5% non-fat milk for 1 h at 4°C under agitation. The membranes were incubated with the primary antibody (Tab. 4), diluted in blocking solution, overnight (ON) at 4°C, under agitation. The membranes were successively incubated with HRP-conjugated secondary antibodies (Tab. 4), diluted in TBS-T, for 1 h at RT under agitation. The protein was detected, developing by the chemiluminescent system (Clarity™ Western ECL Substrate BioRad, cat.170-5060), after a reaction of five min at RT. For re-probing the membranes, it was used Restore™ Western Blot stripping buffer (ThermoFischer Scientific, cat.21059) ON at RT. Western blots were repeated in triplicate and every experiment was followed by negative control in which the step of the primary incubation was skipped.

Buffers:

- lysis buffer: composed by a mix of protease inhibitors (in ratio 1:1000)
    - Pepstatin A (synthetic, Enzo® Life Sciences, ALX-260-085-M005)
    - Antipain (synthetic, Enzo® Life Sciences, ALX-260-093-M005)
    - Leupeptin (synthetic, Enzo® Life Science, ALX-260-009-M005)
    - Phenylmethylsulfonyl Fluoride or PMSF (synthetic, Enzo® Life Sciences, ALX-270-184-G005)

    - RIPA buffer
        - 150 mM NaCl
        - 50 mM tris HCl, pH 8.0
        - 1% Triton X-100
        - 0.5 % Sodium deoxycholate
        - 0.1% SDS

- loading buffer: 5x Leammli loading dye, pH 6.8
    - 4% SDS,
    - 20% Glycerol
    - 10% β-mercaptoethanol,
    - 0.125 M Tris HCL
    - 0.004% Bromophenol blue

- migration buffer: 1x Tris-glycine, pH 8.3
    - 25 mM Tris base
    - 190 mM Glycine
    - 0.1% SDS

- transfer buffer
    - 25 mM Tris base
    - 190 mM Glycine
    - 20% Isopropanol

- Ponceau S staining solution
  - 0.5% (w/v) Ponceau S
  - 1% Acetic acid

- 10x Tris-Buffered Saline (TBS): for 1l, pH 7.6
  - 24.23 g Tris base
  - 80.06 g NaCl
  - Ultra-pure H_2O

- 1x TBS-T: 1l, pH 7.4
  - 100 ml 10x TBS
  - 900 ml ultra-pure H_2O
  - 1 ml Tween 20

3.4. *In situ* hybridisation

RNA probe generation: primer design, amplification of target region and sequencing

A pool of RNA, extracted from brain of MZM and GRZ strains of *N. furzeri* at different age, was used to synthesise cDNA (protocol elucidated before) to serve as template for the following reactions. Oligonucleotide primers were designed according to standard methods (product length: minimum 400pb), using Primer3 software (Tab. 3). Each reverse primer contained a T7-promotor sequence to allow direct *in vitro* transcription (probes localization whithin the CDS in Fig. 5). The primers were dissolved to a final concentration of 10 pM. A standard PCR was run to amplify the target region, using an annealing temperature of 60°C. 5 µl of each product was loaded in an analytical 1% agarose gel to check for the expected length of the amplicon. Preparative 1% agarose gel was used to cut out the band of interest. Visualisation of gels was done by ethidium bromide staining on UV transilluminator (ChemiDoc™ MP System, #1708280) and DNA was cleaned by use of Illustra GFX PCR DNA and Gel Band Purification Kit (GE Healthcare Life Science, 28-9034-70), following the manufacture protocol. 300 ng of the products were sequenced by the Laboratory of Genome analysis (Platzer laboratory, Leibniz Institute on Aging - Fritz Lipmann Institute). Alignment of the obtained sequences was performed by MEGA6 software (Molecular Evolutionary Genetics Analysis from www.megasoftware.net) to validate the expected sequence of the amplicon.

RNA probe generation: in vitro transcription and probe testing

RNA labelling with Digoxigenin-11-dUTP (DIG) by *in vitro* transcription with T7 polymerase was carried out with DIG RNA labelling mix (Roche, 11277073910) following the manufacturer´s protocol, using 200 ng of PCR product as template (Fig. 6a-c). After Lithium-chloride precipitation, the concentration of RNA was measured with spectrophotometer. Dot blot was performed to guarantee the proper DIG incorporation into the newly synthesised transcript (protocol: Zimmerman *et al., 2013*) (Fig. 7a). In addition, to verify the efficiency of the reaction, the length of the transcript was checked on a denaturing 4% Urea-TBE polyacrylamide gel (Fig. 7b).

Sample preparation for ISH and IF/IHC

Brain was dissected on ice and fixed in 4% RNAase-free paraformaldehyde at 4°C for 24 h. Tissue was treated with 20% sucrose for 12 h and 30% sucrose ON at 4°C. Brain was embedded in cryo-embedding-medium (O.C.T. tissue tek Richard-Allan Scientific™ Neg-50™, #6502) with dry ice to ensure optimal cutting temperature and kept at -80°C. Cryostat sectioning were performed in coronal orientation with 10 µm thickness.

Pre-treatment, incubation and developing

Coronal sections were treated with Proteinase K (5 µg/ µl) for 10 min at RT and, after several washes first with glycine and RNAase-free 1x PBS, fixed again with 4% paraformaldehyde for 15 min at RT. After washing away fixing solution, slides were pre-hybridised for 30 min with the hybridisation buffer in a humid chamber. Hybridisation temperature was chosen depending on the GC content of the probes: 55°C was used for NPY and HCRT (GC content 54%) and 42°C was used for NUCB2 (GC content 50%). Probes were denatured at 80°C and cooled on ice before use. Sections were incubated ON with 200 ng of respective probes. After hybridisation, wash steps (each 10 min at RT) using 0.5x, 0.1x Saline-Sodium Citrate (SSC) and RNAase-free 1x PBS were performed. Sections were treated with blocking solution for 30 min at RT and immediately incubated with anti-DIG-Alkaline Phosphatase Fab fragments (1:2000 Roche, cat. 11093274910) at 4°C ON. After washing in RNAase-free 1x PBS and levamisole (Vector Labs., SP-5000), sections were stained with Fast Red substrate (Roche, 11496549001) and with DAPI mounting medium (IBSC, cat # AR-6501-01) before sealing with a coverslip.

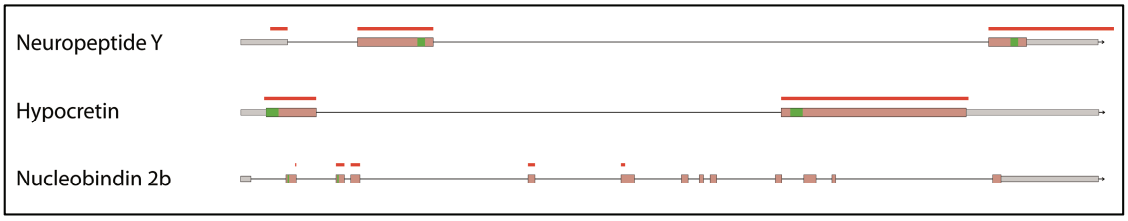

Figure 5. Genomic structure of analysed genes and localisation of qPCR primer (green) and probe sequences (red) within the CDS (light orange).

Buffer and solutions:

- Hybridisation Buffer
  - 50% formamide (deionised)
  - 5x Saline Sodium Citrate (SSC, pH 7.0)
  - 0.1% Tween-20
  - 9.2 mM citric acid
  - 50 µg/ µl heparin
  - 500 µg/ µl yeast t-RNA
  - DEPC H_2O

- Blocking Solution
  - 1x PBS
  - 10% goat serum (heat inactivated, see IHC)
  - 0.5% blocking reagent (Roche, #11096176001)
  - 0.1% tween-20
  - DEPC H_2O

- 20x Saline Sodium Citrate (SSC stock, pH 7.0)
  - 3M NaCl
  - 300 mM Sodium Citrate
  - DEPC H_2O

Table 3. ISH primer pair sequences (Eurofin genomics). In bold italic is marked T7 promotor.

Gene	ISH primer sequence	Product size
NPY_fw	GAA AGC CAC TGG GAC AAA TC	514
NPY_rv	***GGT AAT ACG ACT CAC TAT AGG*** GCC CCA TCT CCG TTT TCT AT	
HCRT_fw	ATC AGA TGA CTG CCC TCC AT	404
HCRT_rv	**GGT AAT ACG ACT CAC TAT AGG** AGT TCA CTG CTC CCC AGT TG	
NUCB2_fw	CCA CCA GCG AGC ACT GAC ACC	416
NUCB2_rv	**GGT AAT ACG ACT CAC TAT AGG** ATA CCT CTT GAA CTC ATC ATG	

a. NPY *N. furzeri* riboprobe GC 54.58

```
GAAAGCCACTGGGACAAATCTCGCTCCAATCTTCTGGACAAATGCATCCTAACT
      C
TGGTGAGCTGGCTGGGGACGCTGGGCTTCCTGCTGTGGGCGCTGGTCTGCCT
GGGAGCCTTGACGGAGGGGTACCCGGTGAAACCGGAGAACCCCGGGGAGGA
CGCTCCGGCCGAGGAACTGGCCAAGTACTACTCAGCCCTGAGACACTACATCA
                                                      A
ACCTGATAACGAGACAGAGGTATGGGAAAAGGTCCAGTCCAGAGAGTCTGGTC
                    G
ACACTGATCTCAGAGCTGCTGCTGAAGGAGAGCAGAGACATACTTCCACAGTC
GAGATACGACCCATCATCGTGGTGATGCTGTCGTCAGCCTGCTGCACTCTATC
                                    A
ACGTCTGTCCGTTCACCACATCCAAGCAGCCTGGTCCTCCTCTTGTCCCCATG
          C         T
CAGCTTCAAAGTTCTGTAGTACACCGTGTGCCATACAACTGTAAATAGTTTATG
CCGTCATTGTCTGTGAAATAGAAAACGGAGATGGGGC
```

b. HCRT *N. furzeri* riboprobe GC 54.46

```
ATCAGATGACTGCCCTCCATAAAAGCCTGAAGATGACGTGGAGCCCCTCCAAG
ATCCAGAAAGCTGCTAGGATGGACACAACGCACAAGAAAGCCCTGGTGTTCGT
TTTGATGTTGCTGCTGTCTCAGCTGGATTGTAACGCCCAAATTGTGTCTGAGTG
CTGCAGACAGCCTCCTCACTCCTGCCGCCTCTATGTCTTACTGTGCCGTTCTG
GCAGCAATAGCATGGGGGGAACAATTGTAGAAGATGCAGCTGCTGGGATCCTC
ACGCTGGGTAAACGGGACGAGAATGAGTATCGCTTGCAGAGCCGACTCCACC
AGCTTCTTCACAGCTCCAGGAACCAAGCAGCAGGGATCCTGACGATGGGGAG
GAGGACCACTGGGCCAACTGGGGAGCAGTGAACT
```

c. NUCB2 *N. furzeri* riboprobe GC 50.12

```
CCACCAGCGAGCACTGACACCGGGCTGCACTATGACCGTTACCTCAGGGAAG
TCATCGAATACCTTGAGAAAGACCCGCACTTTAGAGAAAAGCTGCAAAATGCCA
GTATTGAGGACATCAAGCAAGGCAAACTTGCCAAAGAGCTGGACTTTGTCCAT
CGCAATTTTCGAACTAAGCTGGACGAGTTGAAGAGGGAGGAGATGAACCGGCT
                                                      T
GAGGATGCTTATTAAAGCCAAACATGACCTCCAGGACAGGAATGGCCGTGCCA
TGGACCGCCAGGCCCTGCTGAAACAGTTTGAGCATCTCAACCATGTGAACCCA
CACACCTTTGAGGTGGAGGATCTGGACCGCCTCATCCAGTCGGCAACTAAAGA
TCTGGAAAACTTTGACAAGACACACCATGATGAGTTCAAGAGGTAT
```

Figure 6. (continued)

d. Differences between MZM and GRZ strains

Gene	Lenght of the probe	Single nucleotide variance	Similarity MZM- GRZ
NPY	513	6 nt	98.83%
HCRT	404	0 nt	100%
NUCB2	416	1	99.76%

Figure 6. Riboprobe sequences **a)** NPY; **b)** HCRT; **c)** NUCB2 referred to the genome annotation in GRZ (http://nfingb.leibniz-fli.de/). In yellow and red are marked the different nucleotide between MZM and GRZ. **d)** Summary table with the length of the probes and grade of similarity between MZM and GRZ.

a.

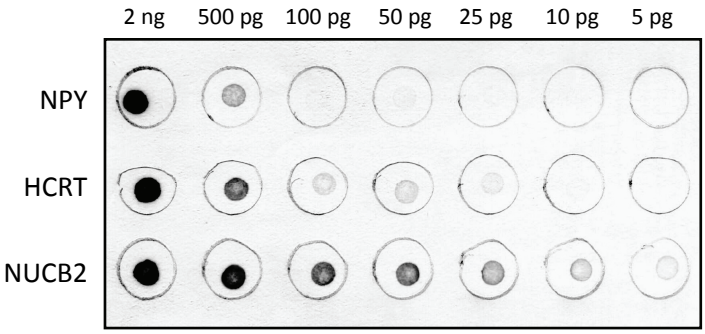

b.

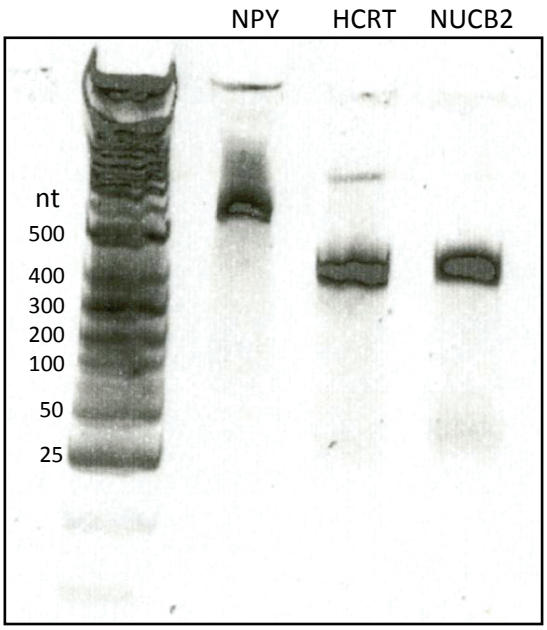

Figure 7. Quality control of probe synthesis. **a)** Dot Blot to verify DIG labelling during IVT: line 1) NPY; 2) HCRT; 3) NUCB2; **b)** denaturing 4% Urea-TBE polyacrylamide gel.

3.5. Immunohistochemistry (IHC)

Immunohistochemistry on paraffin sections

Sample preparation

Brain was dissected and fixed in Bouin's fluid ON at RT, progressively dehydrated in ascendant gradient of ethanol and then transferred to the organic solvent xylene. The tissue was finally embedded in low melting temperature paraffin and microtomical coronal sections of 7 µm thickness were processed.

Pre-treatment and incubation

After dewaxing in xylene and rehydrating in progressively diluted alcohols, serial sections were treated 30 min with 3% H_2O_2 and, after washing with 1x PBS, normal goat serum blocking solution (NGS 1:5 in 1x PBS, ImmunoBioScience Corp., IHR-8136) or normal rabbit serum blocking solution (NRS 1:5 in 1x PBS, Vector, S-5000) was used at RT for 30 min. Incubation with each of primary antibody (Tab. 4) diluted with dilution buffer in a humid chamber was performed at 4°C ON. After incubation, different treatment was carried out according to the primary antibody in use: incubation with rabbit antibodies was followed by incubation with EnVision reagent (DAKO, K406511), a peroxidase-conjugated polymer backbone, which carries anti rabbit- secondary antibody (Tab. 4), for 30 min at RT. Instead, primary incubation with antibodies hosted in goat, were followed by incubation with anti-goat secondary antibody biotinylated (Tab. 4) and treated with the avidin-biotin-based peroxidase system (VECTASTAIN Elite ABC Kit, PK-6100).

Developing and visualisation

The immunoreactive sites were visualised using a fresh solution of 10 µg of 3,3'-diaminobenzidine tetrahydrochloride (DAB, Sigma-Aldrich, #D5905) in 15 ml of a 0.5 M Tris buffer.

Immunohistochemistry on frozen sections

Sample preparation

Brain preparation was carried out following the same protocol applied for ISH. Cryostat sectioning were performed in coronal orientation with 7 µm thickness.

Pre-treatment, incubation and developing

Sections were fixed with pure ice-cold acetone for 10 min at RT. Normal goat serum (NGS, ImmunoBioScience Corp., IHR-8136) or normal donkey serum (NDS, ImmunoBioScience Corp., IHR-8135) solution were used for blocking at RT for 2 h. The slides were incubated with the primary antibody (Tab. 4) diluted in dilution buffer at 4°C ON. The sections were incubated with fluorochrome conjugated-secondary antibody (Tab. 4) diluted in 1x PBS for 1 h at RT and nuclei were stained with DAPI mounting medium (IBSC, cat # AR-6501-01) before sealing with coverslips.

Buffers:

- Bouin Solution:
  - 70 ml Picric acid (saturated)
  - 25 ml Formaldehyde (37-40%)
  - 5 ml Glacial acetic acid

- 1x Phosphate Buffered Saline (PBS):
  - 137 mM NaCl
  - 2.7 mM KCl
  - 10 mM Na_2HPO_4
  - 2 mM KH_2PO_4

- Dilution buffer:
  - 0.2% TritonX-100,
  - 0.1% bovine serum albumin,
  - 4% normal goat serum (NGS).
  - 0.5 M Tris buffer, pH 7.6
  - 1.5 ml 0.03% H_2O_2

Table 4. Antibodies used in WB, IHC, IF experiments.

Antibody	Dilution WB	Dilution IHC-IF	Catalogue code
Anti-rabbit neuropeptide Y polyclonal	-	1:1000 P 1:100 FoFr	Abcam ab30914
Anti-rabbit neuropeptide Y polyclonal	1:500	-	Abcam ab186440
Anti-rabbit prepro- orexin polyclonal	1:300	-	EDM Millipore AB3096
Anti-goat orexin A polyclonal	-	1:500 P 1:10 FoFr	Santa Cruz Biotecnology sc-8070
Anti-rat nesfatin 1 polyclonal	1:2000	1:3000 P 1:3000 FoFr	Phoenix Pharmaceuticals, Inc. H-003-22
Anti-rabbit phospho-S6 ribosomal protein monoclonal	1:2000	1:1000 FoFr	Cell Signaling Tec. #4858
Anti-rabbit S6 ribosomal protein monoclonal	1:1000	-	Cell Signaling Tec. #2217
Anti-biotin, HRP-linked	1:1000	-	Cell Signaling Tec. #7075
Anti-rabbit IgG, HRP-linked	1:2000	-	Cell Signaling Tec. #7074
Goat anti-rabbit (H+L), Alexa Fluor® 488 conjugate	-	1:1000 FoFr	Invitrogen Molec. Probes A-11008
Biotinylated rabbit anti-goat (H+L)	-	1:200 P	Vector Laboratories BA-5000
Donkey anti-goat (H+L), Alexa Fluor® 488 conjugate	-	1:1000 FoFr	Invitrogen Molec. Probes A-11055

4. RESULTS

The results refer to the characterisation of neuropeptide Y (NPY) orexin (HCRT/ORX-A) and nesfatin-1 (NUCB2) in the brain of two strains, MZM and GRZ, of *Nothobranchius furzeri*. The expression and distribution, of either mRNA (*In Situ* Hybridisation, ISH) and protein (Immunohistochemistry, IHC) are restricted to the areas responsible for the regulation of the food intake: the forebrain, including the ventral part of the telencephalon and the diencephalon *in toto*. Positive areas, which are not reported as neuroendocrine structures, are also described when signal was detected, in particular, olfactory bulbs and dorsal telencephalon, regarding the forebrain, optical tectum and semicircular tori in the mesencephalon (midbrain). The morphological description is referred to young subjects of both strains, sexually mature (5 weeks old), using as template *N. furzeri* brain atlas (D'Angelo, 2013). The differences between the two strains, young and elderly subjects and between regularly fed animals (controls) and starved after 96 hours of food deprivation are reported. Gene regulation is based on the extraction of the mRNA from the whole brain, as well as the results of protein identification (Western Blot, WB).

4.1. Gene regulation

4.1.1. Neuropeptide Y

NPY regulation during ageing

In MZM strain, comparing animals regularly fed, but at distant age, NPY expression significantly upregulated and the fold change of old subjects was 2.45 ± 0.27 times higher than the young (Fig. 8 top-left). Also in GRZ strain, the regulation was significantly higher in elderly fish than in young, with a fold change increase of 1.54 ± 0.29 times (Fig. 8 bottom-left).

NPY regulation upon starvation

In MZM strain, comparing control and starved (96 hours) fish at young age, NPY significantly upregulated in subjects under starvation with an increase of 1.36 ± 0.12 times higher than controls (Fig. 8 top-middle). Analysing the starvation effect between old controls and starved, the expression level was almost identical (Fig. 8 top-middle and -right). In GRZ strain, in the young subjects, food deprivation led to significant NPY upregulation of 1.54 ± 0.29 times higher in starved than in controls

(Fig. 8 bottom-middle). Also in old starved fish there was a significant increase of 2.81 ± 0.38 times compared with controls (Fig. 8 bottom-right).

4.1.2. Hypocretin/ Orexin

HCRT regulation during ageing

In MZM strain, HCRT in old subjects has a significant decrease of 0.52 ± 0.66 fold as young (Fig. 9 top-left). In GRZ strain, no regulation during ageing was revealed (Fig. 9 bottom-left).

HCRT regulation upon starvation

In MZM strain, in starved young fish, after 96 hours of food deprivation, HCRT expression level was 1.77 ± 0.49 times significantly higher than the animals of the same age with regular feeding (Fig 9 top-middle). The starvation didn't have an effect on the regulation in old fish (Fig. 9 top-right). In GRZ strain, starved young subject showed a not significant upregulation of 1.29 ± 0.52 times compared with controls (Fig. 9 bottom-middle). Also in old fish, HCRT expression showed same level in starved and control animals (Fig. 9 bottom-right).

4.1.3. Nucleobindin-2/ Nesfatin-1

NUCB2 regulation during ageing

In MZM strain, old animals had significantly 1.27 ± 0.31 fold higher levels than young (Fig. 10 top-left). Also in GRZ strain, there was a significant increase of 1.47 ± 0.37 times in elderly subjects compared with young (Fig. 10 bottom-left).

NUCB2 regulation upon starvation

NUCB2 expression level didn't chance significantly after 96 hours of food deprivation, whether in young or old animals of both strains (Fig. 10 top-middle and -right, bottom-middle and -right).

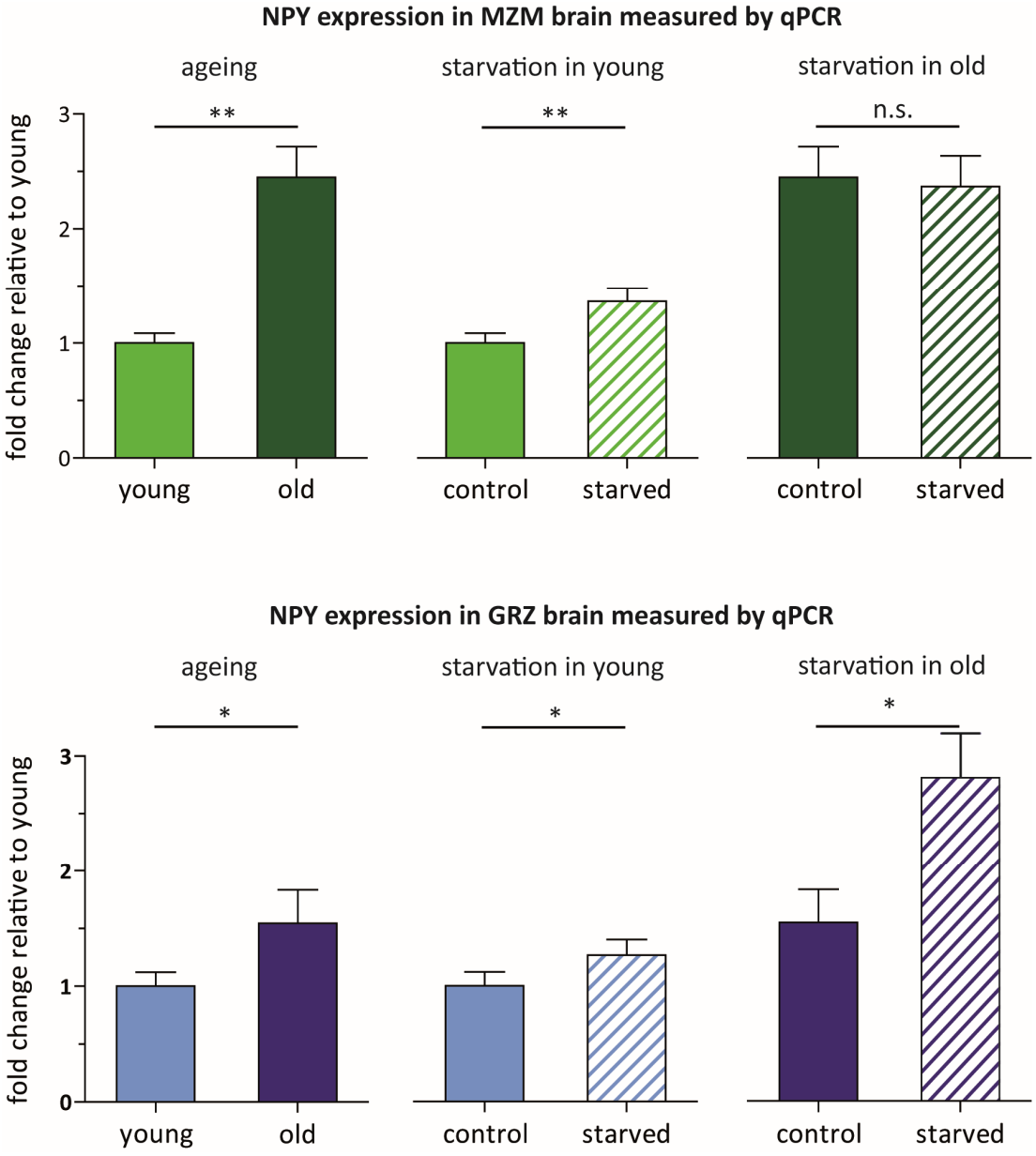

Figure 8. NPY expression in MZM (green) and GRZ (blue) strains measured by qPCR. Light colour indicates young subjects and dark indicate old subjects; full column indicates control condition, strips pattern indicates fasting condition. n=8. Bars= SD. n.s. $p > 0.05$; * $p \leq 0.05$; ** $p \leq 0.01$.

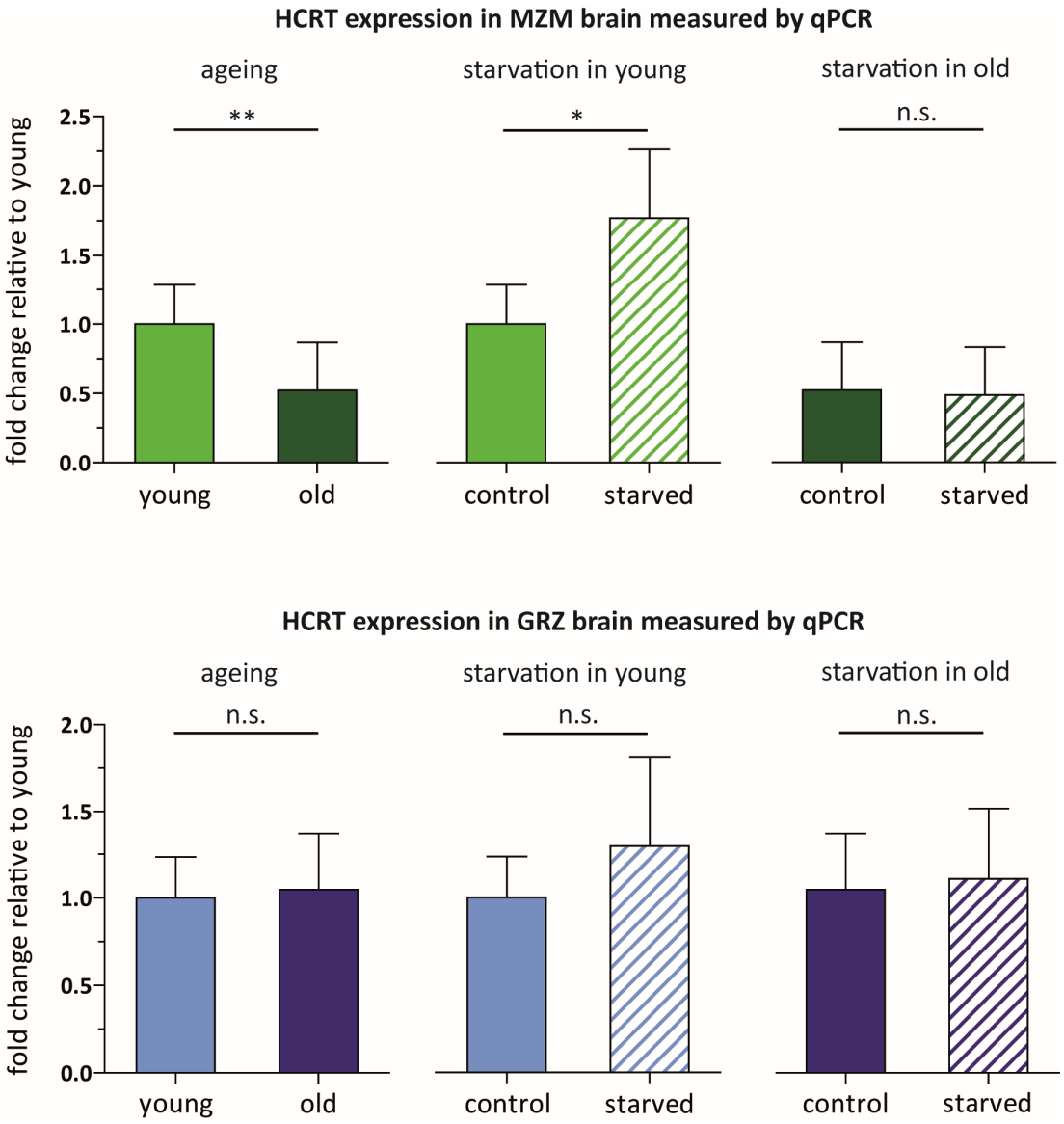

Figure 9. HCRT expression in MZM (green) and GRZ (blue) strains measured by qPCR. Light colour indicates young subjects and dark indicate old subjects; full column indicates control condition, strips pattern indicates fasting condition. n=8. Bars= SD. n.s. $p > 0.05$; * $p \leq 0.05$; ** $p \leq 0.01$.

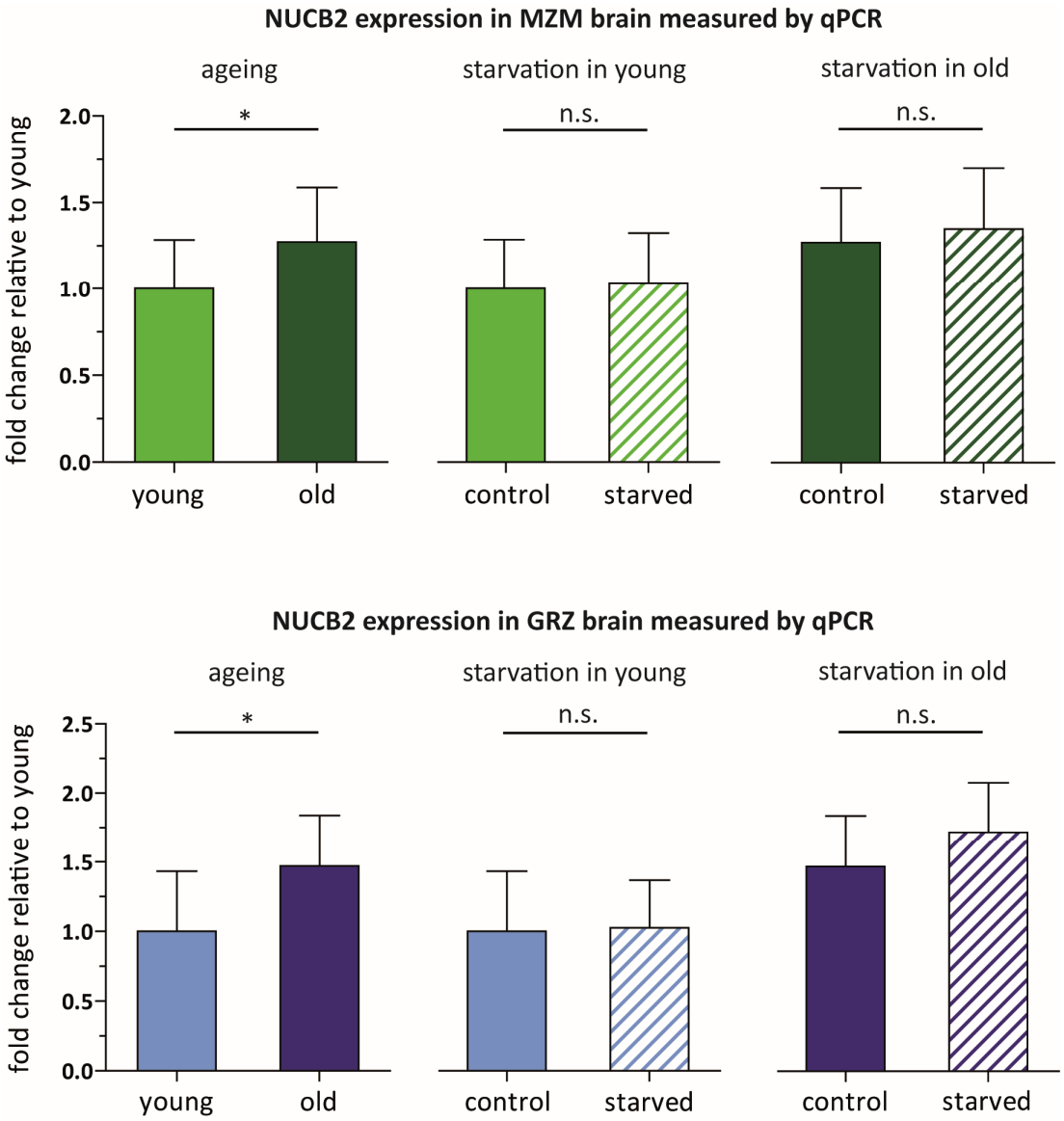

Figure 10. NUCB2 expression in MZM (green) and GRZ (blue) strains measured by qPCR. Light colour indicates young subjects and dark indicate old subjects; full column indicates control condition, strips pattern indicates fasting condition. n=8. Bars= SD. n.s. $p > 0.05$; * $p \leq 0.05$; ** $p \leq 0.01$.

4.2. Protein expression

4.2.1. Phosphorylation of S6 ribosomal protein

Blotting S6 Ribosomal Protein (5G10) detected endogenous levels of total S6 ribosomal protein independent of phosphorylation. In MZM strain, one single band was detected at the molecular weight of ~35 kDa (between ~25 and ~37 kDa). None evident difference of intensity was observed between young control (Fig. 11a right, line 1), young starved (Fig. 11a right, line 2). In GRZ strain homologues pattern was detected, but the intensity of signal was much lower than MZM expression (Fig. 11a right and left). Blotting Phospho-S6 Ribosomal Protein detects endogenous levels of ribosomal protein S6 only when phosphorylated at serines 235 and 236. In MZM strain, all conditions showed double bands around ~30-32 kDa (between ~25 and ~37 kDa); compared to young control (Fig. 11b right, line1), signal was more intense in the young starved animal (Fig. 11b right, line 2). In GRZ strain, one clear single band was detected around ~35 kDa (between ~27 and ~37 kDa), in starved fish (Fig. 11b left, line 2) the signal was more intense than in control (Fig. 11b, line 1).

4.2.2. Neuropeptide Y

Immunoblotting of neuropeptide Y detected the following peptide sequence: CLGALAEAYPSKPDNPGEDAPAEDMARYYSALRHYINLITRQRYGKRSSP and, in all studied conditions, 3 bands were detected. In MZM strain (Fig. 11c right), a lower band was detected ~10 and other two bands were identified ~37 and ~50 kDa. These latter bands showed higher intensity in both young control and starved (Fig. 11c right, lines 1-2). The old control animal (Fig. 11c right, line 3) showed darker bands at ~40 kDa and ~11 kDa. In GRZ strain (Fig. 11c left), the lower band was detected at ~10 kDa and two other close bands were found close to ~50 kDa. The young control (Fig. 11c left, line 1) showed just a higher intense band between ~37 and 50 kDa. The starved fish (Fig. 11c left, line 2) revealed high intensity in all 3 bands and the total signal was more intense than other conditions. In the old control (Fig. 11c left, line 3), the intermediate band at ~40 kDa was not distinguishable.

4.2.3. Hypocretin/ Orexin

The binding of prepro-orexin was close to C-terminus of the peptide. In MZM strain (Fig. 11d right), young control (Fig. 11d right, line 1), showed an irregular but clear band at ~14 kDa and in starved fish (Fig. 11d right, line 2) the band, at analogues molecular weight, was more intense. Old control (Fig. 11d right, line 3) showed different smeared bands on background from ~10 to ~20 kDa with a more recognisable bands at ~14 kDa and ~20 kDa. In GRZ strain (Fig. 11d left), identifiable bands were found in all specimens at ~14 kDa, but any clear difference was notable between young control, young starved and old control fish (Fig. 11d left, lines 1-3).

4.2.4. Nucleobindin-2/ Nesfatin-1

The binding of nesfatin-1 precursor, recognised the amino acid sequence: VPIDIDKTKVQNIHPVESAKIEPPDTGLYYDEYLKQVIDVLETDKHFREKLQKADIEEI KSGRLSKELDLVSHHVRTKLDEL. In MZM strain (Fig. 11e right), a clear stained band was detected at ~40 kDa. None qualitative difference was distinguished between young control, young starved and old control (Fig. 11e right, lines 1-3). In the GRZ strain (Fig. 11e left), similar pattern as MZM was noted, with the difference that several others smeared bands were detected in the range between ~25 and 100 kDa and their intensity was higher in young starved (Fig. 11e right, line 2) and old (Fig. 11e right, line 3) fish than young control (Fig. 11e right, line1).

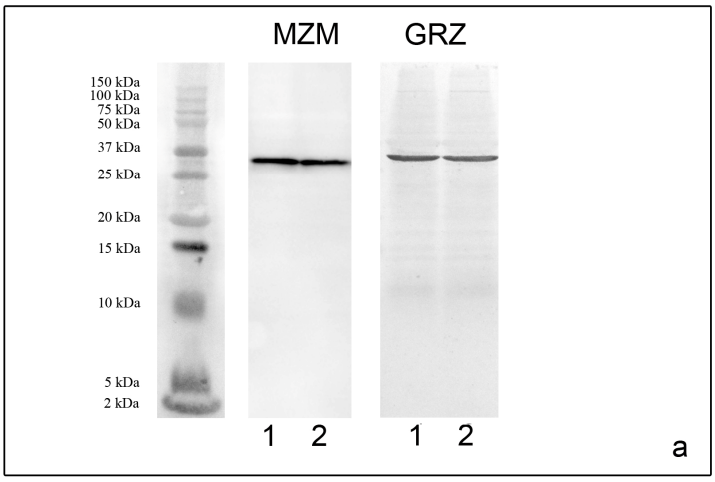

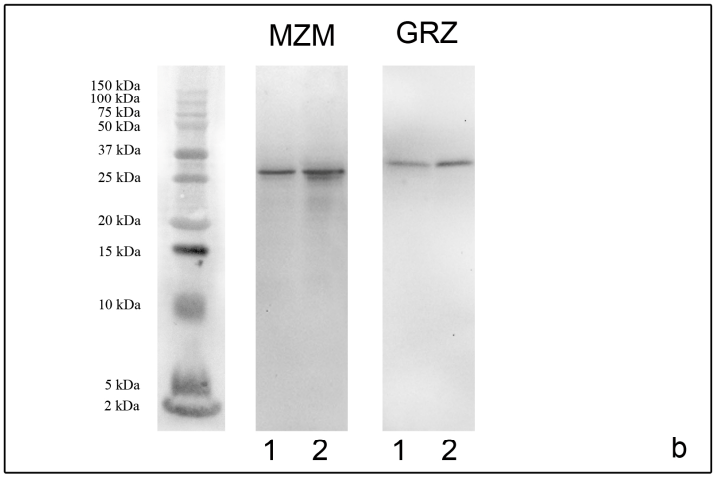

Figure 11. (continued)

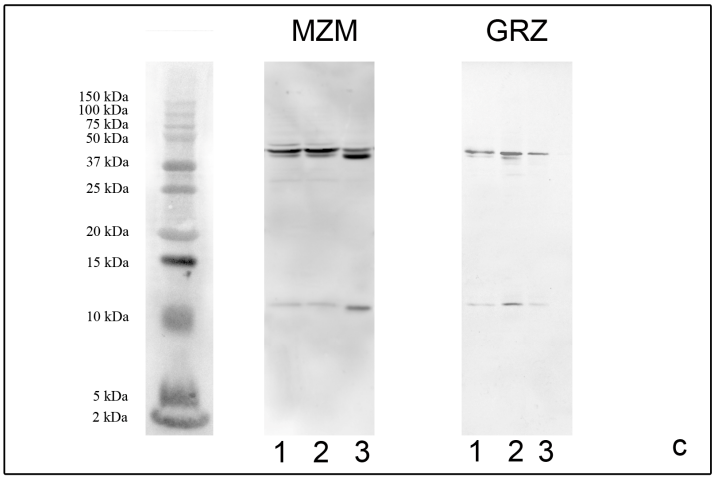

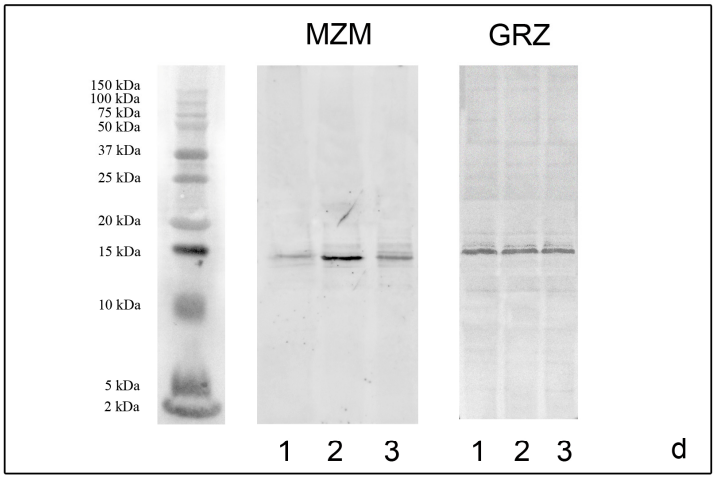

Figure 11. (continued)

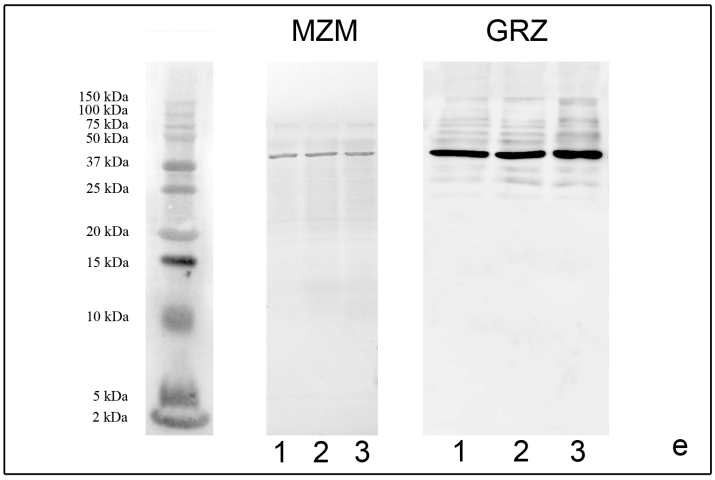

Figure 11. Protein expression **a)** S6RP in MZM and GRZ; **b)** pS6RP in MZM and GRZ; **c)** NPY; **d)** Prepro- ORX; **e)** NUCB2. Line 1: young control; line 2: young starved; line 3: old control.

4.3. Morphological description of mRNA and protein distribution

4.3.1. Phosphorylated ribosomal protein S6

pS6 Immunohistochemistry

Distribution in the brain of young fish upon starvation.

In subjects fasted for 96 hours, the preoptic nuclei contain neurons stained pS6 immunoreactive (Fig. 12a-a'). Specifically, labelled neurons were detected in the parvocellular portion of preoptic nucleus and positive fibres were in dorsal and ventral parts of accessory optic nucleus (Fig. 12b-b'). Moreover, some projections were weakly stained in cortical nucleus. In the diencephalon, immunoreactive neurons were located in the cranial part of the anterior and ventro- lateral thalamic nuclei; many positive fibres were revealed in the dorsal hypothalamus and in glomerular nucleus (Fig. 12c-c'). In the midbrain, few neuronal cells, with intense staining, were observed in the cranial part of the first layer of semicircular tori (Fig. 12d-d'). Positive neurons were also identified in periventricular nucleus of posterior tuberculum, in the paraventricular organ, in the anterior tuberal nucleus and in dorsal hypothalamus. These neuronal patterns were surrounded from a diffuse, but not tight net of labelled projections. In addition, in the medial part of the diffuse inferior hypothalamic lobe (Fig. 12e-e'), several widespread immuno-positive neurons were observed in the medial part. In the subject regularly fed some positive neurons were detected in dorsal, lateral and in the diffuse inferior lobe of hypothalamus. Some positive fibres were also detected in the optic tectum (Fig. 12f-f'). The distribution pattern of activated neurons didn't change between MZM and GRZ strains.

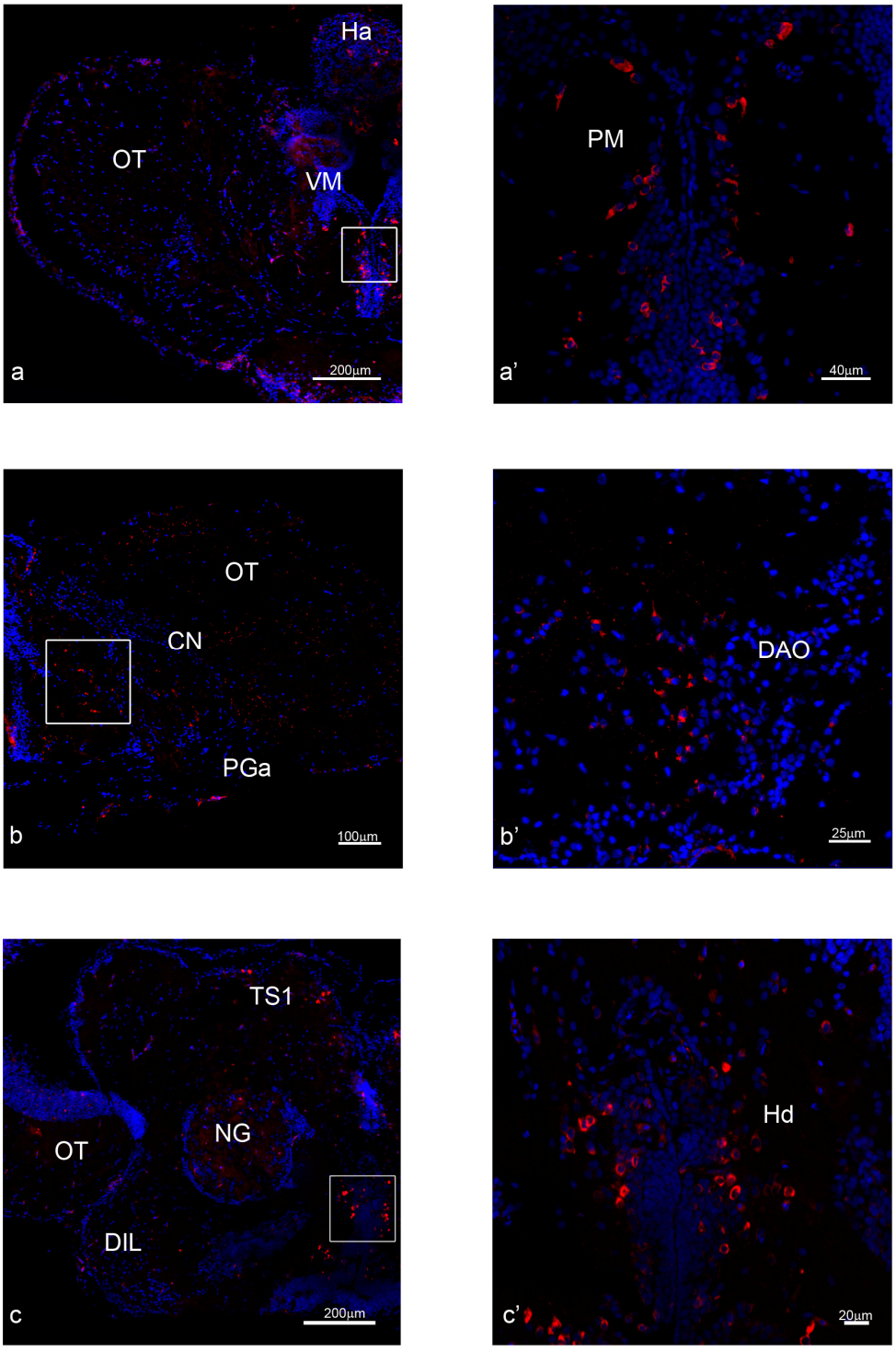

Figure 12. (continued)

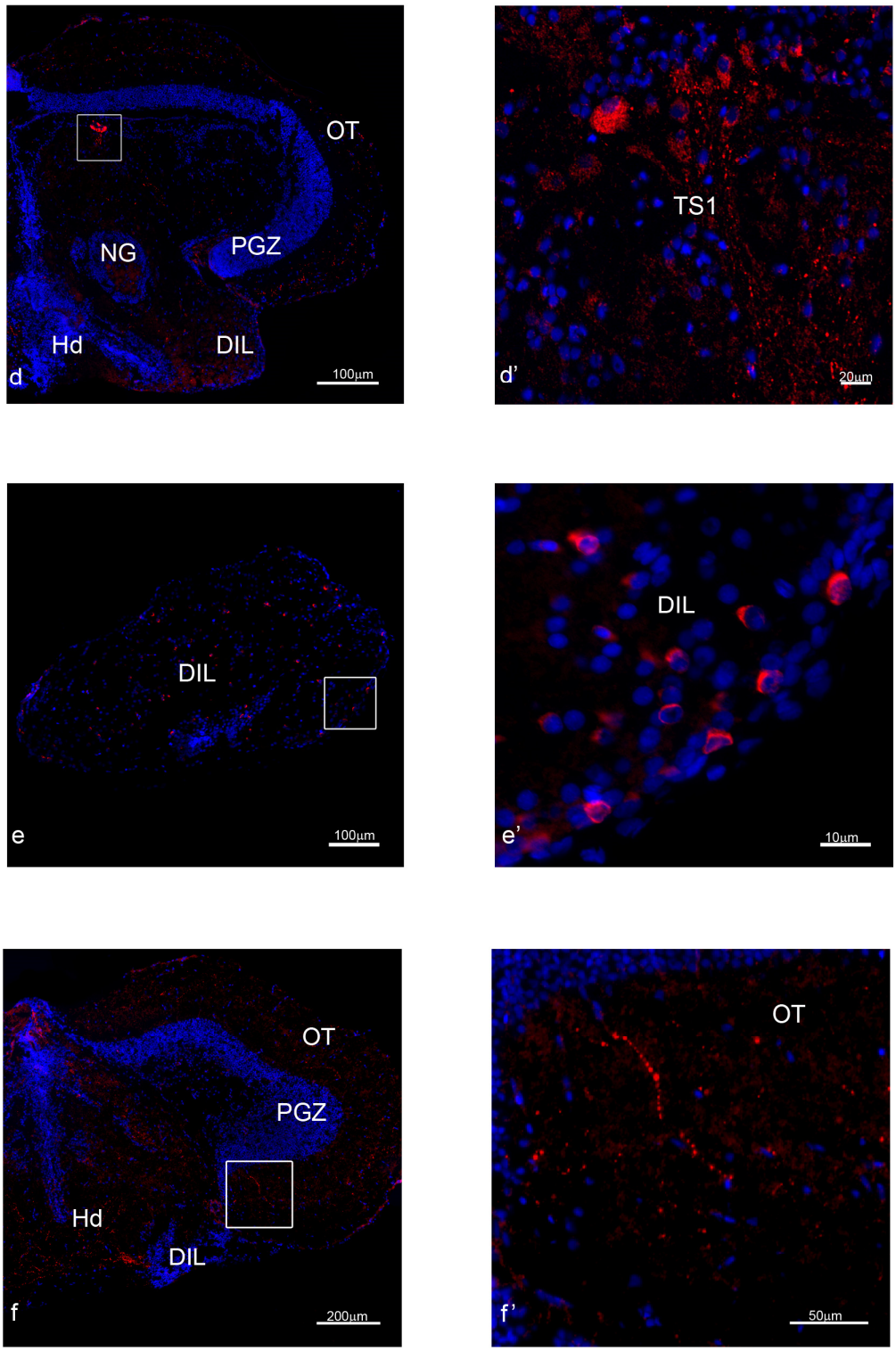

Figure 12. Phosphorylated S6 ribosomal protein localisation (IHC); **a-a')** neurons of magnocellular part of proptic nucleus; **b-b')** neurons of dorsal accessory optic nucleus; **c-c')** neurons of dorsal hypothalamus ; **d-d')** neurons of semicircular tori; **e-e')** neurons of diffuse inferior lobe; **f-f')** fibres in the ventral part of optic tectum. Red: positive neurons and fibres; blue: DAPI nuclear staining dye.

4.3.2. Neuropeptide Y

NPY *in situ* hybridisation

Distribution in the neuroendocrine brain of young fish

Proceeding in craniocaudal direction, Neuropeptide Y (NPY) mRNA positive neurons were detected in the area between posterior diencephalon and the rostral part of the midbrain, in details between the preoptic region and the tuberal hypothalamus. Specifically, positive round neurons were localised in the magnocellular pars of the preoptic nucleus (Fig. 13d-f), smaller neurons around the anterior and medial preglomerular nucleus (13f) and sporadically in ventral, medial and posterior thalamic nucleus (Fig. 13d-h). Moreover, positive neurons were detected in the periventricular nucleus of posterior tuberculum and paraventricular organ (Fig. 13g-l). In the dorsal hypothalamus numerous neurons, characterised by thin but intensively marked cytoplasm, were localised close to the ventricle (Fig. 13g-l). Packed neurons were organised on the basal part of the ventral hypothalamus (Fig. 13g-i) and very intense positive neurons were detected also in the lateral (Fig. 13i), caudal (Fig. 13l) and dorsal parts (Fig. 13g-l) as well as in the anterior tuberal nucleus (Fig. 13h-l). The neurons were intensively positive in the nucleus of posterior recess and around the glomerular nucleus (Fig. 13l-m). Few neurons were labelled in the diffuse inferior lobe of hypothalamus (Fig. 13h, m-o): some elongated ones were disposed mostly around the lateral perimeter and few others more intense stained were localised in the caudal part of the dorsal hypothalamus. Summary of positive nuclei is shown in Tab. 5.

Extra- neuroendocrine regions

Only in MZM strain NPY mRNA positive neurons were distributed in the rostral part of telencephalon, specifically in the optic nerve (Figs. 13l, 14a), and in the dorsal accessory optic nucleus (Figs. 13f-g, 14b). In both strains positive neurons were detected in the optic tectum, specifically in periglomerular grey zone and in the outer layer (Figs. 13g-o, 14c-e). In MZM, more than GRZ, also the external layer of the semicircular tori showed few neurons with probe signal (Figs. 13m, 14f).

Differences during ageing

In the elderly subjects of both strains, thalamic nuclei showed intensely positive large neurons widespread in the anterior and ventro-medial parts (Fig. 15a-b). The neurons of the periglomerular grey zone were positive and intensely distributed along the optic tectum (Fig. 15c). Also the dorsal accessory optic nucleus (Fig. 15d) contained labelled neurons with a rich cytoplasm. The pretectal nucleus, more in its magnocellular than in the parvocellular part, showed high density of stained neuronal populations (Fig. 15e). In the dorsal and caudal hypothalamus, around the recess, the number of positive cell bodies were notably increased compared with the pattern found in the young fish (Fig. 15f). In the diffuse inferior lobe, intense staining was seen in some neurons, almost absent in young subjects, scattered in the medial part and along the margin. Neurons in the central portion of the lobe displays large positive perikarya, those displaced at the margin were smaller.

Differences upon starvation

In young fish brain, after 96 hours of starvation, both magnocellular (Fig. 16a) and parvocellular (Fig. 16b) portions of preoptic nucleus showed intensely labelled neurons. In the ventral hypothalamus (Fig. 16c) dense quantity of elongate neurons was distributed around the basal part and in the dorsal hypothalamus (Fig. 16d-e), positive small neurons were observed. In all layers of the optic tectum (Fig. 16f), many round positive neuronal cells were diffused. In the tuberal nuclei, both posterior and anterior, a packed group of neurons close to the ventricle was present. These pattern were more evident in MZM strain.

NPY Immunohistochemistry

Distribution in the neuroendocrine brain of young fish

In ventral telencephalon (Figs. 13b-c, 17a-b) several fibres were immunolabelled. In the diencephalic region, many immunolabelled neurons with a round shape were detected in the cortical nucleus (Figs. 13e-g, 17c) and some smaller were scattered in the ventral accessory optic nucleus (Fig. 13f-g). Neuronal perikarya with intense immunostaining were observed in the dorsal part of hypothalamus (Figs. 13g-l, 17c) especially in proximity of the ventricle, whereas, few neurons weakly stained were detected at the margin of ventral hypothalamus (Figs. 13g-l, 17c-d). Abundant positive fibres and some scattered neurons were found in the central pretectal

nucleus (Fig. 13j-l). Weakly stained neurons were dispersed in the periventricular nucleus of posterior tuberculum (Fig. 13g-l), surrounded by a dense net of fibres projecting to the ventricle. Strongly immunopositive fibres and many weakly stained neurons were detected in the anterior and posterior parts of tuberal nucleus (Fig. 13h-m). The neurons located in dorsal part of the glomerular nucleus (Figs. 13l-m, 17d) showed stronger immunoreactivity than those in the ventral side. Few large neurons were spread in the medial part of diffuse inferior lobe of hypothalamus (Figs. 13i,l,o, 17e) and some smaller, but more intensely stained were located laterally. Summary of positive neurons and fibres localisation is shown in Tab. 5.

Extra-neuroendocrine regions

In young animals of both strains NPY protein distribution was detected in the telencephalon. In addition, to the neuroendocrine ventral parts, also a homogeneously pattern of stained fibres was found diffuse in the central and lateral zones (Figs. 13a-c, 17a-b, 18a-b). Moreover, numerous fibres projecting in medial-lateral direction were detected in the external layer of the optic tectum, and small spread neurons were labelled in the media-ventral part of periglomerular grey zone (Figs. 13g-m, 17c-d, 18c-d).

Differences during ageing

In the elderly fish, the diencephalic region, particularly the ventral accessory optic nucleus, was disseminated of positive fibres (Fig. 19a). In the ventro-medial thalamic nucleus (Fig. 19b), labelled neurons were displayed close to the ventricle, in the lateral and ventral hypothalamus (Fig.19c) they were surrounded by a considerable amount of projections and at the periphery of the diffuse inferior lobe (Fig. 19d) there were also positive neurons detected in medial part with several fibres around.

Differences upon starvation

The comparison between control and starved young animals didn’t show remarkable differences in the distribution pattern of NPY protein in MZM as well as GRZ strains. In the diencephalon the presence of immunoreactive fibres in preoptic and pretectal nuclei was notable and completely absent in control brains (Fig. 20a). Few projections were also detectable in the optical nerve. In the hypothalamus the main difference was observed in the ventral part (Fig. 20b), where several distinct

projections took an oblique course, from the ventricle part to the preglomerular nucleus (Fig. 20a). Around the glomerular nucleus (Fig. 20c), small neurons were intensely stained and many fibres were marked in its central part. In the diffuse inferior lobe (Fig. 20d) several projections were evident in the area close to the tuberal hypothalamus.

Table 5. NPY protein and mRNA distribution in the main neuroendocrine territories of *N. furzeri* brain. + few; ++ moderately dense; +++ very dense.

	Protein		**mRNA**
	Neurons	Fibres	Neurons
Telencephalon			
Ventral zone of ventral telencephalon (Vv)		++	
Supracommissural zone of the ventral telencephalon (Vs)			
Central part of the ventral telencephalon (Vc)	+++	+++	
Preoptic area			
Suprachiasmatic nucleus (SC)			
Preoptic nucleus, parvocellular part (PPp)			
Preoptic nucleus, magnocellular part (PM)			+++
Dorsal periventricular pretectal nucleus (PPd)			
Ventral periventricular pretectal nucleus (PPv)			
Intermediate superficial pretectal nucleus (SPNi)			
Magnocellular superficial pretectal nucleus (SPNm)			
Parvocellular superficial pretectal nucleus (SPNp)			
Cortical nucleus (CN)	+++	++	
Ventral accessory optic nucleus (VAO)	++	+++	
Central pretectal nucleus (CPN)	++	+++	
Anterior preglomerular nucleus (PGa)			+
Lateral preglomerular nucleus (PGl)			
Medial preglomerular nucleus (PGm)			++

Tuberal hypothalamus			
Dorsal hypothalamus (Hd)	+	+++	++/+
Ventral hypothalamus (Hv)	++		+++
Caudal hypothalamus (Hc)	+	+++	+++
Lateral hypothalamus (Hl)			+++
Anterior tuberal nucleus (TNa)	+	+++	+++
Posterior tuberal nucleus (TNp)	+	+++	
Periventricular nucleus of posterior tuberculum (TPp)	++	++	++
Glomerular nucleus (NG)	+/++		++
Hypothalamic recess (rec)			+++
Nucleus of posterior recess (NRP)			+++
Diffuse inferior lobe of hypothalamus (DIL)	++		
Posterior tubercle			
Paraventricular organ (PVO)			++
Thalamus			
Dorsal posterior thalamic nucleus (DP)			+
Anterior thalamic nucleus (A)			
Central posterior thalamic nucleus (CP)			+
Ventro-medial thalamic nucleus (VM)	+++	+++	+
Intermediate thalamic nucleus (I)			
Ventro-lateral thalamic nucleus(VL)	++	+++	

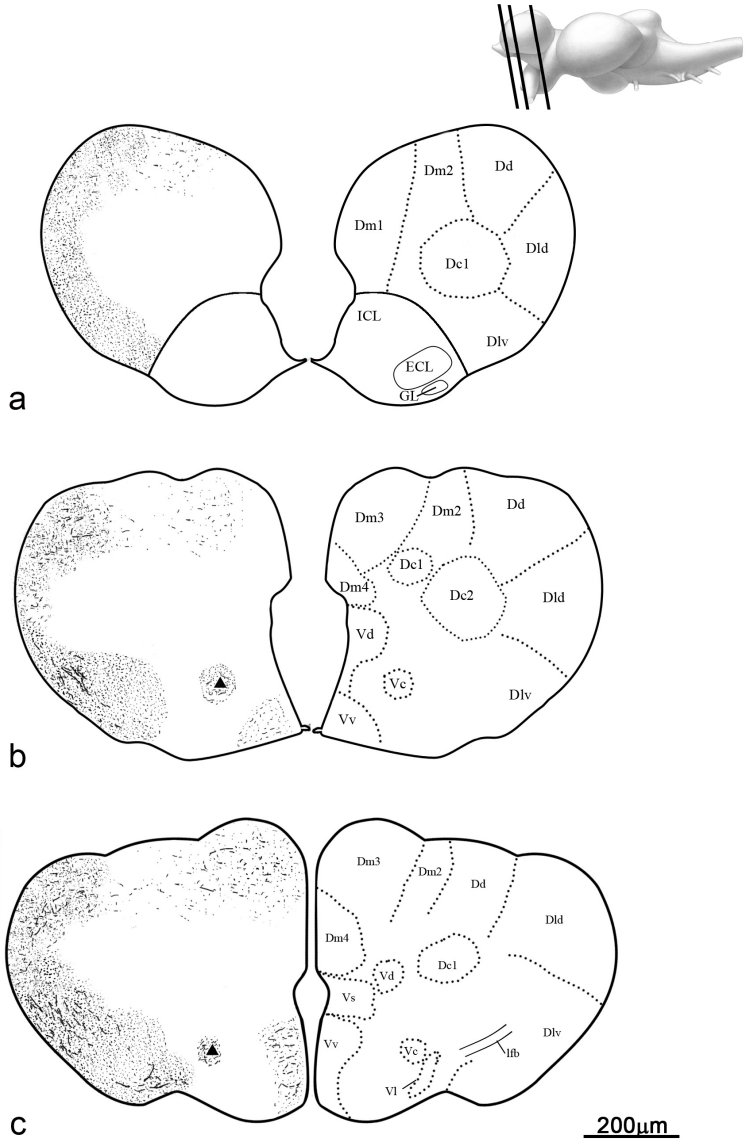

Figure 13. (continued)

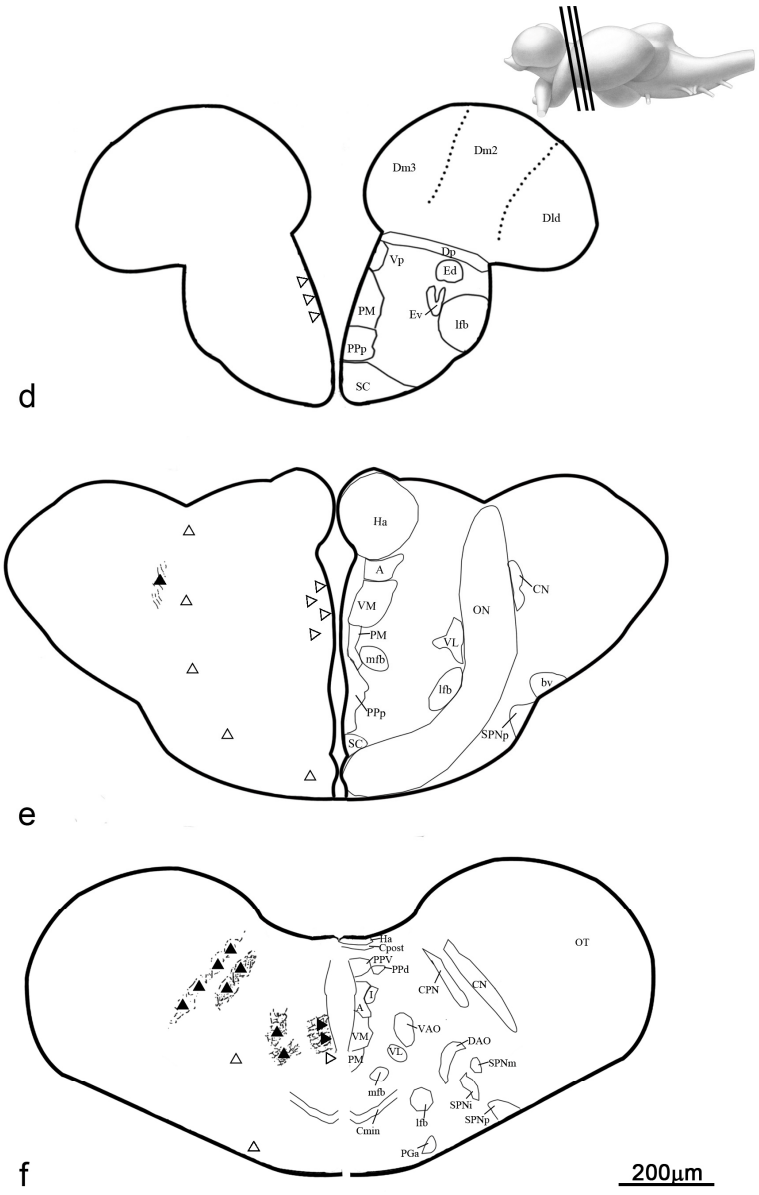

Figure 13. (continued)

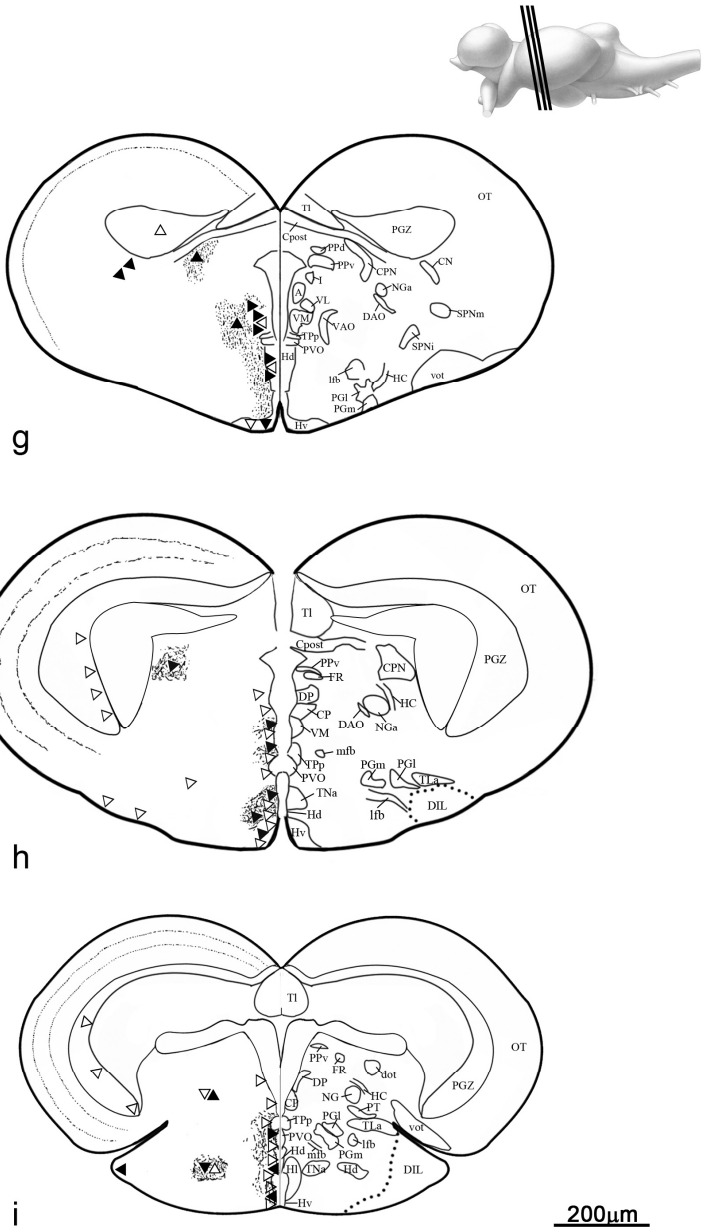

Figure 13. (continued)

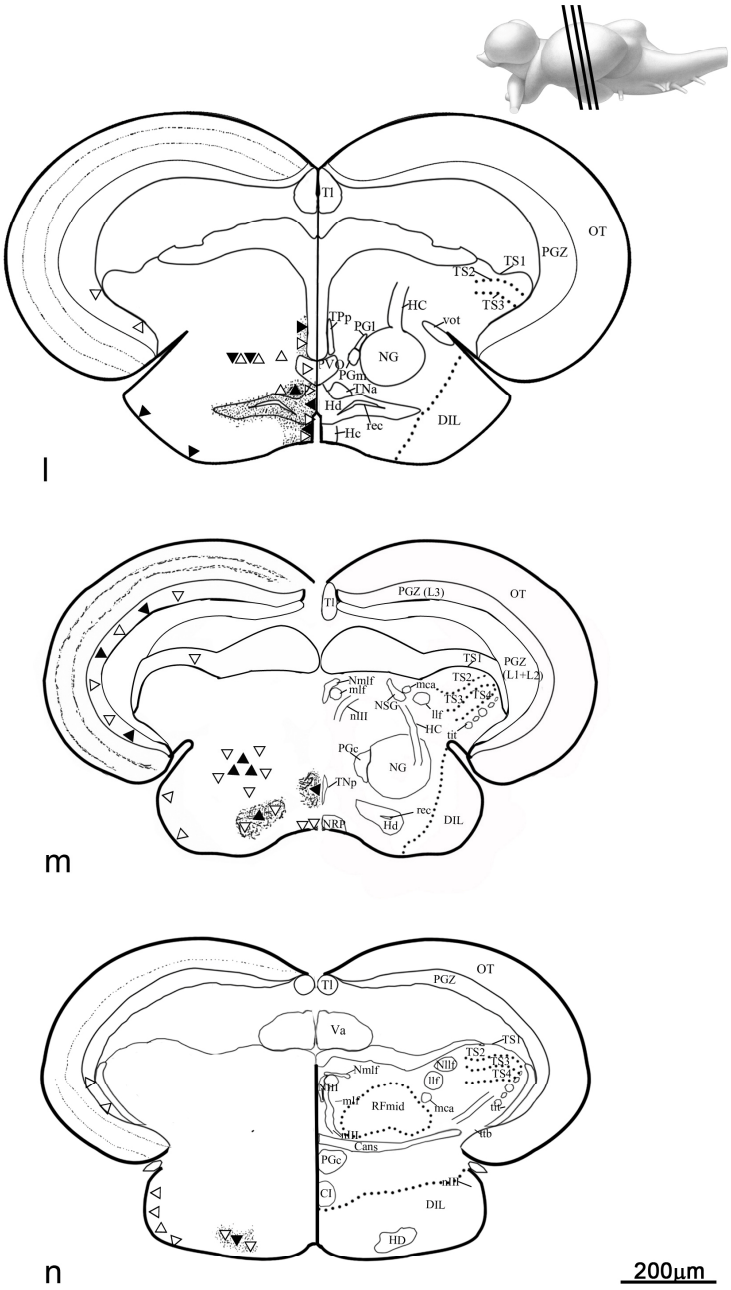

Figure 13. (continued)

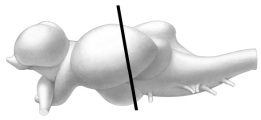

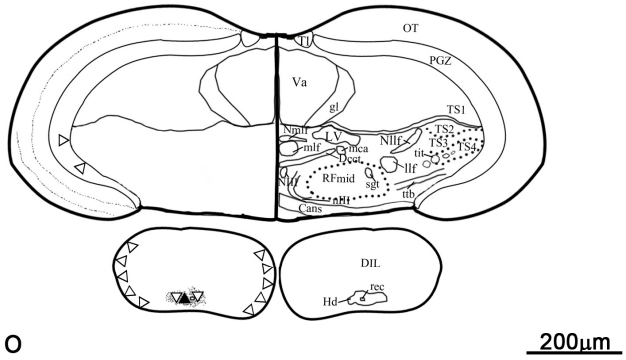

Figure 13. Atlas of NPY gene and protein distribution: white triangles indicate sites of mRNA positive neurons (ISH); black tringles indicate sites of immunopositive neurons (IHC); small dots indicate immunoreactive fibres (IHC); **a-f**) forebrain; **g-o**) midbrain.

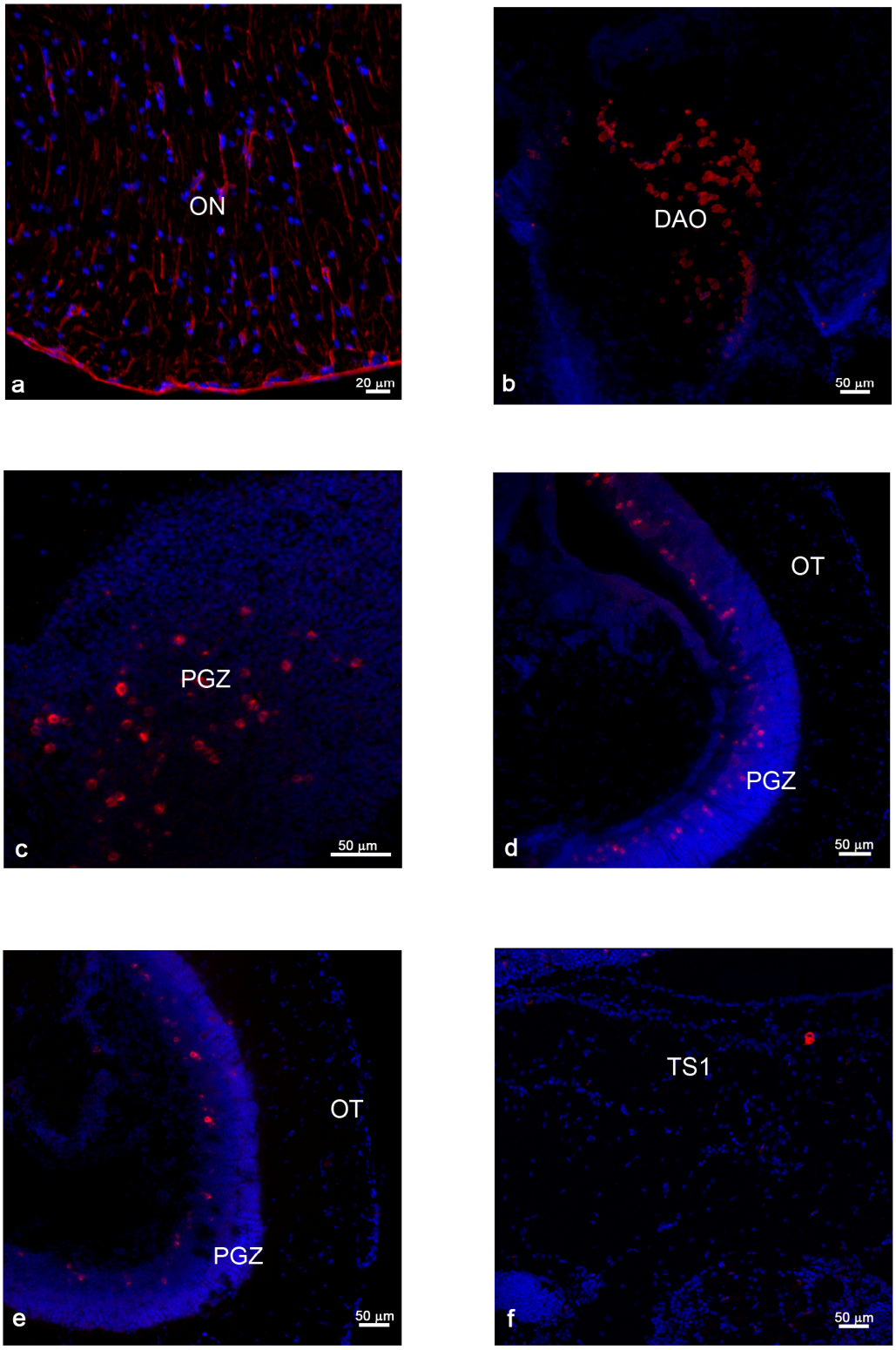

Figure 14. NPY mRNA extra-neuroendocrine localisation between two strains (ISH): **a-d)** MZM; **e-f)** GRZ. Red: positive neurons and fibres; blue: DAPI nuclear staining dye.

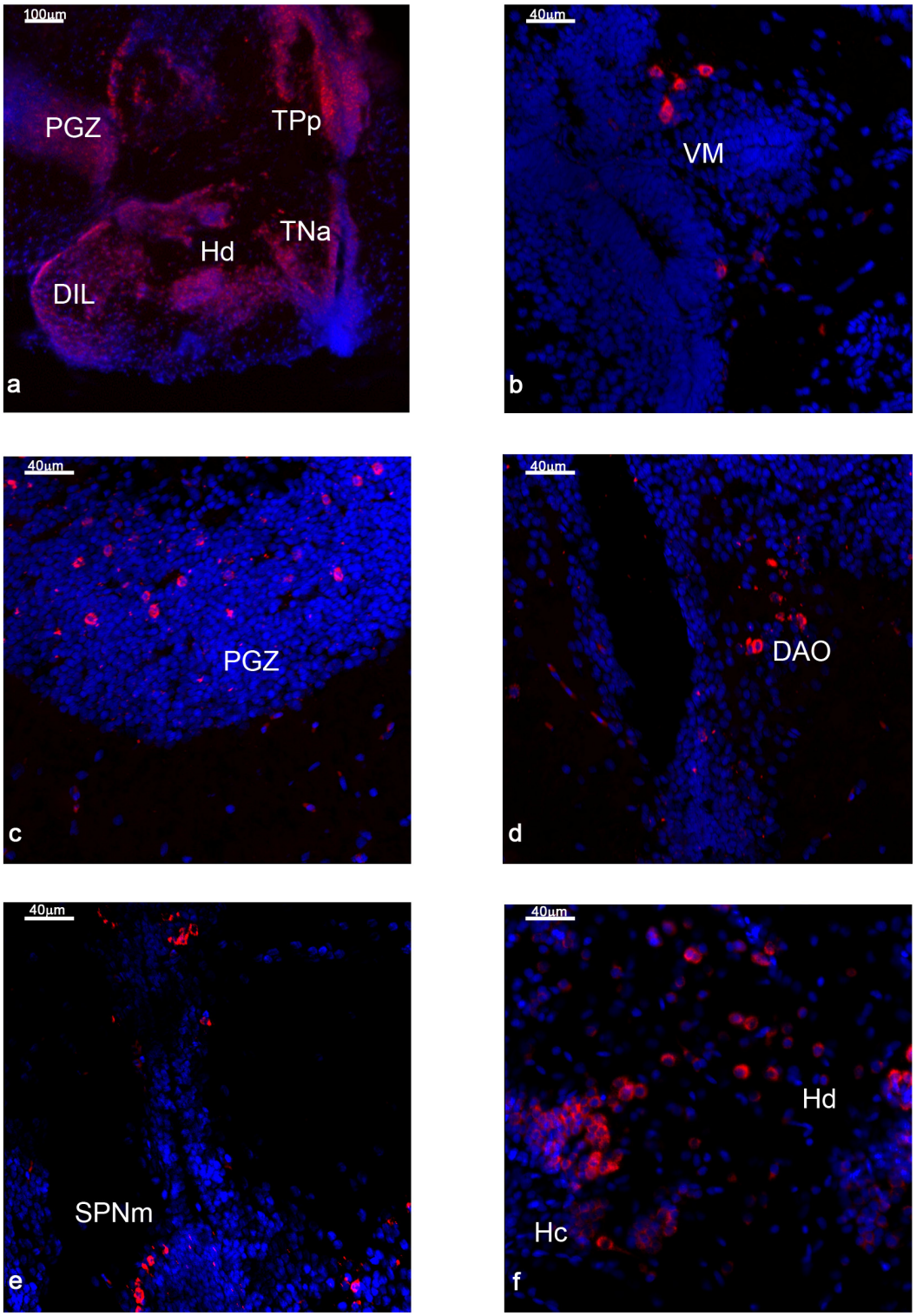

Figure 15. NPY mRNA localisation in elderly subject (ISH): **a)** thalamus and hypothalamus overview; **b)** detail of thalamic nuclei; **c)** neurons distributed in PGZ; **d)** detail of accessory optic tectum; **e)** neurons of magnocellular part of superficial pretectal nucleus; **f)** detail of hypothalamic nuclei. Red**:** positive neurons and fibres; blue: DAPI nuclear staining dye.

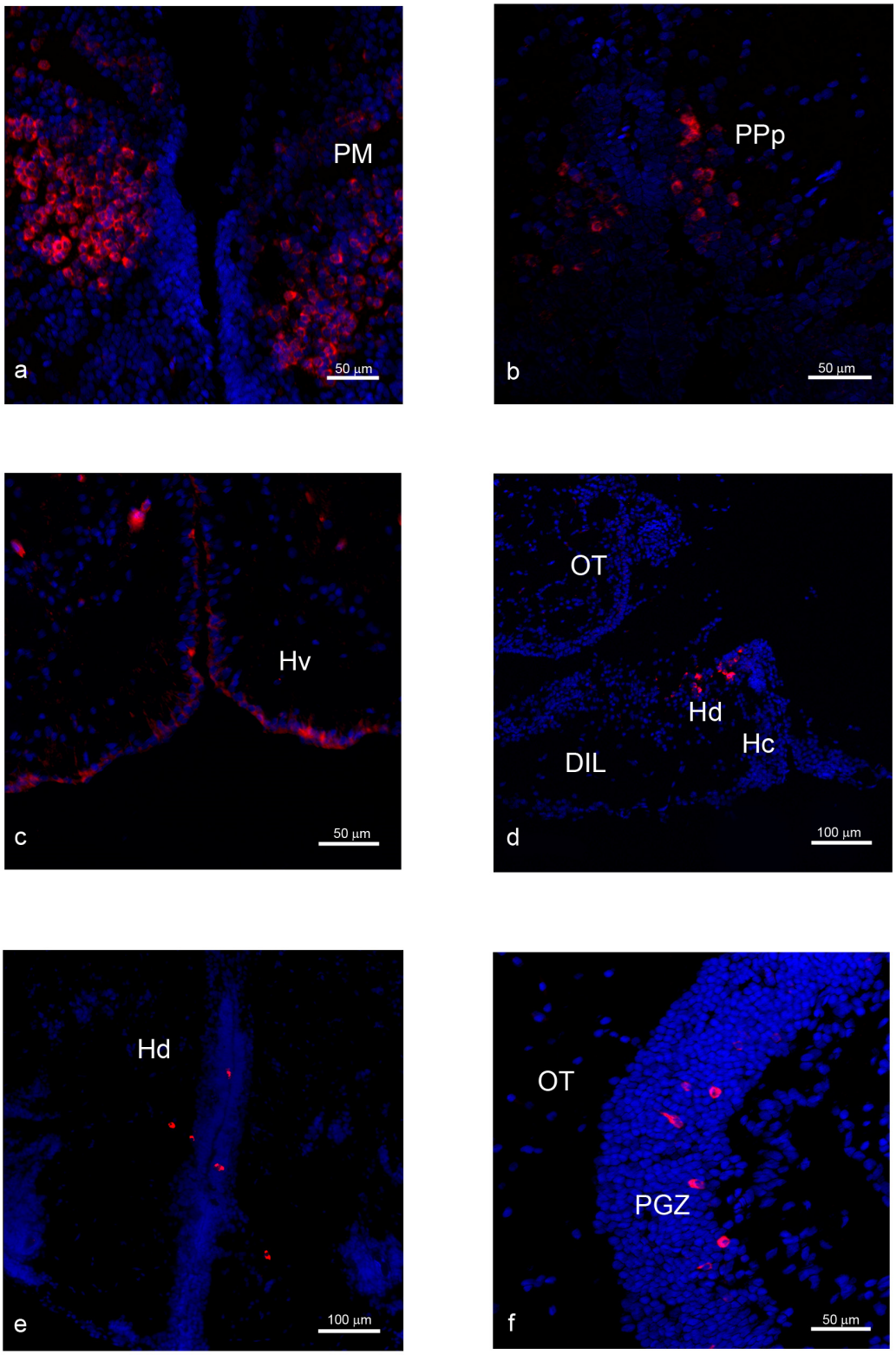

Figure 16. NPY mRNA localisation in fasted subject (ISH): **a-b)** details of magnocellular and parvocellular parts of preoptic nucleus; **c-e)** neurons of ventral and dorsal hypothalamus; **f)** neurons of periglomerular gray zone. Red: positive neurons and fibres; blue: DAPI nuclear staining dye.

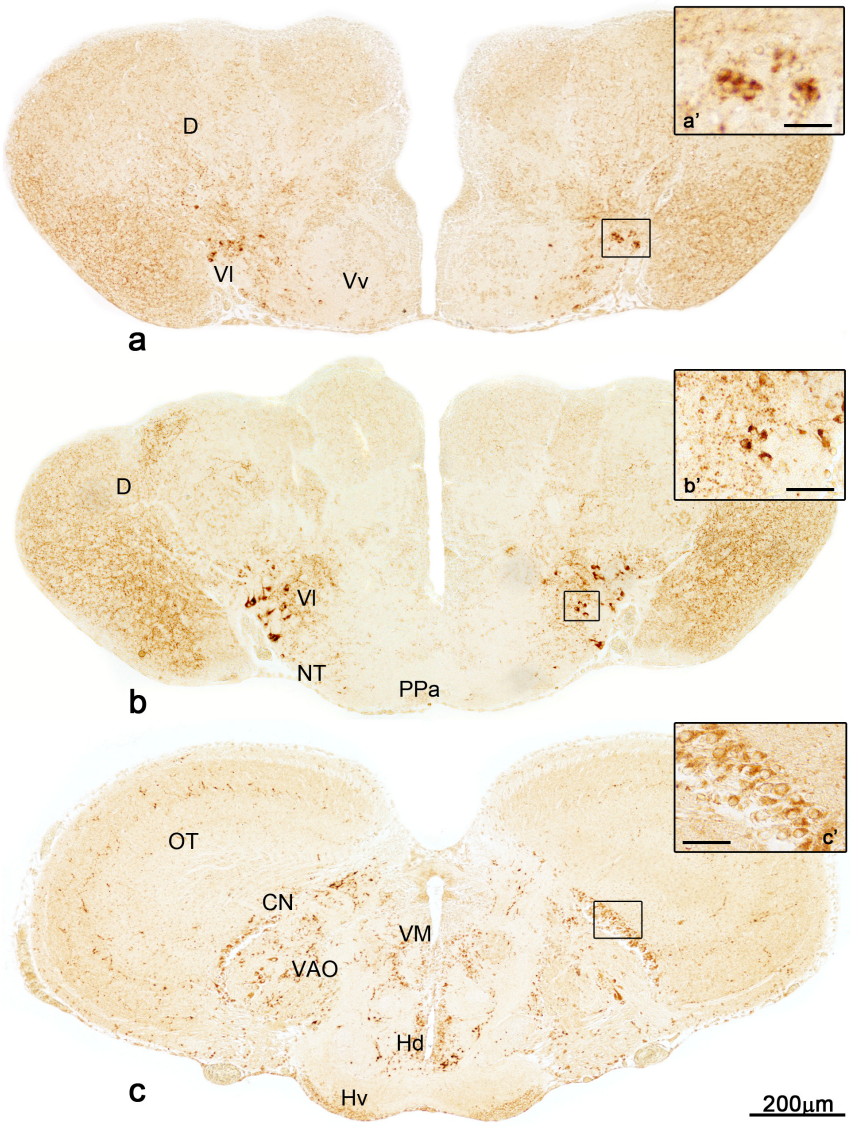

Figure 17. (continued)

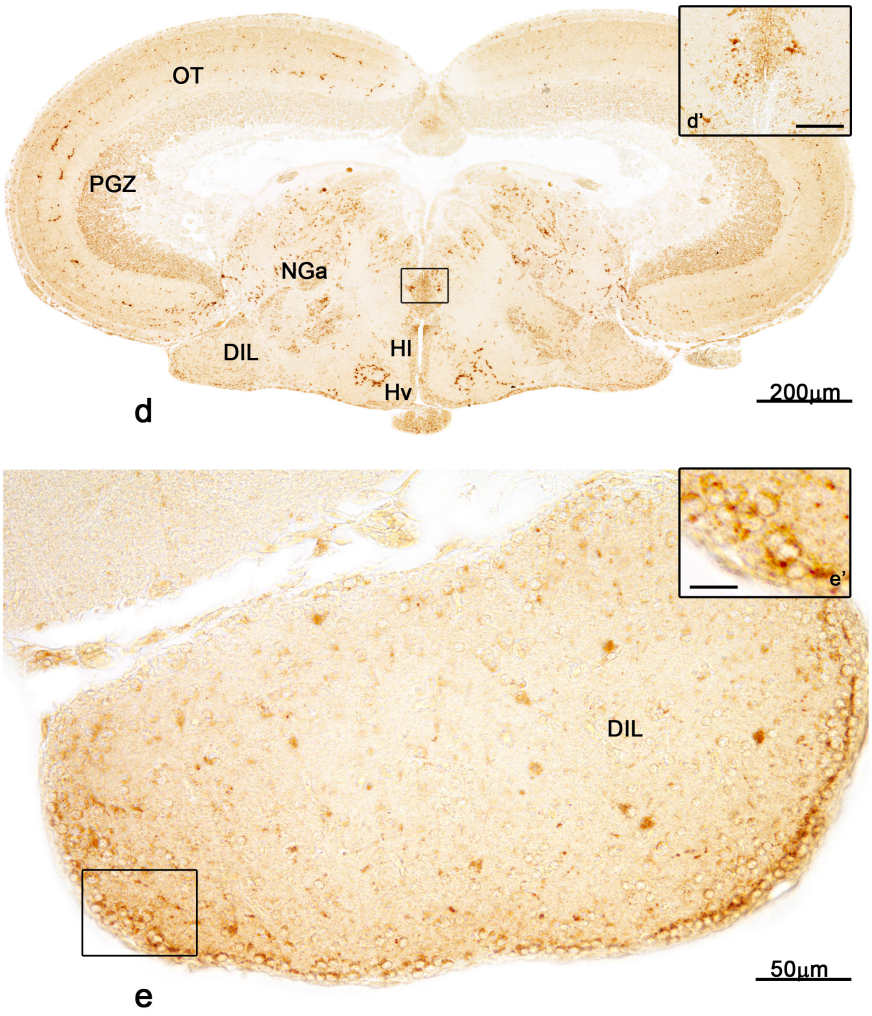

Figure 17. NPY peptide distribution (IHC): **a-c)** telencephalic and preoptic regions; **c-e)** hypothalamic and thalamic regions. DAB staining. High magnification: 25 µm.

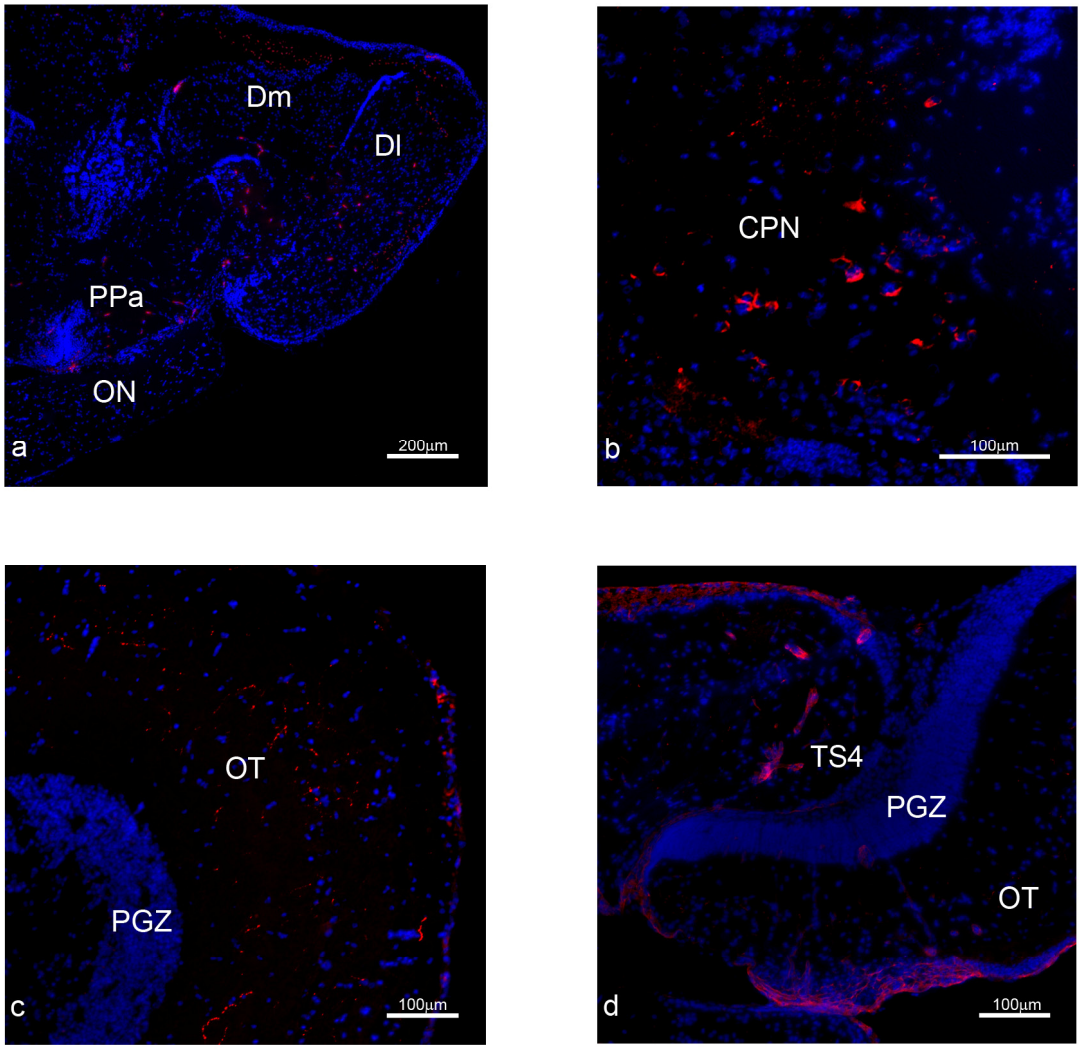

Figure 18. NPY peptide localisation in extra-neuroendocrine regions (IHC): **a)** overiview of the telencephalon; **b)** detail of central pretectal nucleus; **c)** fibres in the optic tectum; **d)** overview of ventral part of optic tectum and semicircular tori. Red: positive neurons and fibres; blue: DAPI nuclear staining dye.

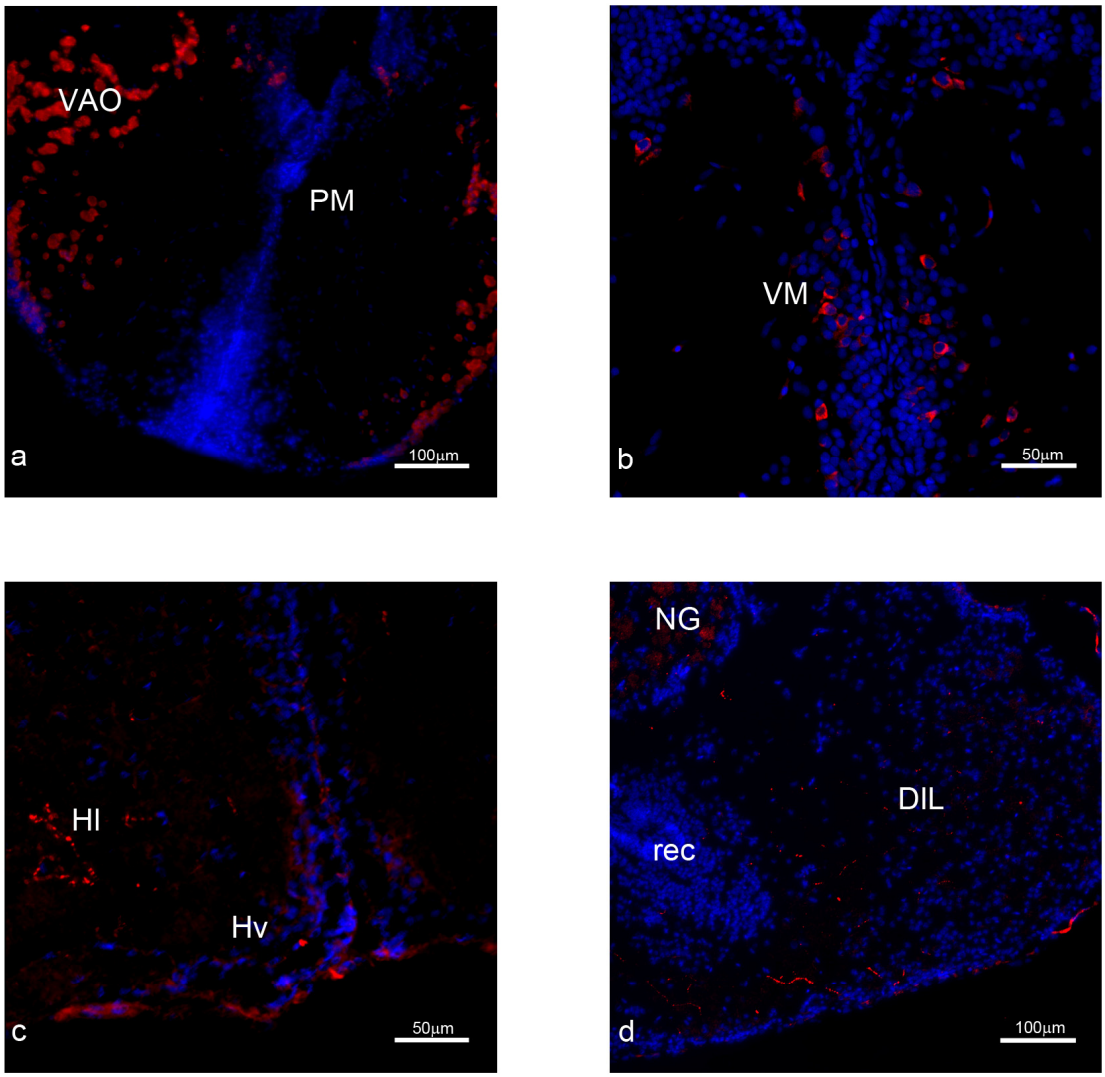

Figure 19. NPY peptide localisation in elderly subject (IHC): **a)** positive neurons in ventral accessory optic nucleus; **b)** detail of thalamic nucleus; **c-d)** ventral hypothalamus and diffuse inferiore lobe. Red: positive neurons and fibres; blue: DAPI nuclear staining dye

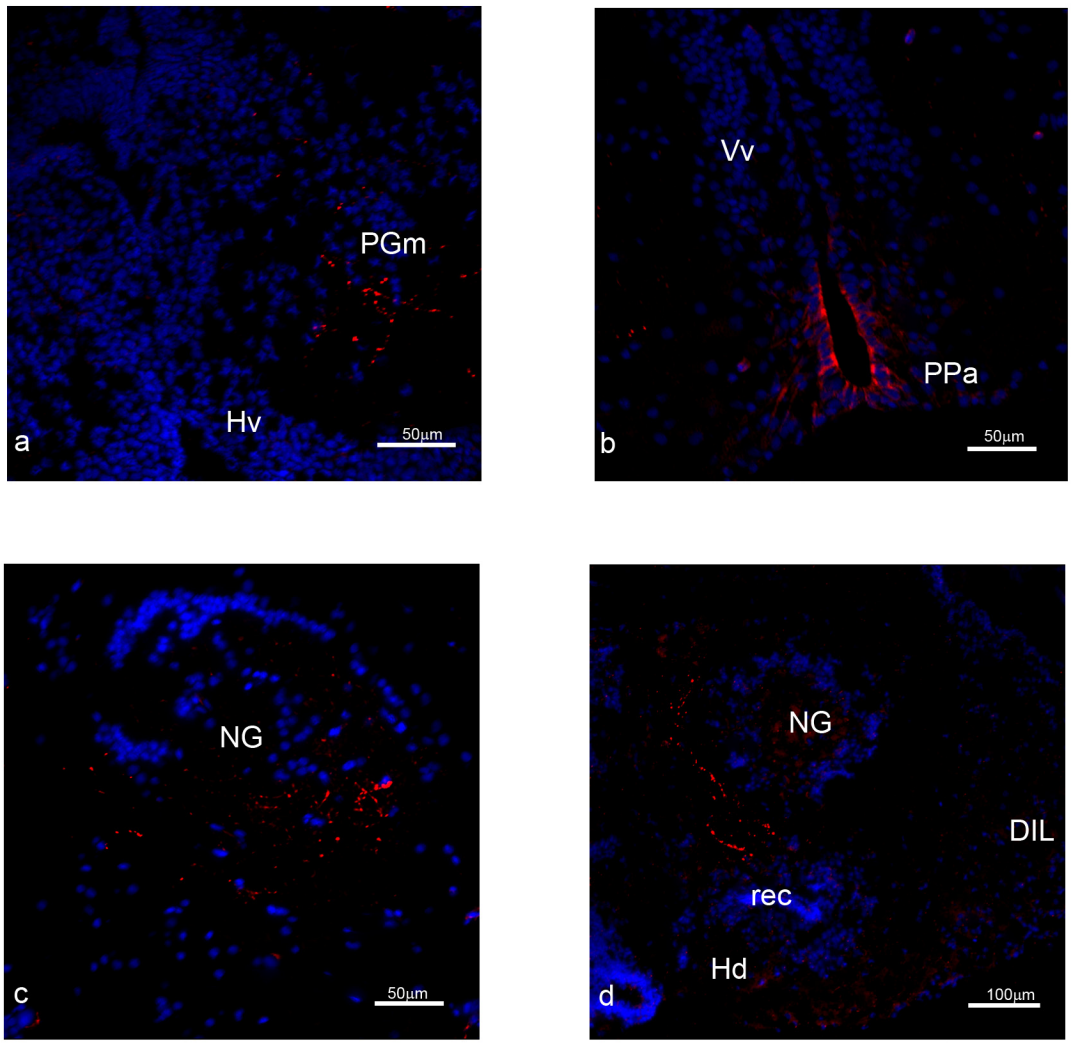

Figure 20. NPY peptide localisation in fasted subject (IHC): **a-b)** details of preglomerular and preoptic nuclei; **c-d)** fibres in glomerular nucleus and in diffuse inferior lobe of hypothalamus. Red: positive neurons and fibres; blue: DAPI nuclear staining dye.

4.3.3. Hypocretin/ Orexin

HCRT *in situ* hybridisation

Distribution in the neuroendocrine brain of young fish

The HCRT mRNA distribution was homologous in MZM and GRZ strains. In the diencephalic region, the pretectal nucleus showed intensely stained neurons in the ventral part and weak label in dorsal part (Fig. 21f-i). Similar expression pattern appeared also in neurons of thalamic nucleus whereas higher intensity was seen in the dorsal, ventro-medial and ventro-lateral parts (Fig. 21f-i). The ventral accessory optic nucleus (Fig. 21f-g) showed scattered labelled neurons. The periventricular nucleus of posterior tuberculum and paraventricular organ (Fig. 21g-l) contained few small positive neurons close to ventricle. In the tuberal hypothalamus, HCRT mRNA distribution differs between the two strains, in fact in GRZ very few neurons were detected. Also, in MZM the dorsal hypothalamus (Fig. 21l-o) showed few neurons with large cytoplasm and remarkable signal close to the ventricle, but the nucleus of posterior recess and diffuse inferior lobe of hypothalamus (Fig. 21m-o) were characterised by many intensely stained neurons, located both in the medial and peripheral parts. Summary of positive nuclei is shown in Tab. 6.

Extra-neuroendocrine regions

In the MZM strain, positive neurons were found also in the external layer of periglomerular zone and in the rest of optic tectum (Figs. 21g-o, 22a). These areas result negative in the strain GRZ.

Differences during ageing

Upon ageing, the two strains showed quite divergent regulation. The elderly MZM animals showed HCRT mRNA localisation in the most cranial portions of the brain. In the strain MZM, the elderly subjects showed positive neurons in areas which were different as in young ones. Specifically, olfactory bulbs (Fig. 22b) of the old fish were rich of small round neurons, mostly located around the external perimeter. In addition, in the telencephalon in *sensu strictu,* positive neurons were found in the dorsal part (Fig. 22c). The hypothalamic nuclei (Fig. 22d) showed less positive neurons in old subjects compared ton young. Those differences between juvenile and aged fish were not visible in GRZ.

Differences upon starvation

In the young fish of MZM strain, after starvation a higher amount of positive neurons was found in dorsal hypothalamus (Fig. 22e) and some positive ones in lateral preglomerular nucleus (Fig. 22f).

ORX-A Immunohistochemistry

Distribution in the neuroendocrine brain of young fish

The immunoreactivity to orexin A (ORX-A) was detected in neurons and some fibres of the ventral telencephalon (Fig. 21a-c). Positive neurons were detected in the parvocellular part of the preoptic nucleus and pretectal nucleus (Figs. 21d, 23a). Moreover, many neurons were labelled in cortical nucleus (Figs. 21e-g, 23a), in ventral accessory optic nucleus (Fig. 21f-g), in anterior and ventro-medial thalamic nucleus and along the ventricle (Fig. 21h-l). Few positive neurons were observed in lateral and anterior part of dorsal hypothalamus; some large neurons were instead scattered in the caudal part (Figs. 21h-l, 23b-c). Strongly positive neurons characterised the diffuse inferior lobe of the hypothalamus, along the external perimeter (Figs. 21h-o, 23c-d'). Positive neurons were found in the paraventricular organ (Figs. 21g-l, 23c) and in the glomerular nucleus (Figs. 21l-m, 23c). The distribution of the protein is homologous between the two strains MZM and GRZ and in both was restricted to neuroendocrine parts of the brains. Summary of positive neurons and fibres localisation is shown in Tab. 6.

Differences during ageing

Independently from the strain, elderly subjects showed very rare positive staining in all neuroendocrine regions of the brain. Few neurons (in the order of 2-3 cells) were detected in the dorsal hypothalamus (Fig. 24a-b), located close to the ventricle. Some widespread fibres were seen in the medial part of the diffuse inferior lobe of hypothalamus (Fig. 24c-d).

Differences upon starvation

The starvation led to visible effects on ORX-A protein distribution in the tuberal hypothalamus, especially in MZM strain. Particularly positive neurons and a certain amount of fibres were detected in the dorsal, ventral and caudal hypothalamus (Fig. 25a-c) of starved fish, higher than controls. In addition, big round immunoreactive

neurons were widespread in diffuse inferior lobe of hypothalamus (Fig. 25d) and numerous smaller ones were displayed along the margins.

Table 6. HCRT/ ORX-A protein and mRNA distribution in the main neuroendocrine territories of *N. furzeri* brain. + few; ++ moderately dense; +++ very dense.

	Protein		**mRNA**
	Neurons	Fibres	Neurons
Telencephalon			
Ventral zone of ventral telencephalon (Vv)	+	++	
Sopracommissural zone of the ventral telencephalon (Vs)	+		
Central part of the ventral telencephalon (Vc)			
Preoptic area			
Suprachiasmatic nucleus (SC)			
Preoptic nucleus, parvocellular part (PPp)	++	+	
Preoptic nucleus, magnocellular part (PM)			
Dorsal periventricular pretectal nucleus (PPd)			+
Ventral periventricular pretectal nucleus (PPv)			++
Intermediate superficial pretectal nucleus (SPNi)	+	++	
Magnocellular superficial pretectal nucleus (SPNm)	+	++	
Parvocellular superficial pretectal nucleus (SPNp)	+	++	
Cortical nucleus (CN)	+++		
Ventral accessory optic nucleus (VAO)	++		++
Central pretectal nucleus (CPN)			
Anterior preglomerular nucleus (PGa)			
Lateral preglomerular nucleus (PGl)			
Medial preglomerular nucleus (PGm)			

Tuberal hypothalamus			
Dorsal hypothalamus (Hd)	+		++
Ventral hypothalamus (Hv)			
Caudal hypothalamus (Hc)			
Lateral hypothalamus (Hl)	+		
Anterior tuberal nucleus (TNa)			
Posterior tuberal nucleus (TNp)			
Periventricular nucleus of posterior tuberculum (TPp)			+
Glomerular nucleus (NG)	+++		
Hypothalamic recess (rec)	++		
Nucleus of posterior recess (NRP)			++
Diffuse inferior lobe of hypothalamus (DIL)	+++	++	++
Posterior tubercle			
Paraventricular organ (PVO)	++		+
Thalamus			
Dorsal posterior thalamic nucleus (DP)			
Anterior thalamic nucleus (A)	++		++
Central posterior thalamic nucleus (CP)			
Ventro-medial thalamic nucleus (VM)	++		++
Intermediate thalamic nucleus (I)			+
Ventro-lateral thalamic nucleus(VL)			++

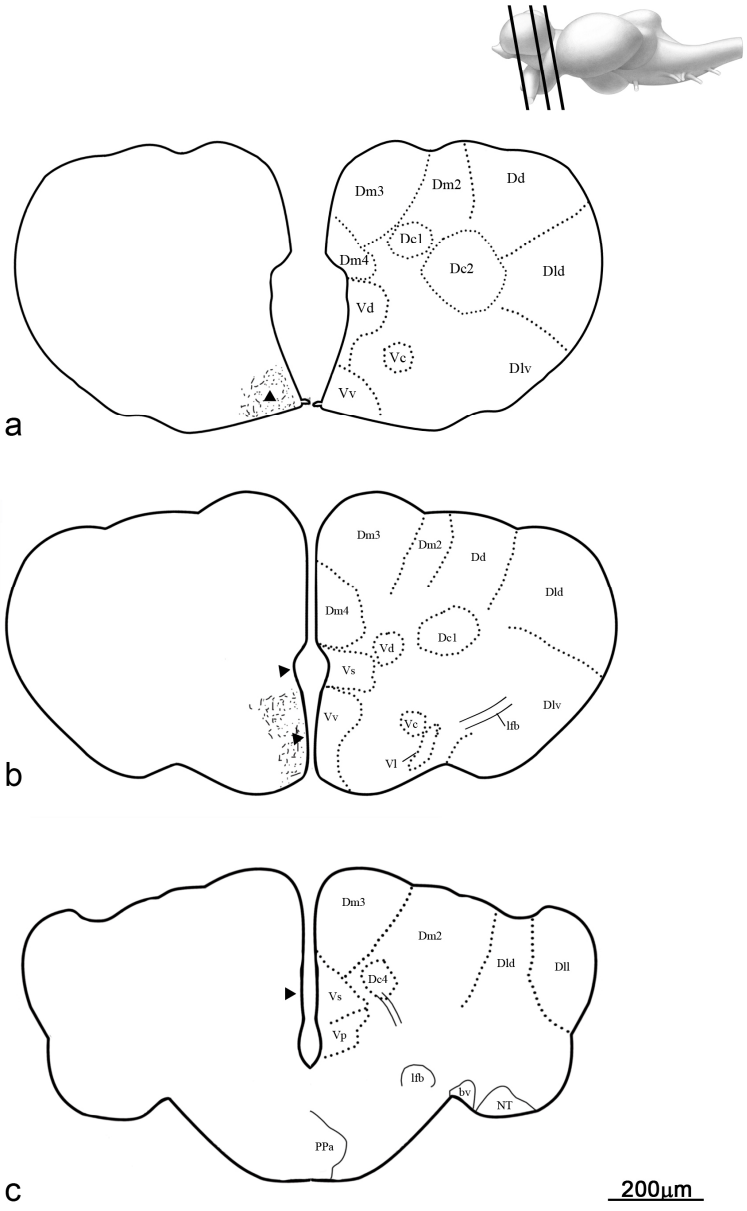

Figure 21. (continued)

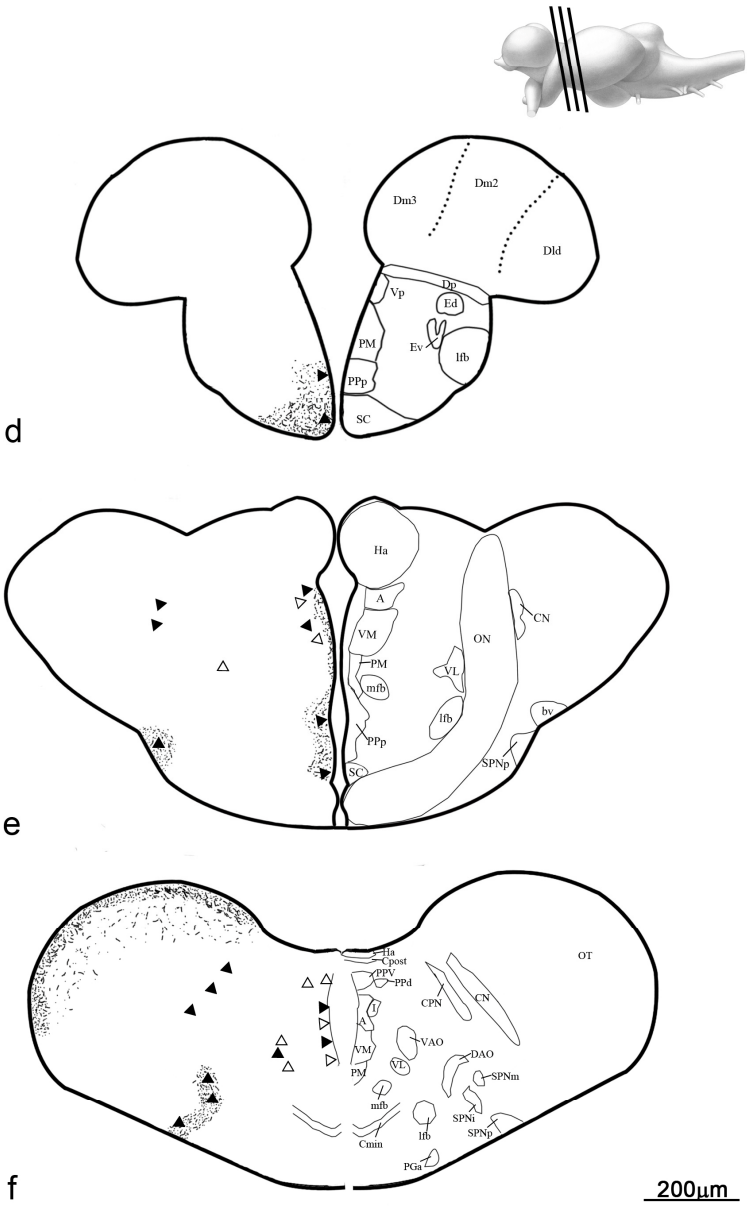

Figure 21. (continued)

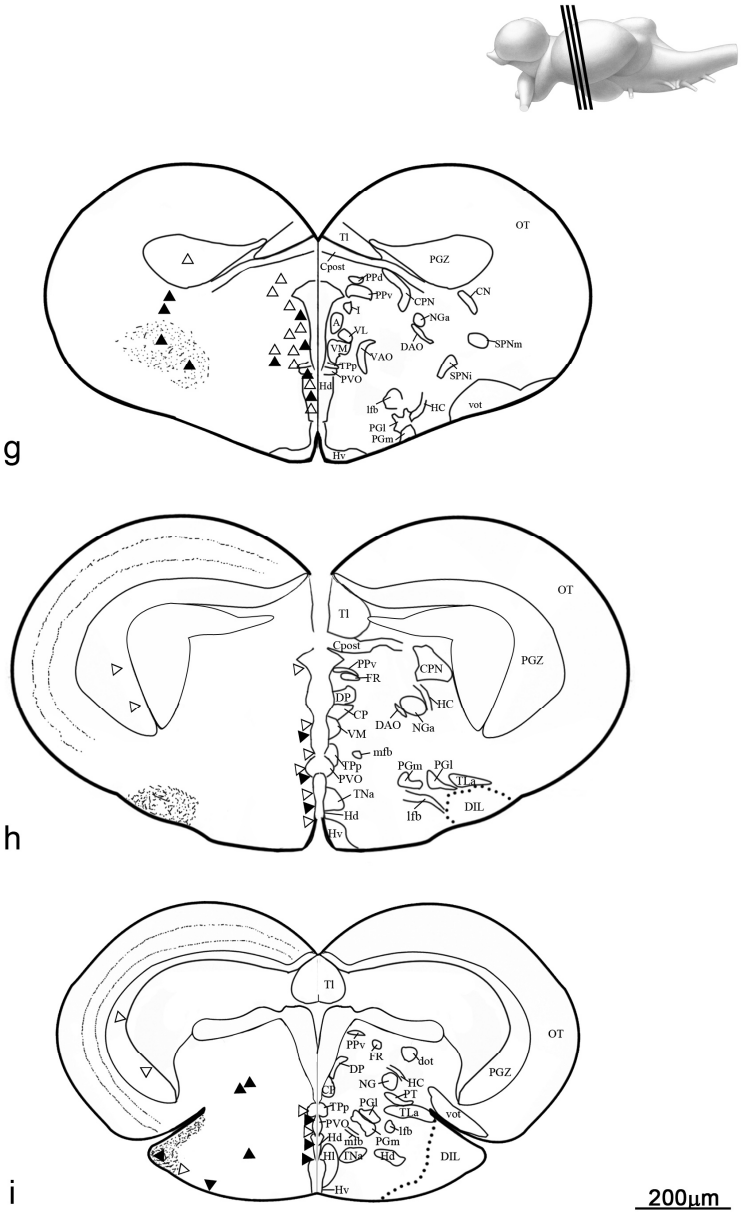

Figure 21. (continued)

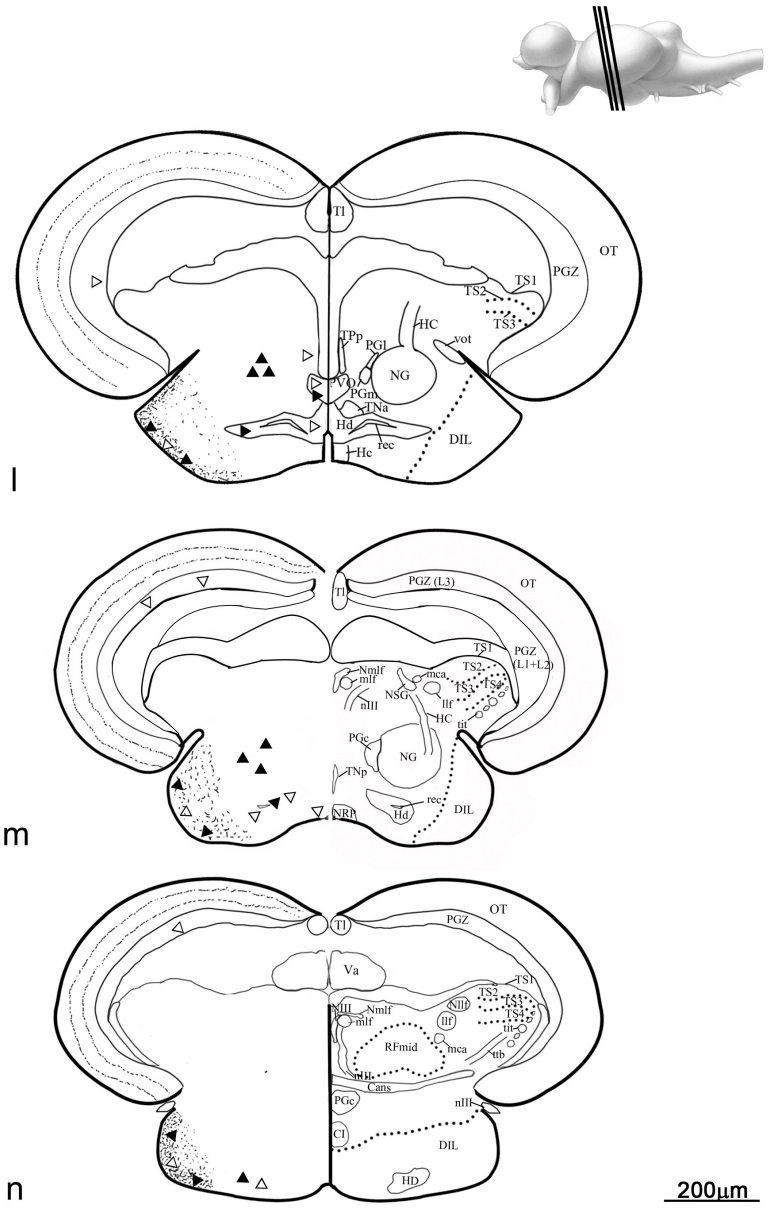

Figure 21. (continued)

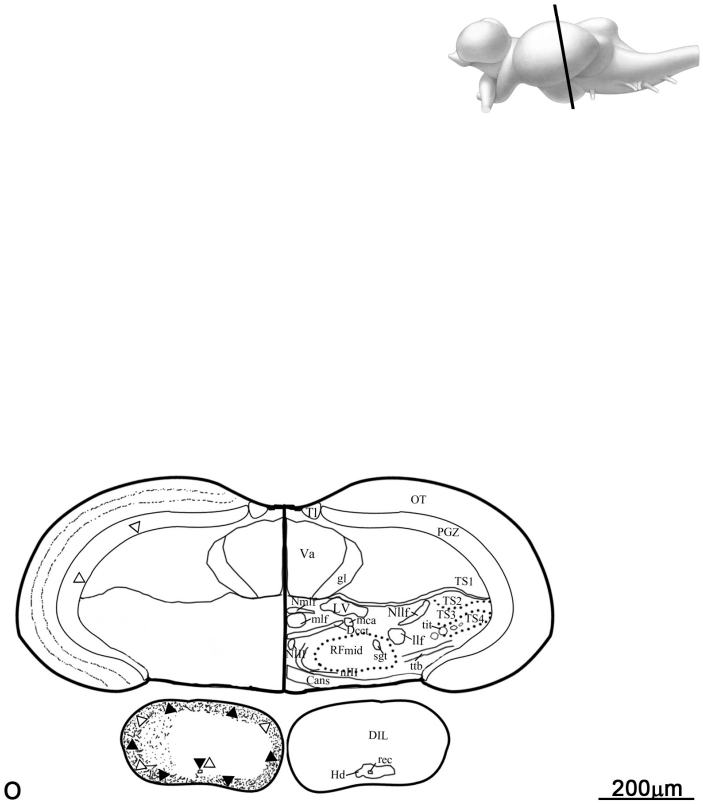

Figure 21. Atlas of HCRT/ORX-A gene and protein distribution: white triangles indicate sites of mRNA positive neurons (ISH); black tringles indicate sites of immunopositive neurons (IHC); small dots indicate immunoreactive fibres (IHC); **a-f**) forebrain; **g-o**) midbrain.

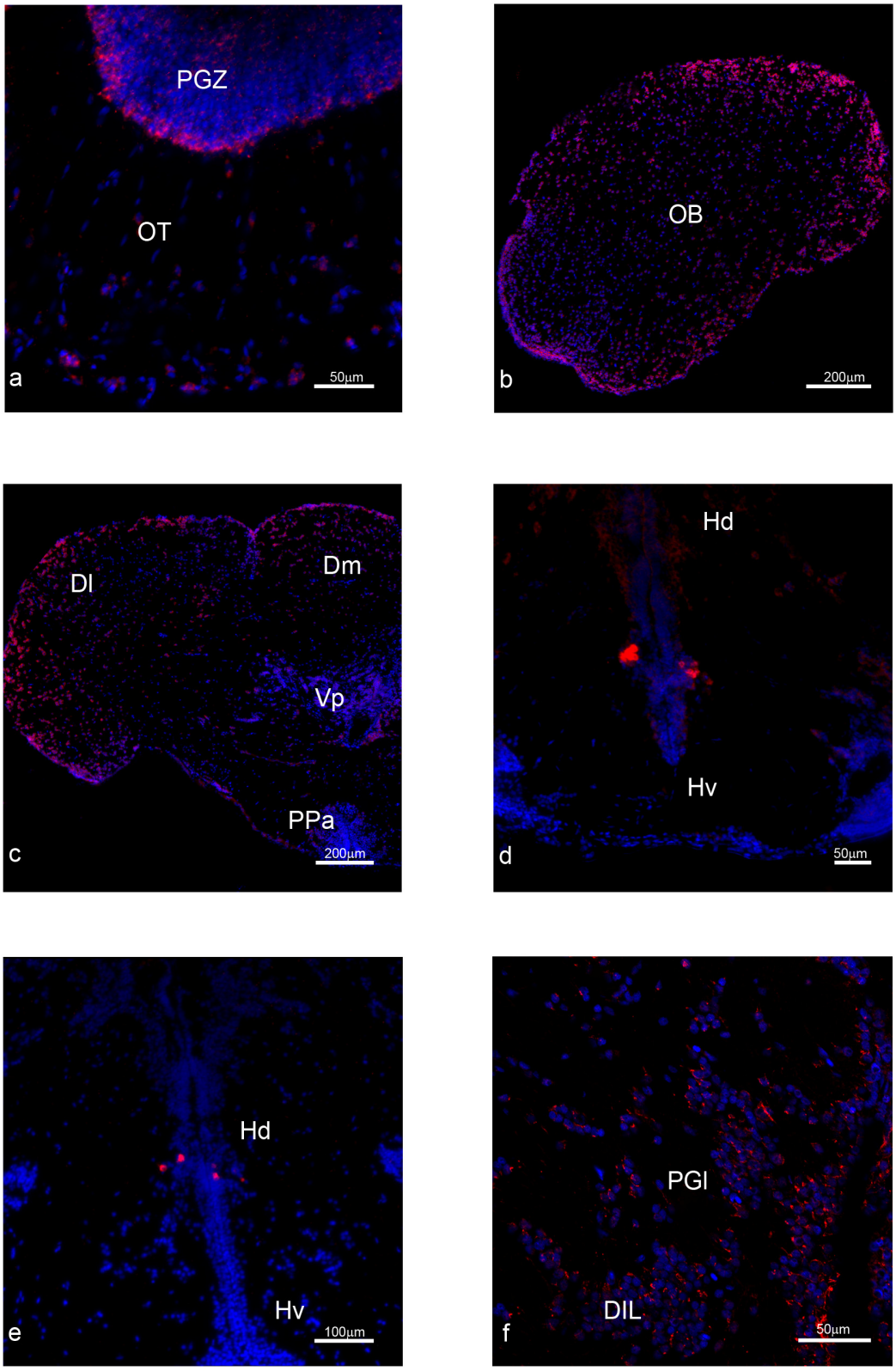

Figure 22. HCRT mRNA localisation (ISH): **a)** extra-neuroendocrine region in young MZM control (PGZ-OT); **b-c)** details of extra-neuroendocrine regions in elderly subject: **b)** olfactory bulbs, **c)** telencephalon; **d)** low positive neurons in dorsal hypothalamus in elderly subject; **e-f)** details of fasted subject: high signal in dorsal hypothalamus and lateral preglomerular nucleus. Red neurons and fibres; blue: DAPI nuclear staining dye.

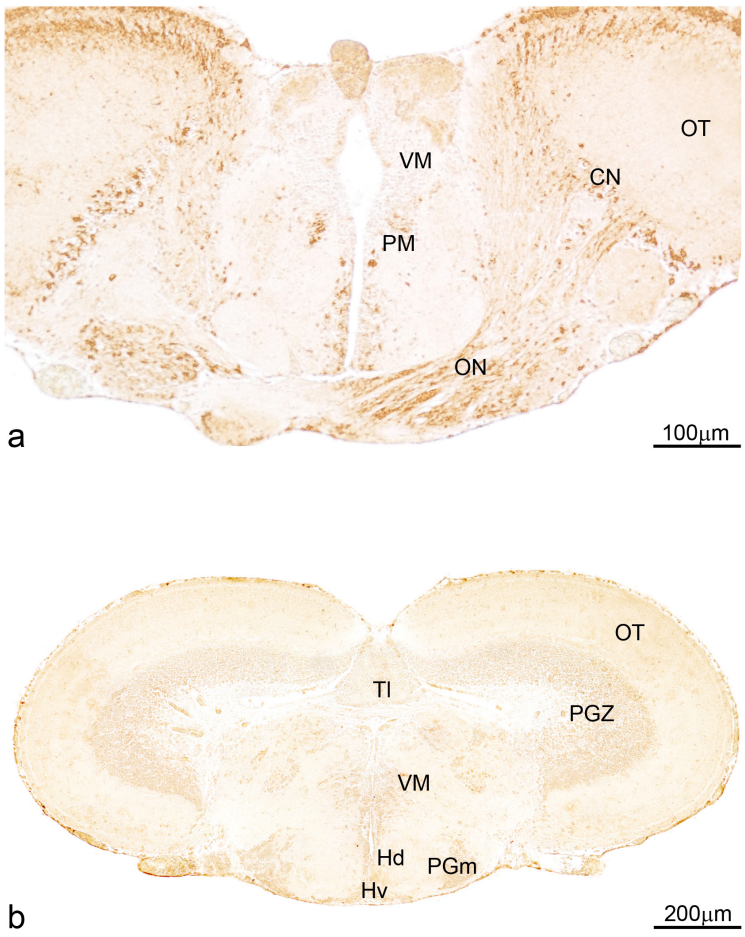

Figure 23. (continued)

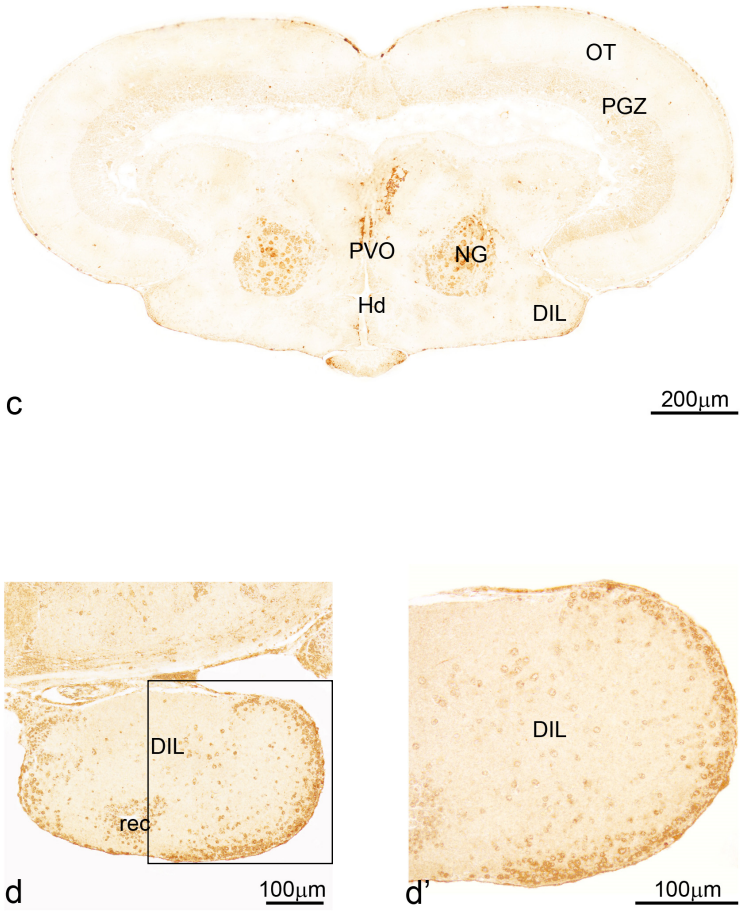

Figure 23. ORX-A peptide distribution (IHC): **a)** preoptic region; **b-c)** thalamic and hypothalamic regions; **d)** diffuse inferior lobe of hypothalamus. DAB staining.

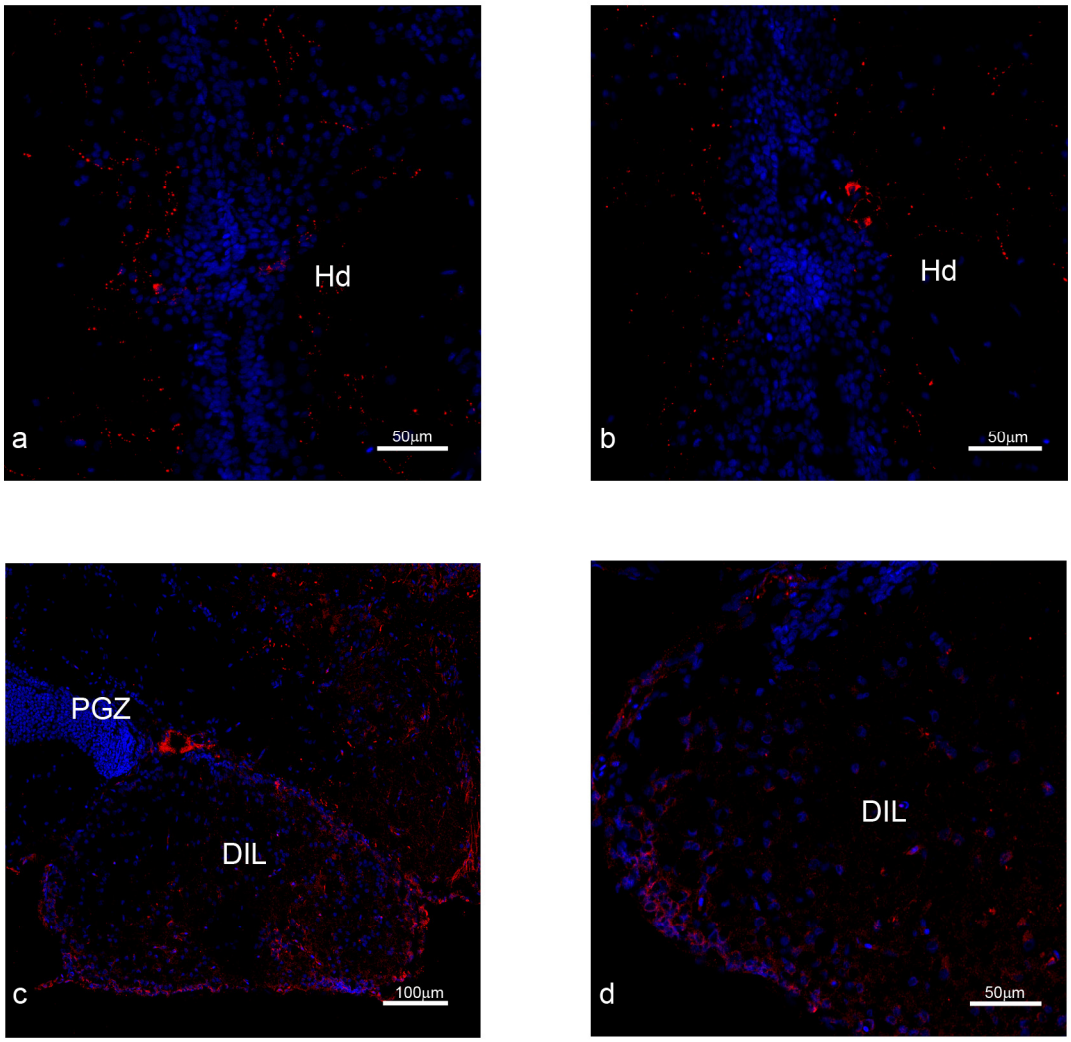

Figure 24. ORX-A peptide localisation in elderly subject (IHC): **a-b)** dorsal hypothalamus**; c-d)** diffuse inferior lobe of hypothalamus. Red: positive neurons and fibres; blue: DAPI nuclear staining dye.

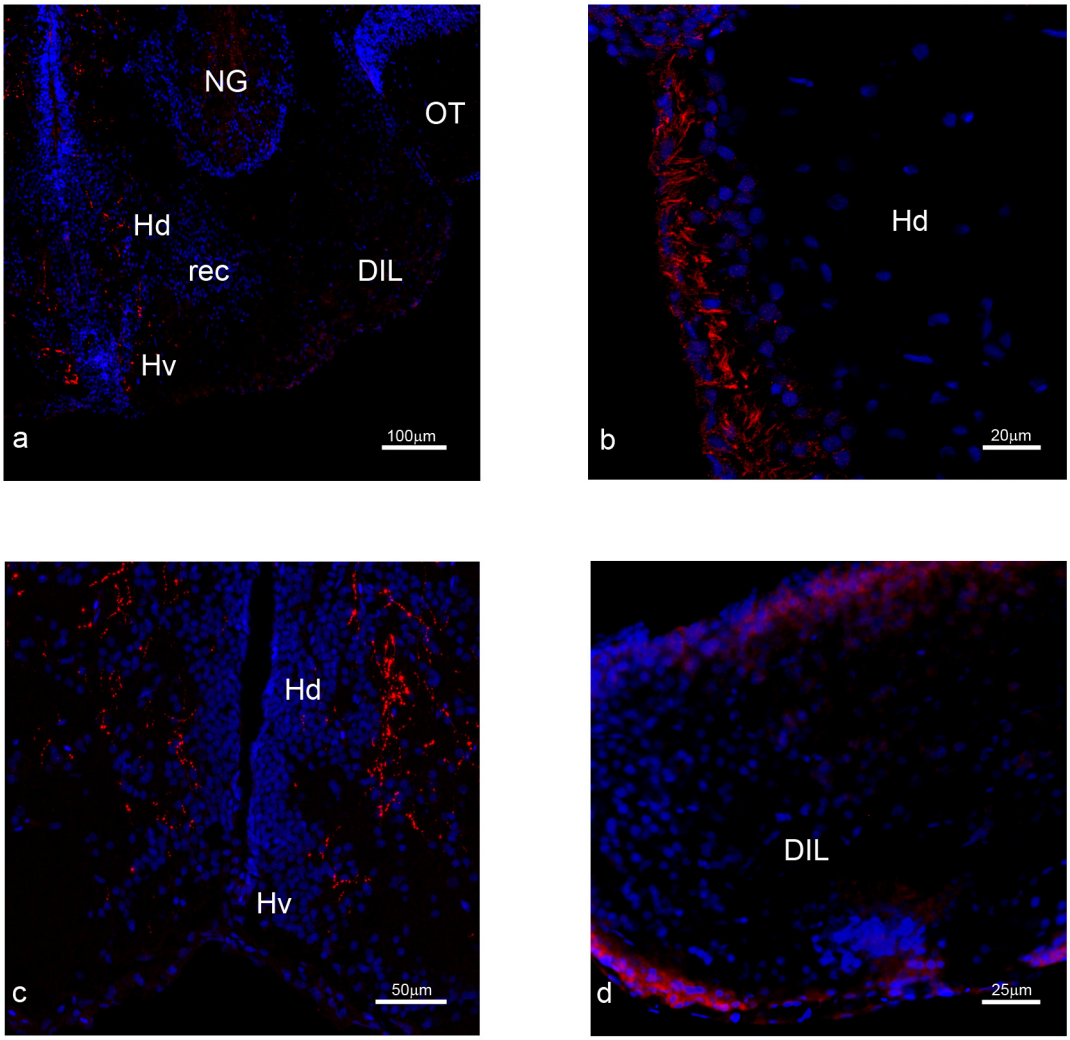

Figure 25. ORX-A peptide localisation in fasted subject (IHC): **a-c)** dorsal, ventral and caudal hypothalamus; **d)** diffuse inferior lobe. Red: positive neurons and fibres; blue: DAPI nuclear staining dye.

4.3.4. Nucleobindin-2/ Nesfatin-1

NUCB2 *in situ* hybridisation

Distribution in the neuroendocrine brain of young fish

Nucleobindin-2 mRNA (NUCB2) precursor was expressed in the forebrain, particularly in the diencephalon. Labelled neurons with a big round cytoplasm were detected in the cortical nucleus (Figs. 26e-g, 29c-c'). Positive neurons were displayed in the ventro-medial thalamic nucleus (Fig. 26e-h), in the paraventricular organ (Fig. 26g-l) and also the posterior tubercle (Fig. 26g-l), along the ventricle. Labelled neurons were found in the dorsal and ventral part of hypothalamus (Figs. 26g-l, 29d-d'), close to the ventricle. Also, small and intensely positive neurons were detected in the diffuse inferior lobe of hypothalamus (Figs. 26n-o, 29b). No differences were noticed between MZM and GRZ strains. Summary of positive nuclei is shown in Tab. 7.

Extra-neuroendocrine regions

In young control fish of both strains, positive neurons were detected along the margin of the dorsal telencephalon (Figs. 26a-c, 27a, 29a). Big amount of packed neurons, with a thin layer of cytosol, were labelled in the periglomerular grey zone of optic tectum (Figs. 26g, 27b).

Differences during ageing

In the elderly fish of both strains, less positive neurons were detected along the margin of the dorsal telencephalon (Fig. 28a), compared with those positive in young subjects, as described above. In the diencephalon, some positive neurons were detected in the periventricular nucleus of posterior tuberculum (Fig. 28b). Also, many packed positive neurons were observed in hypothalamic region, particularly in dorsal, ventral and especially in the caudal parts (Fig. 28c). Moreover, in old animals many neurons were positively stained in the nucleus of posterior recess, in contrary in young subjects no positive cells were found (Fig. 28d).

Differences upon starvation

No differences were found comparing control animals with starved ones of both strains.

Nesfatin-1 Immunohistochemistry

Distribution in the neuroendocrine brain of young fish

Immunoreactivity to the nesfatin-1 (NUCB2) protein was found in the ventral telencephalon and diencephalon of *N. furzeri*. In the telencephalic ventral areas abundant positive fibres, especially in sopracommisural zone, were observed (Fig. 26c). In the diencephalon, positive neurons were detected in the magno- and parvocellular parts of the preoptic nucleus (Figs. 26d-f, 30a). Also, many neurons enveloped in a tight net of projections were visible in the cortical nucleus (Fig. 26e-g), preglomerular nucleus, especially in its medial part (Fig. 26g), pretectal nucleus (Fig. 30b), as well as in the paraventricular organ (Figs. 26g-l, 30d). A big amount of labelled neurons, with a notable quantity of fibres surrounding, was identified in the ventral, dorsal and caudal parts of tuberal hypothalamus. Several stained neurons and fibres were recognised in the thalamic nucleus, both dorsal posterior and ventro-medial parts (Figs. 26g-l, 30c-d). Labelled perikarya were located around the margin of periventricular nucleus of posterior tuberculum (Fig. 26g-e). Many projections were found in the medial part of glomerular nucleus (Figs. 26l-m, 30e). Conspicuous amount of positive neurons was located on the external margin of diffuse inferior lobe of hypothalamus (Figs. 26m-o, 30l) with some fibres spread in the medial zone. No differences of distribution pattern were seen in neuroendocrine areas between MZM and GRZ. Summary of positive neurons and fibres localisation is shown in Tab. 7.

Extra-neuroendocrine regions

Only in MZM strain, several positive neurons were detected in the optic tectum, especially packed in the periglomerular grey zone, with remarkable projections towards the external margin (Figs. 26g-o, 27c). Moreover, weakly stained neuronal cells were widespread in the different layers of semicircular tori (Figs. 26l-m; 27d-f). These localisations were not detectable in the brain of GRZ.

Differences during ageing

The nesfatin-1 protein distribution didn't show notable differences between the young and elderly subjects in both strains.

Differences upon starvation

As well as in ISH, also the nesfatin-1 protein distribution didn't change between the control and starved subjects of MZM and GRZ strains.

Table 7. NUCB2/nesfatin-1 protein and mRNA distribution in the main neuroendocrine regions of *N. furzeri* brain. + few; ++ moderately dense; +++ very dense.

	Protein		**mRNA**
	Neurons	Fibres	Neurons
Telencephalon			
Ventral zone of ventral telencephalon (Vv)			
Sopracommissural zone of the ventral telencephalon (Vs)		+++	
Central part of the ventral telencephalon (Vc)		++	
Preoptic area			
Suprachiasmatic nucleus (SC)			
Preoptic nucleus, parvocellular part (PPp)			
Preoptic nucleus, magnocellular part (PM)	+		
Dorsal periventricular pretectal nucleus (PPd)			
Ventral periventricular pretectal nucleus (PPv)			
Intermediate superficial pretectal nucleus (SPNi)			
Magnocellular superficial pretectal nucleus (SPNm)			
Parvocellular superficial pretectal nucleus (SPNp)			
Cortical nucleus (CN)	+++		+++
Ventral accessory optic nucleus (VAO)			
Central pretectal nucleus (CPN)			
Anterior preglomerular nucleus (PGa)			
Lateral preglomerular nucleus (PGl)	+		
Medial preglomerular nucleus (PGm)	++		

Tuberal hypothalamus			
Dorsal hypothalamus (Hd)	++	+	+++
Ventral hypothalamus (Hv)	+++	++	+
Caudal hypothalamus (Hc)	+		++
Lateral hypothalamus (Hl)			
Anterior tuberal nucleus (TNa)			
Posterior tuberal nucleus (TNp)			
Periventricular nucleus of posterior tuberculum (TPp)		++	
Glomerular nucleus (NG)	+	++	
Hypothalamic recess (rec)			
Nucleus of posterior recess (NRP)		++	+++
Diffuse inferior lobe of hypothalamus (DIL)	+++	+++	++
Posterior tubercle			
Paraventricular organ (PVO)	+++	+	++
Thalamus			
Dorsal posterior thalamic nucleus (DP)	+		
Anterior thalamic nucleus (A)			
Central posterior thalamic nucleus (CP)			
Ventro-medial thalamic nucleus (VM)	++		++
Intermediate thalamic nucleus (I)			
Ventro-lateral thalamic nucleus(VL)			

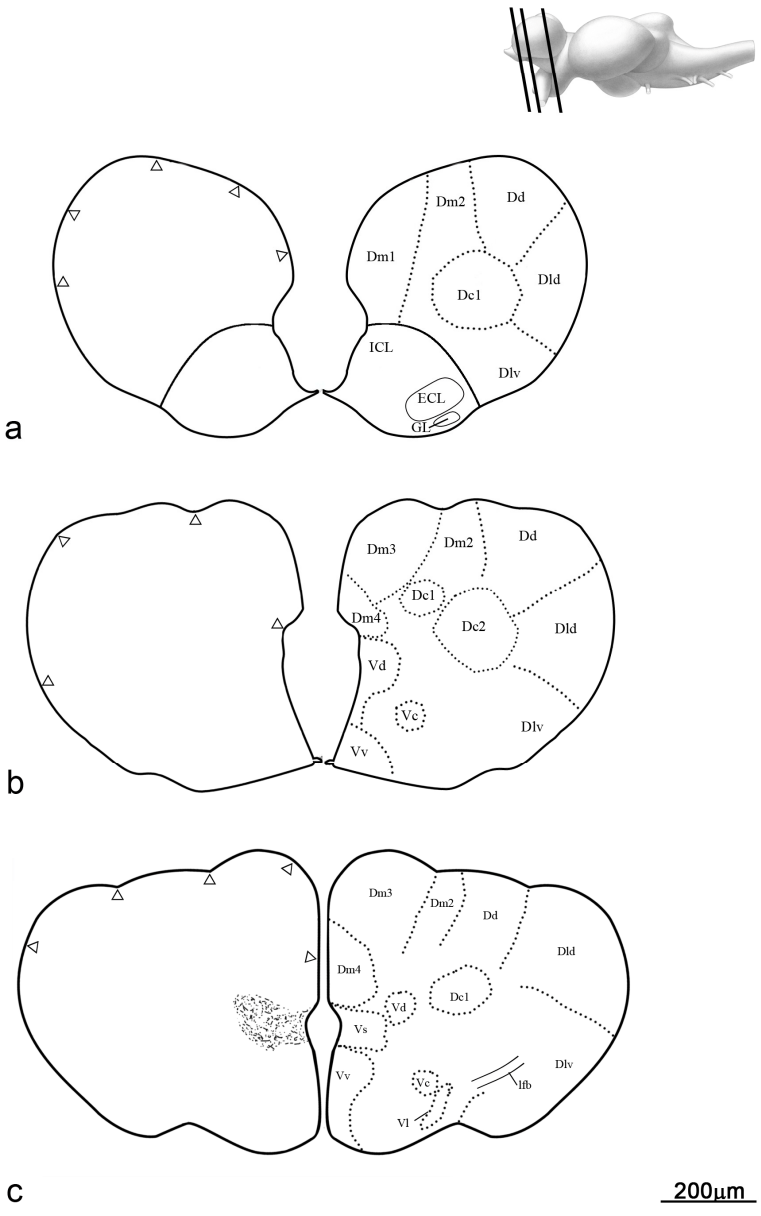

Figure 26. (continued)

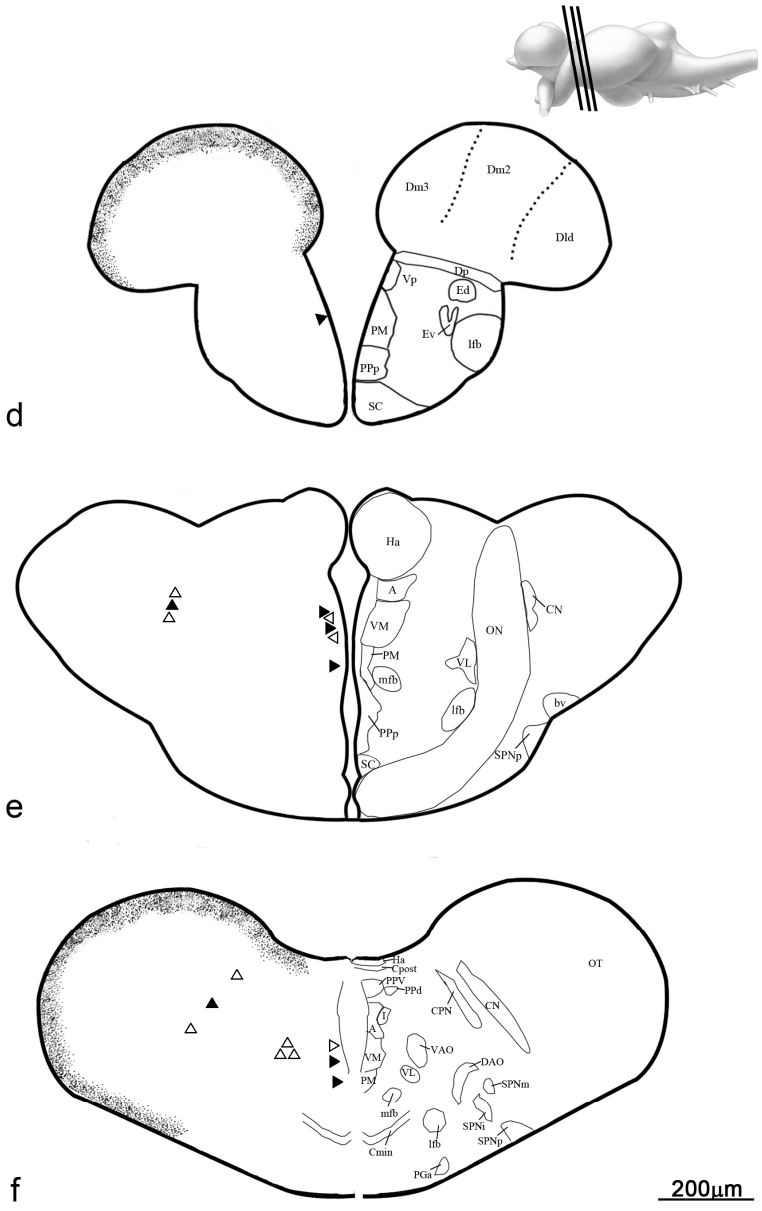

Figure 26. (continued)

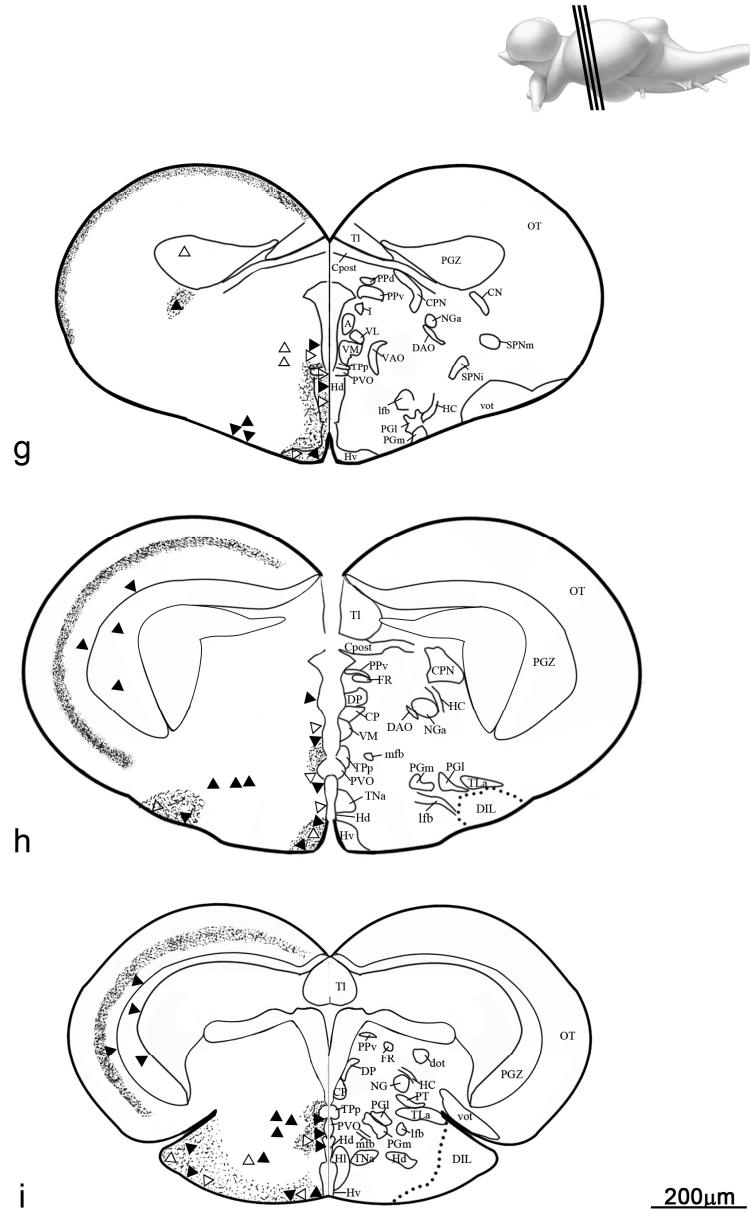

Figure 26. (continued)

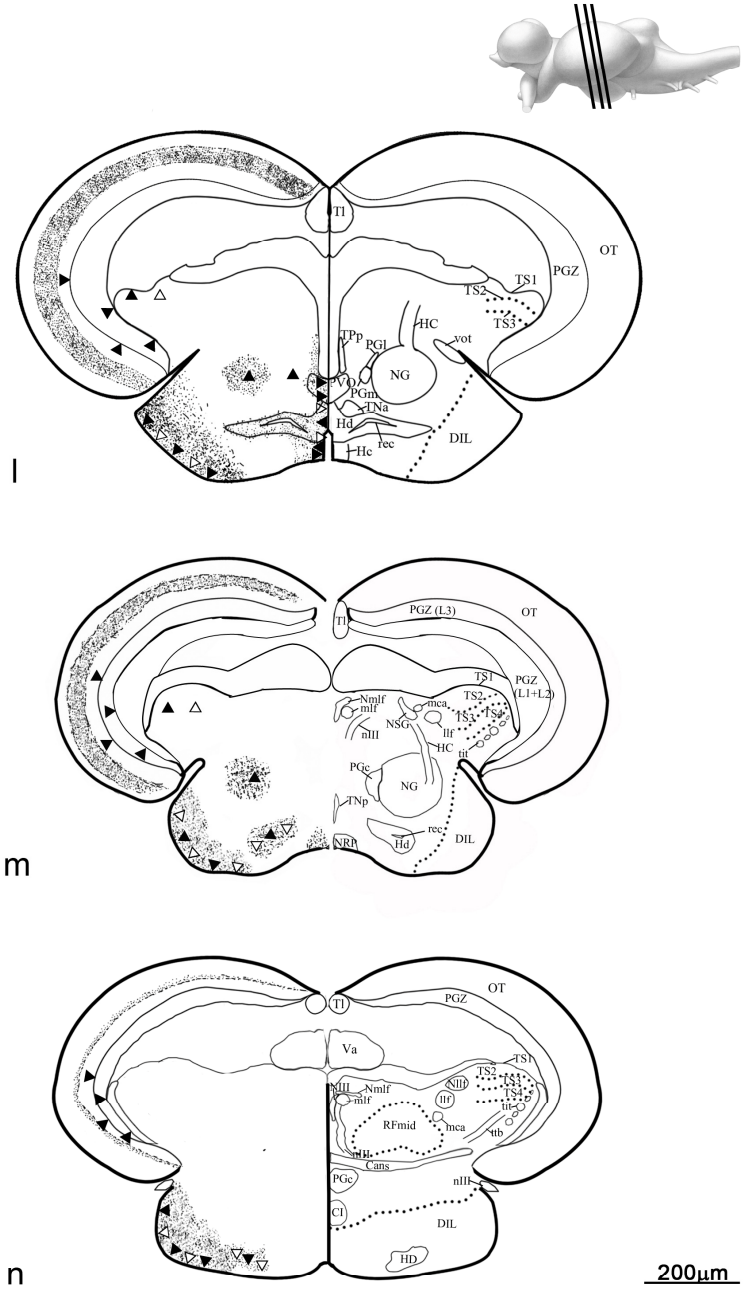

Figure 26. (continued)

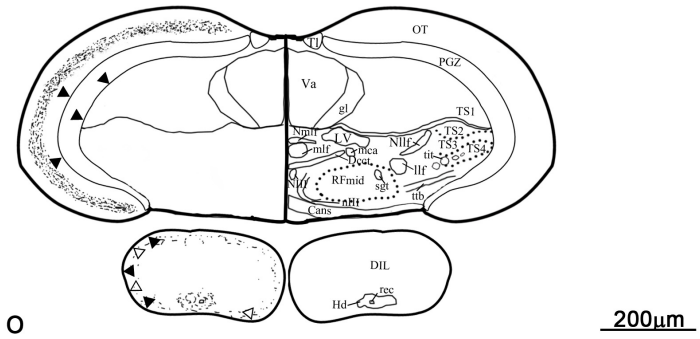

Figure 26. Atlas of NUCB2 gene and protein distribution: white triangles indicate sites of mRNA positive neurons (ISH); black tringles indicate sites of immunopositive neurons (IHC); small dots indicate immunoreactive fibres (IHC); **a-f)** forebrain; **g-o)** midbrain.

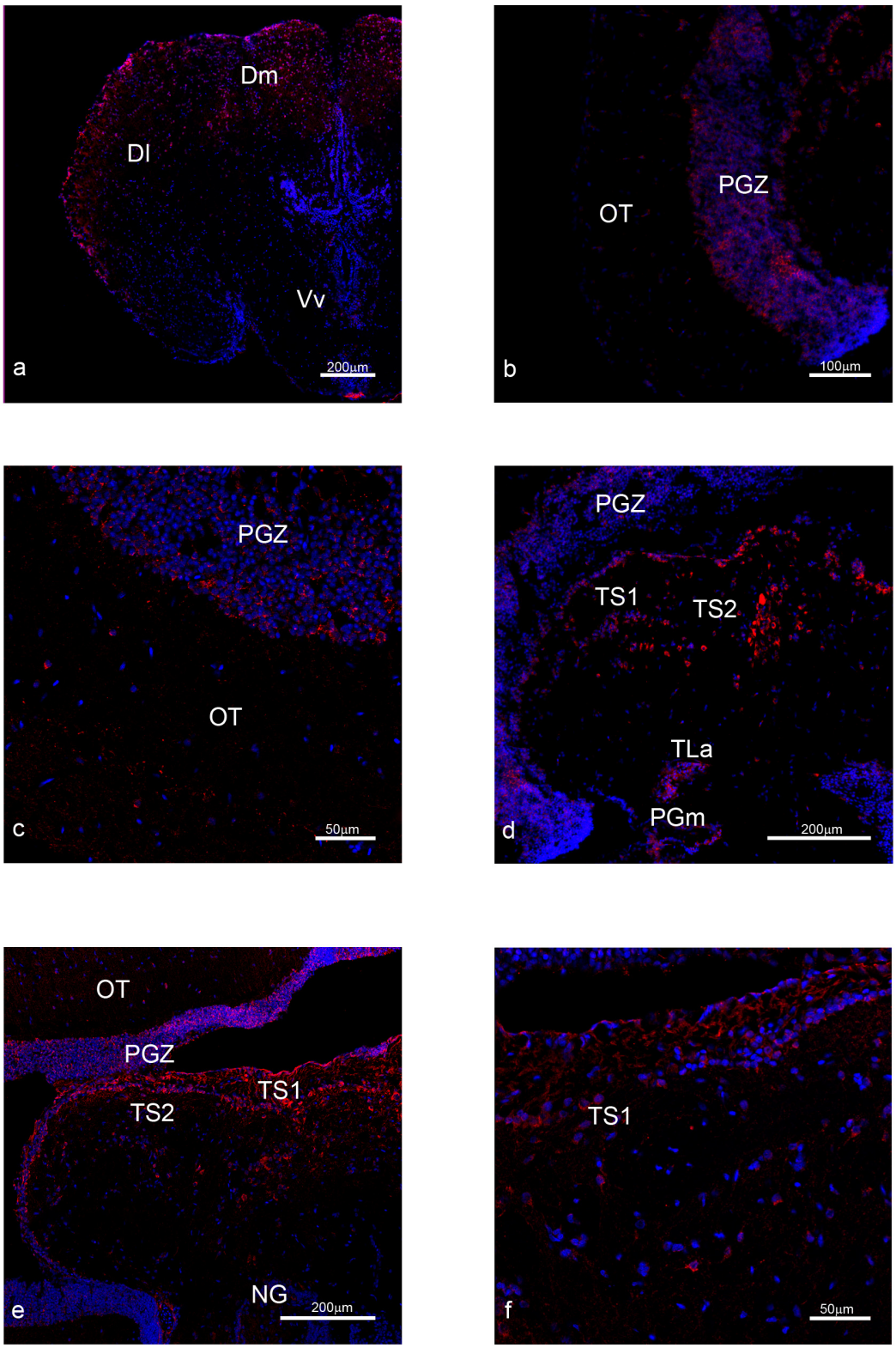

Figure 27. NUCB2 mRNA and peptide localisation in extra-neuroendocrine regions (ISH/IHC): **a)** ISH detail of telencephon; **b)** ISH detail of optic tectum (PGZ); **c)** IHC detail of positive neurons and fibres in optic tectum (MZM); **d-f)** IHC details of neurons and fibres in layers of semicircular tori. Red: positive neurons and fibres; blue: DAPI nuclear staining dye.

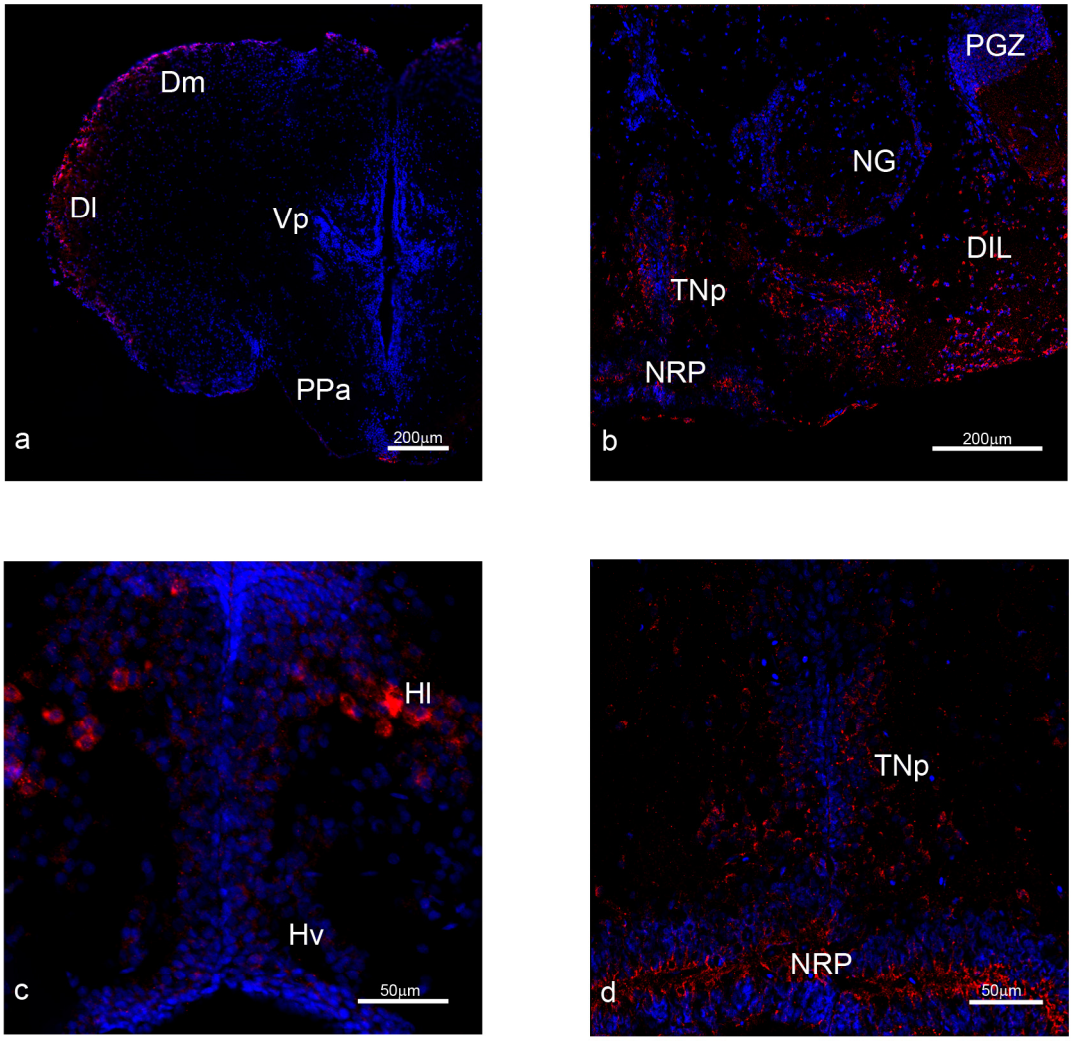

Figure 28. NUCB2 mRNA localisation in elderly subject (ISH): **a)** overview of telencephalon; **b)** overview of tuberal hypothalamic region; **c)** detail of hypothalamic nuclei; **d)** detail of the posterior recess. Red: positive neurons and fibres; blue: DAPI nuclear staining dye.

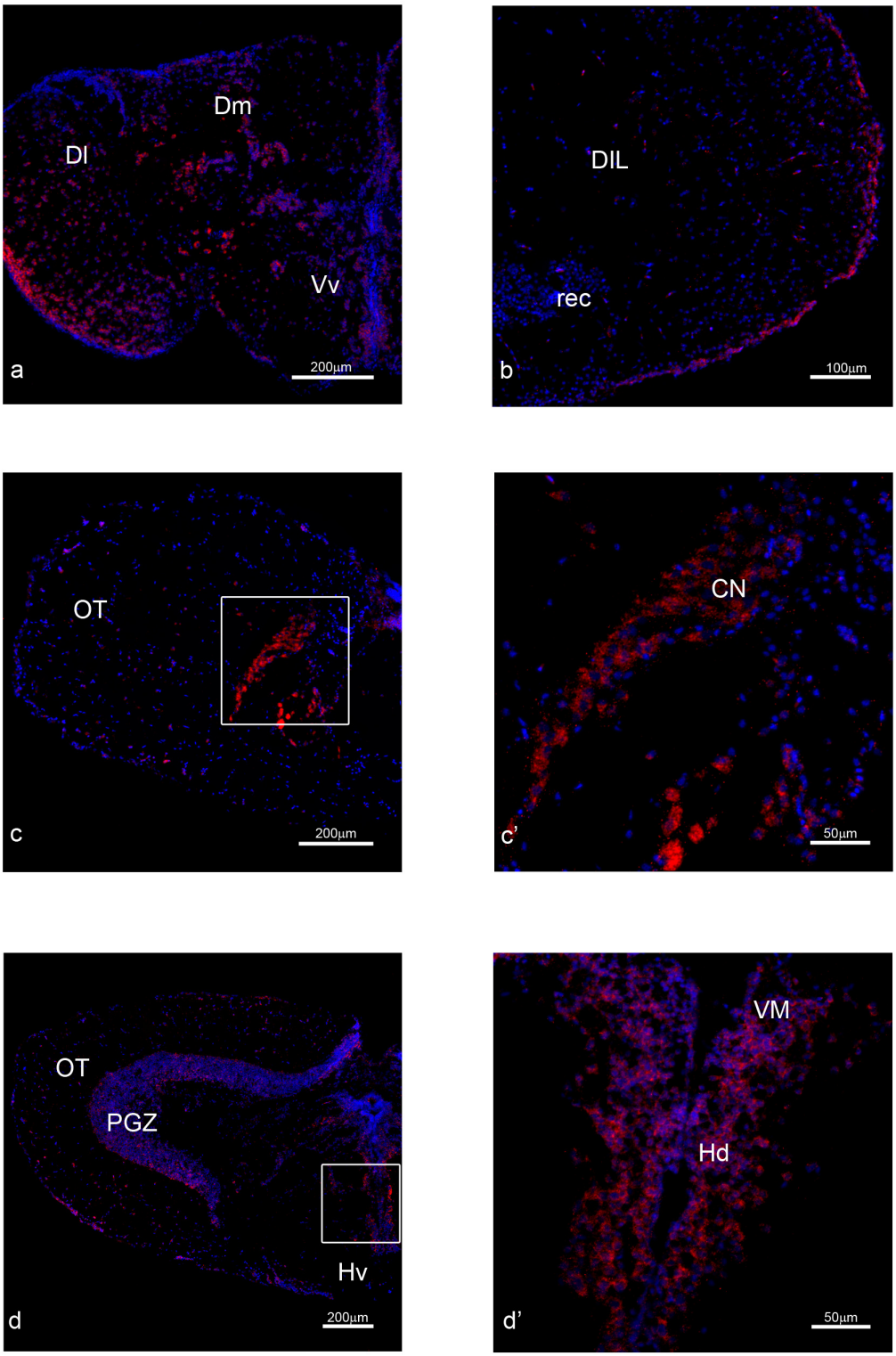

Figure 29. NUCB2 mRNA localisation in young control (ISH): a) telecephalon overview; b) detail of diffuse inferior lobe of hypothalamus; c-c') detail of the cortical nucleus; d-d') detail of dorsal hypothalamus. Red: positive neurons and fibres; blue: DAPI nuclear staining dye.

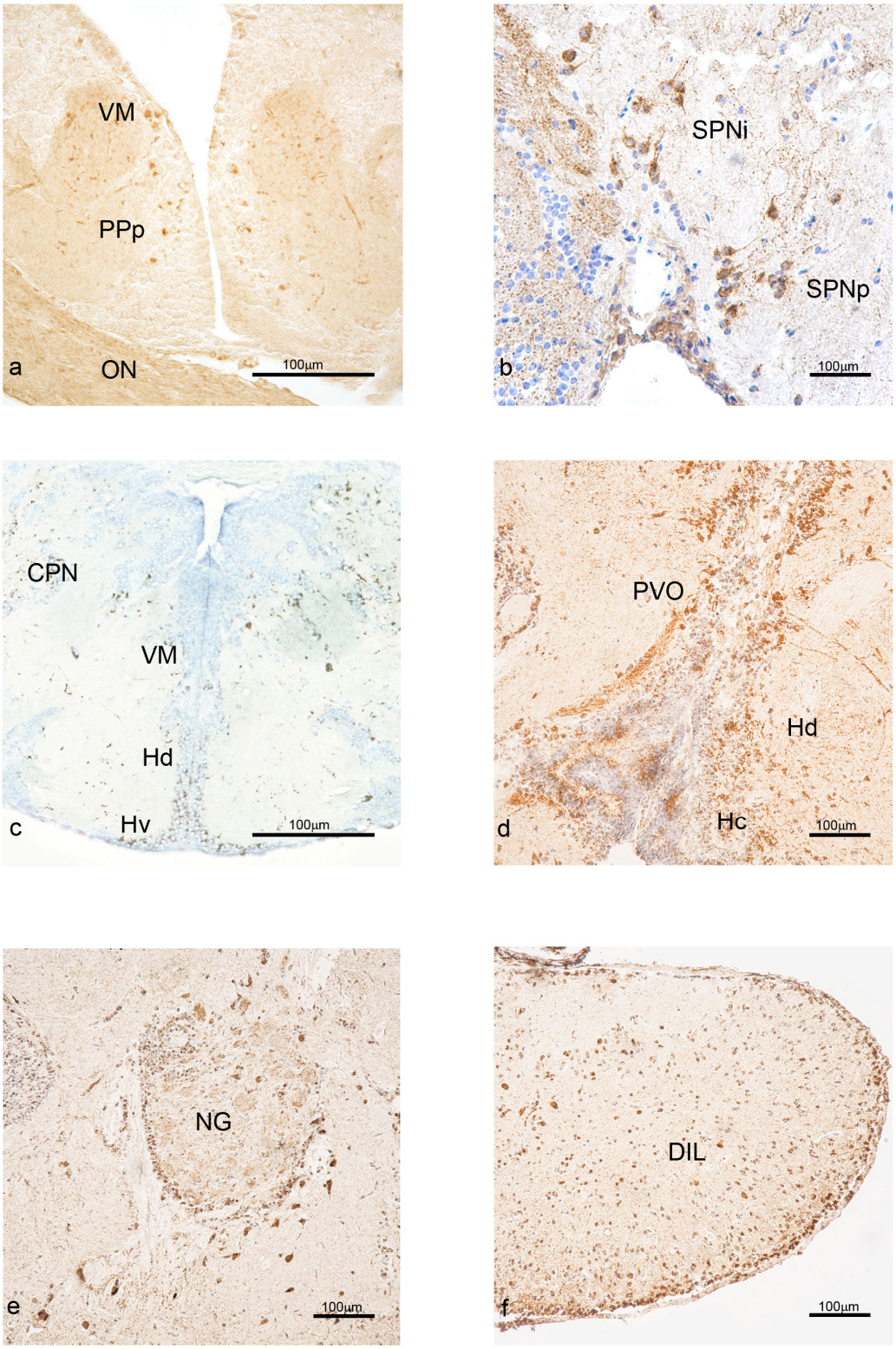

Figure 30. NUCB2 peptide localisation in young control (IHC): **a)** overview of preoptic region; **b)** detail of pretectal nucleus; **c)** overview of tuberal hypothalamus; **d)** details of paraventricular organ and hypothalamus; **e)** detail of glomerular nucleus; **f)** detail of diffuse inferior lobe of hypothalamus. DAB staining with eosin differentiation.

5. DISCUSSION

5.1. Neuropeptide Y

NPY represents one of the best conserved neuroendocrine peptides known and we demonstrated that *N. furzeri* amino acid sequence was highly conserved compared with zebrafish, medaka and mouse, sharing 83% of identity with mouse. In literature, NPY is described as the most potent orexigenic factor in fish and rodents (Matsuda *et al*., 2012). In the present survey we documented the expression of NPY in the brain of *N. furzeri*, under standard laboratory condition, as well as starvation and ageing. We showed that NPY is expressed in the CNS, as also documented in brain, pituitary and some peripheral tissues of other teleost (Chen *et al*., 2005; Leonard *et al*., 2001; Liang *et al*., 2007; Murashita *et al*., 2009). We observed the NPY levels increase upon 96 hours of starvation in the brain of both strains MZM and GRZ, confirming that in this species NPY acted as regulator of food intake and had an orexigenic function, as in zebrafish (Yokobory *et al*., 2012) and goldfish (Narnaware and Peter, 2001), whereas in the brain of Atlantic cod (Kehoe and Volkoff, 2007), Atlantic salmon (Murashita *et al*., 2009), and blunt snout bream (Ji *et al*., 2015), the role of NPY is not clear, since no significant differences in its expression were observed. In the winter skate, *R. ocellata*, NPY mRNA expression increased in the telencephalon but not the hypothalamus after 2 weeks of fasting (MacDonald and Volkoff, 2009). Nevertheless, for the first time in a piscine model, the conserved capability of regulating the food consumption has been analysed during ageing. In fact, in GRZ strain, the upregulation was preserved also during ageing; in contrary, in MZM, acute starvation didn't show any significant difference in the regulation of elderly subjects. Moreover, these results evidenced that the difference ageing time-points between the two strains (Terzibasi *et al*., 2008; Ptezold *et al*., 2013) also involved the loss of metabolic regulative drive, which probably happen in different stages. Further investigation and progressive monitoring of NPY level would be necessary to understand the end-points of driving expression in both strains. The increasing NPY-ergic activity upon ageing was in contrast with the phenomenon of anorexia of ageing described in several models, characterised by a decreasing of food intake (Morley *et al*., 2001). However, the increased levels of NPY mRNA in the brain of old *N. furzeri* could be due to insulin resistance leading to obesity, diabetes, and other metabolic disorders, typical of

senescence process (Botelho and Cavadas, 2015). In mammals some studies showed that NPY system was differentially changed, in fact in genetically modified obese rodent models levels and release of NPY were increased and receptor density was reduced (Beck, 2006). Interestingly in the aged MZM we could observe a reduced food intake despite of increased NPY levels. By contrast, in rodents with diet-induced obesity and in obese humans, hypothalamic NPY levels were lower, compared to controls with a normal body mass index (Goldstone *et al*., 2002; Hansen *et al*., 2004; Beck, 2006). Since we observed typical features of normal ageing in both strains, with gradual decrease of food intake and muscle mass, we would have expected lower levels of NPY expression in the brain. We argued that these discrepancies in NPY regulation between young and old animals could be correlated to alterations in energy homeostasis. It is widely documented that in course of ageing both MZM and GRZ strains undergo a high percentage of lesions in the liver, referable to fatty degeneration up to steatosis (Di Cicco *et al*., 2011). When *N. furzeri* was deprived of food for 96 hours, NPY expression increased in the brain, as also reported in numerous studies in mammals (Beck, 2006). It could be possible that the hypoglycaemia caused by starvation induced a larger orexigenic stimulus and activates the hypothalamic NPY neurons increasing NPY expression (Sindelar *et al*., 2004). In addition, we identified neurons expressing NPY mRNA in neuroendrocrine areas by ISH in control, starved and aged animals. The distribution of the NPY mRNA positive neurons in the was conserved in the two analysed strains of *N. furzeri*. Slight differences in the expression of neurons were observed between aged and starved animals. Compared to young animals, increased amount of intense labelled neurons was seen in the diffuse inferior lobe of hypothalamus and in the thalamic nuclei of old animals. In goldfish (Peng *et al*., 1994; Vecino *et al*., 1994), ISH signal was detected mainly in the ventral telencephalon, the preoptic area, the olfactory bulbs, and also in several thalamic nuclei. NPY mRNA was expressed in the hypothalamus of *N. furzeri*, whose neurons were activated upon starvation, as clearly demonstrated by pS6 labelling. This observation led us to affirm that in *N. furzeri* the main central feeding centres are localised in the hypothalamus and partly in preoptic area, and that NPY could modulate feeding behaviour. Furthermore, we observed NPY mRNA expression in preoptic area, mainly in young specimens. In other teleost, occurrence of NPY in this area has been described (Chiba *et al*., 1996; Subhedar *et al*., 1996; Cerda-Reverter *et al*., 2000; Mathieu *et al*., 2002; Gaikwad *et al*., 2004; Sakharkar *et al*., 2005), although

with some differences among species. The preoptic area is known to modulate also sexual behaviour in fish (Munchrath and Hofmann, 2010), and it could be possible that in *N. furzeri*, NPY is implicated in modulating the reproduction system functions, taking into account that we observed higher expression in young animals which already reached sexual maturity. Further studies are necessary to analyse this hypothesis. In addition, we have undertaken an immunohistochemical study, by using commercial antibodies recognising an amino acid sequence highly conserved in *N. furzeri* (~98%). The protein was expressed in the brain of young, starved and old samples, of both strains, showing the expected molecular weight. The localisation of NPY protein was seen in neuronal bodies and fibres of numerous diencephalic nuclei, not only in the hypothalamic region. Numerous descriptions have been addressed to the study of immunoreactivity in fish; in the goldfish, immunopositivity to NPY was detected in areas associated with control of food intake, such as hypothalamus, including the periventricular and lateral regions and the region near the lateral recess of the third ventricle in the inferior lobe (Huesa *et al*., 2005; Nakamachi *et al*., 2006). NPY immunoreactivity was reported also in zebrafish, mainly in the preoptic, thalamic and hypothalamic areas, and in the medulla oblongata (Yokobori *et al*., 2012). In the tiger puffer, immunoreactivity to NPY was detected in the telencephalon, hypothalamus, mesencephalon and medulla oblongata, and fibres widespread throughout the brain (Kamijo *et al*., 2011). In mammals, NPY for feeding regulation is synthesised in the arcuate nucleus, where the peptide is active in the paraventricular, dorsomedial and ventromedial nuclei and perifornical area (Beck, 2006). In *N. furzeri*, we observed an increased density of immunopositive projections in the CNS of starved animals, when comparing with controls. The increased number of immunopositive projections could represent a physiological response to fasting conditions, upon peripheral or central stimulation. NPY positive neurons could project to other brain areas to stimulate the feeding behaviour, for searching and acquiring food. Interestingly, we observed strong immunoreactivity in numerous varicose fibres and neurons of ventral, supracommissural and central zone of ventral telencephalon. In the ventral telencephalon of another killifish, *Fundulus heteroclitus* (Subhedar *et al.*, 1996), NPY positive neurons were documented; in fact, in fish, the ventral telencephalon, corresponding to the mammalian subpallial region, is considered as the major component of NPY-ergic system (Cerda-Reverter and Larhammar, 2000). The distribution of NPY in extrahypothalamic regions suggest that NPY could act in the

CNS of *N. furzeri* as neurotransmitter (or neuromodulator) and as a hypophysiotropic neuro-hormone (Danger *et al*., 1990).

5.2. Orexin/ Hypocretin

The HCRT gene has been characterised in several fish species, including pufferfish (Alvarez and Sutcliffe, 2002), zebrafish (Kaslin *et al.*, 2004), goldfish (Hoskins *et al*., 2008), cod (Xu and Volkoff, 2007), winter flounder (Buckley *et al*., 2010), winter skate (MacDonald *et al*., 2010), orange grouper (Yan et al., 2011), Mexican blind cavefish (Wall and Volkoff, 2013) and red-bellied piranha (Volkoff, 2014b). In all teleost species, HCRT/orexin system is related to neuroendocrine functions, being mainly expressed by neurons in the hypothalamic region (Kaslin *et al*., 2004; Huesa *et al*., 2005). Particularly, HCRT plays a role in the feeding physiology of fish, as shown injecting human ORX-A and ORX-B in goldfish brain, causing a significant increase in appetite (Volkoff *et al*., 1999). Also, the number of cells showing orexin-like immunoreactivity in the hypothalamus of goldfish brain increased in fasted fish and decreased in glucose-injected fish (Nakamachi *et al*., 2006). We addressed the study of HCRT/ORX system in the brain of *N. furzeri*, focusing on the regulation during ageing and upon starvation. To our knowledge, this represents the first survey in a teleost that highlights the modification of the orexin regulation during ageing, showing a significant downregulation in MZM strain in the elderly. These results obtained in MZM were congruent with what is described in mammals, showing decreased levels of prepro-orexin expression in the course of ageing (Porkka-Heiskanen *et al*., 2004). The downregulation of HCRT could be due to age-related modification of homeostasis, which affect the efficacy of the orexin system in the CNS of *N. furzeri*, or to reduced number of neurons expressing HCRT, because of degenerative process (Terzibasi *et al*., 2009). Nevertheless, in GRZ, HCRT level stayed stable. This discrepancy could be related to the previously mention intraspecific differences of age time points between two strains (Terzibasi *et al*., 2008; Ptezold *et al*., 2013). However, in elderly subjects of both strains, the response of ORX to acute food deprivation seemed to be lost. In contrary, starvation of 96 hours led to an upregulation of HCRT. This confirmed the role of HCRT/ORX system as appetite stimulator in *N. furzeri*. In GRZ, the upregulation was not statistically significant, but we argue that it was due to a high variability between the specimens, indicated as high standard deviation. Our results were consistent with previous studies showing an orexigenic role for orexin in fish: fasting induced an

increase in orexin expression in the hypothalamus of winter flounder (Buckley *et al*., 2010), barfin flounders (Amyia *et al*., 2012), Nile tilapia (Chen *et al*., 2011), zebrafish (Novak *et al*., 2005) and cavefish (Wall *et al*., 2013). Prepro-orexin mRNA upregulation upon fasting has been also proved in mammals (Sakurai *et al*., 1998). In addition, we identified and characterised the HCRT system in *N. furzeri* by *in situ* hybridisation, in order to study the neuroanatomical distribution. The expression of HCRT mRNA was widespread in the brain of control animals, mainly in the hypothalamic region, and more restricted in starved and aged specimens. The localisation of mRNA is consistent with previous description in the brain of zebrafish (Kaslin *et al*., 2004), and mammals (Sakurai *et al*., 1998), taking into account the different neuroanatomical organisation. Based on these observations we could conclude that HCRT/orexin system is implicated in the central regulation mechanisms of food intake in *N. furzeri*, as described in several other piscine species (Matsuda *et al*., 2012). However, the gene expression was seen also in extra-hypothalamic areas, such as the optic tectum, suggesting a wider role of orexin system in the neuromodulation, as postulated in medaka (Amiya *et al*., 2007), zebrafish (Kaslin *et al*., 2004) and goldfish (Huesa *et al*., 2005; Kojima *et al*., 2009). Coherent with the results of the qPCR, we observed a decrease of HCRT expressing neurons in the brain of old animals, suggesting a downregulation upon ageing in *N. furzeri.* In rats, a progressive age decline has been shown in positive neurons for orexin mRNA, peptide and/or receptors (Terao *et al*., 2002; Porkka-Heiskanen *et al*., 2004; Sawai *et al*., 2010; Kessler *et al*., 2011), including decreased orexin projections into target regions (Zhang *et al*., 2002; Downs *et al*., 2007). Interestingly, in old brains we observed HCRT mRNA labelling in olfactory bulbs and dorsal telencephalon, which was lacking in young animals. This is the first description of HCRT mRNA in olfactory bulbs in fish. In mammals, orexinergic fibres projecting the entire olfactory pathway were reported (Peyron *et al*., 1998). This result could be referred to an ORX signalling activation of alternative pathway during ageing. We first studied the precursor peptide expression and we have seen by Western blot that the prepro-orexin in the whole brain of *N. furzeri* was expressed at molecular weight of ~14 kDa in all samples examined of the strain MZM. Slight shift of molecular mass was detected in the GRZ, but still in the expected range. We also studied the distribution of ORX-A in the brain of *N. furzeri*, by employing a commercial antibody. ORX-A in *N. furzeri* was conserved 33% when compared with the mouse sequence. However, it seemed more conserved than in goldfish and

medaka. On the other hand, ORX-B was conserved 46% compared to mouse. We focus on ORX-A localisation, since it is described to be highly involved in the control of food intake than ORX-B, whose activity is more related to sleep-wakefulness (Nakamachi *et al*., 2006; Matsuda, 2009). Neurons containing ORX-A were detected mainly in the diencephalon of *N. furzeri,* from preoptic nucleus to pretectal, cortical, thalamic nuclei, dorsal hypothalamus, and diffuse inferior lobe of hypothalamus. In other fish species, the distribution of orexinergic neurons was more varied. For example, orexin neurons were localised in the preoptic area and suprachiasmatic nucleus in zebrafish (Kaslin *et al.*, 2004); nucleus posterioris periventricularis in the medaka (Amiya *et al*., 2007); nucleus posterioris periventricularis and nucleus lateralis tuberis in the goldfish (Kojima *et al*., 2009; Huesa *et al*., 2005), and in the suprachiasmatic nucleus and dorsal hypothalamus in lungfishes (Lopez *et al*., 2009). In amphibians, orexin-containing neurons were highly specifically localised in the ventral hypothalamic nucleus. A rich network of immunoreactive fibres was found in telencephalon, diencephalon and mesencephalon of *Xenopus laevis* (Shibahara *et al*., 1999). In the hypothalamus of chick, orexin neurons were detected in the caudal paraventricular nucleus; orexin fibres in the area of the suprachiasmatic nucleus, in the tuberal region and in the median eminence of hypothalamus (Miranda *et al*., 2013). In mammals, orexin neurons were localised in the hypothalamus, precisely in the perifornical and dorsomedial hypothalamic nuclei, dorsal and lateral hypothalamus (Nambu *et al*., 1999; Moore *et al*., 2001; Nixon *et al*., 2007). However, the location of orexin immunoreactive elements, reported following a similar approach in amphibians and amniotes, suggest that the general organisation of this peptidergic system was conserved also in *N. furzeri.* The distribution of immunoreactive fibres to ORX-A was consistent with the pattern of neurons containing ORX-A, with the exception of positive fibres detected in the ventral part of telencephalon and optical tectum of *N. furzeri*. In contrast, data in fish documented that orexin fibres extensively innervate the brain including regions as midbrain, brainstem, raphe, locus coeruleus, the mesopontine-like area, dopaminergic clusters, and histaminergic neurons (Kojima *et al.*, 2009; Nakamachi *et al*., 2006; Huesa *et al*., 2005). However, positive fibres in the subpallial areas of *N. furzeri* forebrain were also documented in zebrafish (Kaslin *et al*., 2004). Similarly, in mammals the major projection patterns of ORX fibres were seen in the homologous of subpallial areas of fish (Kaslin *et al*., 2004).

5.3. Nucleobindin-2/ Nesfatin-1

In the present survey, NUCB2 was characterised in the brain of *N. furzeri* and it was the first report in a teleost of regulation of this gene upon ageing. In *N. furzeri*, as described in other teleost, as zebrafish, goldfish, medaka and stickleback, the structure of the gene was well conserved and consisted in 13 exons and 12 introns. Due to the whole-genome duplication in *N. furzeri* (Reichwald *et al*., 2015), two paralogues were recognised: NUCB2A and NUCB2B. Anyway the differences between the sequences were so exiguous that it was almost impossible to design primers being sure to distinguish them; in fact, we study and detect both paralogues together. In *N. furzeri*, NUCB2 sequence showed an overall identity of 78% with NUCB2 of medaka. Nesfatin-1 is a protein identified in the NUCB2 sequence (Oh-I *et al*., 2006), and constitutes the N-terminal fragment of nucleobindin-2 (NUCB2). Prohormone convertases are predicted to process the pro-nesfatin into three fragments named nesfatin-1 (1-82 amino acids), nesfatin-2 (85-163 amino acids) and nesfatin-3 (166-396 amino acids) (Oh-I *et al*., 2006). The sequence of nesfatin-1 in *N. furzeri* showed 58% identity to the amino acid sequence of mouse. Previous investigations have demonstrated the involvement of nesfatin-1 mRNA in food regulation based on the reduction after 3 and 7 days of food deprivation, in different organs, such as the brain of goldfish (Gonzalez *et al*., 2011), zebrafish (Hatef *et al*., 2014), and Ya-fish (Lin *et al*., 2014). In the rat brain, NUCB2 mRNA expression was significantly reduced (~60%) after food deprivation of 24 h (Mortazavi *et al*., 2015). We observed non-significant regulation upon starvation either in young and aged brain, both in MZM and GRZ strains. No significant changes in the expression under starvation, not necessarily excluded NUCB2 as food intake regulator; in fact, this could be due to low ratio of NUCB2 in the whole brain, which makes detection of the gene difficult and the comparison under fasting. In addition, it was also conceivable that significant expression levels of NUCB2 could have been detected over a longer starvation period, because of intrinsic metabolic need of *N. furzeri.* We analysed also the distribution of NUCB2 mRNA and the transcript was mainly detected in the hypothalamic nuclei, as referred in mammals (Oh-I *et al*., 2006; Brailoiu *et al*., 2007; Kohno *et al*., 2008; Fort *et al*., 2008; Nonogaki *et al*., 2008; Foo *et al*., 2008) and in other vertebrate species (frog, Senejani *et al*., 2014) and goldfish (Gonzalez *et al*., 2011). That report made us confident that maybe the discrepancy with gene regulation could have been related at methodological limits, even if the missing

regulation in dietary restricted regime was also described in rainbow trout (Caldwell *et al*., 2014). Furthermore, our data suggested that in *N. furzeri* NUCB2 regulation could be modulated by peripheral signals from the gastrointestinal tract. In mammals, the expression level of NUCB2 in the stomach was found to be 10 fold higher relative to levels of the brain (Stengel *et al*., 2009). Future experiments in the gastrointestinal tract could help to clarify the regulation of NUCB2/nesfatin-1 in *N. furzeri.* Up to now, this is the first study reporting the regulation of NUCB2 during ageing in the brain of a vertebrate model. Since there is no reported study about any regulation of NUCB2 upon ageing it is difficult to explain the slight increase in elderly animals. It could be related to an energy drive failure or to an altered regulation of insulin (Butler, 2012), which can lead to anorexic phenotype, which indeed is well described and typically occurs during ageing (Morley, 2001). We also studied nesfatin-1 protein expression by IHC. Nevertheless, the commercial antibody available detected the precursor nesfatin-1 (1-82). The protein is expressed in the whole brain of control, starved and aged animals, with the expected molecular weight of about 40 kDa, as also reported in goldfish (Gonzalez *et al.*, 2010) and mammals (Brailoiu *et al*., 2007). In GRZ, beside a very strong 40 kDa band, we observed also several others smeared bands in the range between ~25 and 100 kDa. Immunoreactivity to nesfatin-1 was detected in the hypothalamic area, either in neuronal perikarya and fibres of young and aged brains of both strains. In young control animals of the two strains, neurons expressing NUCB2 mRNA were localised in the cortical nucleus, ventro-medial thalamic nucleus, paraventricular organ, and diffuse inferior lobe of hypothalamus. Some areas, i.e. paraventricular organ and diffuse inferior lobe of hypothalamus, displayed positive neurons in ISH and IHC. Interestingly mRNA expression and protein distribution were detected in extra-neuroendocrine regions, specifically telencephalon, optic tectum and semicircular tori in young and old animals. In mammals, nesfatin-1 immunoreactivity was also detected in extra-diencephalic regions including the nucleus tractus solitarius, another brain region implicated in the regulation of feeding (Brailoiu *et al*., 2007; Kohno *et al*., 2008; Fort *et al.*, 2008). Telencephalon and optic tectum brain regions are known to be involved in the control of appetite of teleost (for review, see Volkoff *et al*., 2004). For example, electrical stimulation of either the ventral telencephalon, the secondary gustatory nucleus or the optic tectum induces feeding behaviour (Demski and Knigge, 1971), whereas feeding behaviour is depressed by olfactory tract lesions (Demski and Knigge, 1971; Stacey and Kyle, 1983). It might be

possible that the presence of NUC2B/nesfatin-1 in the extra-diencephalic areas of *N. furzeri* implicates that these areas could be also involved in the regulation of feeding in *N. furzeri*, and/or several other homeostatic systems (Stengel, 2015).

6. CONCLUSION

In the present study, the appetite regulation in the model for ageing research *N. furzeri,* is analysed for the first time. Moreover, few data are reported in literature about the age-dependent decline of the food intake drive in fish. Also, a comparative study to evidence the differences between the two strains with diverse lifespan has been carried on. In particular, three important neuropeptides, with different roles, are characterised in *N. furzeri*. Neuropeptide Y is the most important orexigenic regulator in vertebrates and it acts in first order neuron of CNS, modulating the message from the peripheral sites, signalling to different specific regions of the brain. We have demonstrated its important role in *N. furzeri* and found, that during ageing, the expression is increased and starvation doesn't have an effect on the modulation anymore. These data suggest, that probably the animals suffer from insulin resistance or similar metabolic syndrome. Since up to now a guide line for the standardisation of the management of *N. furzeri* facility is not available, we could also imagine that the dietary regime conditions in lab are not optimal and the excess of food lead to development of obesity or diabetes type II. This hypothesis is congruent with the prevalence and incidence of neoplasia and liver dysfunction described in literature. To confirm this hypothesis, further investigations are required. HCRT is an orexigenic factor as well but it acts in second order neurons and it coordinates all the outputs in the brain as response to a change in energy metabolism. During the ageing, its downregulation reminds of a similar condition to what happens during anorexia of ageing, but this could also be a response to a paradox effect of insulin intolerance. This could be confirmed by the loss of drive in elderly subjects under acute fasting time. NUCB2 has never been characterised in *N. furzeri* and to best of our knowledge no description of ageing regulation is reported in any vertebrate. We could not confirm its involvement in food intake regulation, since the starvation period didn't have any effect in young and old animals of both analysed strains. Nevertheless, we are confident about its involvement in appetite regulation, since the anatomical localisation was found in the neuroendocrine areas, involved in the food intake, which showed neuronal activation upon starvation. Of course, we cannot exclude methodologic limits of our analysis. Moreover, in basal condition during ageing, we showed upregulation and this, again, is consistent with the increased expression occurring during liver dysfunctions or non-alcoholic fatty liver disease (NAFLD) previously demonstrated in other studies,

both in mammals and fish. Further investigations will be needed. A practical goal is to improve the captivity condition of a model which is becoming more and more utilised, also in pharmacological studies.

7. References

Alvarez CE and Sutcliffe JC (2002). Hypocretin is an early member of the incretin gene family. Neurosci Res, 68: 44-50.

Aveleira CA, Botelho M, Cavadas C (2015). NPY/neuropeptide Y enhances autophagy in the hypothalamus: a mechanism to delay aging? Autophagy, 11: 1431-1433.

Buckley C, MacDonald EE, Tuziak SM, Volkoff H (2010). Molecular cloning and characterization of two putative appetite regulators in winter flounder (*Pleuronectes americanus*): preprothyrotropin-releasing hormone (TRH) and preproorexin (OX). Peptides, 31: 1737-1747.

Bartákova V, Reichard M, Janko K, Polačik M, Blažek R, Reichwald K, Cellerino A, Bryja J (2013). Strong population genetic structuring in annual fish, *Nothobranchius furzeri*, suggests multiple savannah refugia in southern Mozambique. BMC Evol Biol, 13: 196-210.

Baumann C, Ferini-Strambi L, Waldvogel D, Werth E, Bassetti CL (2005). Parkinsonism with excessive daytime sleepiness--a narcolepsy-like disorder? J Neurol, 252: 139-145.

Baumgart M, Priebe S, Groth M. Hartmann N, Menzel U, Pandolfini L, Philipp Koch, Felder M, Ristow M, Englert C, Guthke R, Platzer M, Cellerino A (2016). Longitudinal RNA-Seq Analysis of Vertebrate Aging Identifies Mitochondrial Complex I as a Small-Molecule-Sensitive Modifier of Lifespan. Cell System, 2: 122-132.

Bedoui S, Kromer A, Gebhardt T, Jacobs R, Raber K, Dimitrijevic M, Heine J, von Hörsten S (2008). Neuropeptide Y receptor-specifically modulates human neutrophil function. J Neuroimmunol, 195: 88-95.

Beck B (2006). Neuropeptide Y in normal eating and in genetic and dietary- induced obesity. Phil Trans R Soc B, 361: 1159-1185.

Berthoud HR (2002). Multiple neural systems controlling food intake and body weight. Neurosci Biobehav Rev, 26: 393-428.

Blanton CA, Horwitz BA, Blevins JE, Hamilton JS, Hernandez EJ, McDonald RB (2001). Reduced feeding response to neuropeptide Y in senescent Fischer 344 rats. Am J Physiol Regul Integr Comp Physiol: 280: R1058-R1060.

Blazek R, Polacik MJ, Reichard M (2013). Rapid growth, early maturation and short generation time in African annual fishes. EvoDevo, 4: 24-31.

Botelho M and Cavadas Claudia (2015). Neuropeptide Y: an anti- aging player? Trends Neurosci, 11: 701-711.

Brightman MW, Broadwell RD (1976). The morphological approach to the study of normal and abnormal brain permeability. Adv Exp Med Biol, 69: 41-54.

Brownell SE and Conti B (2010). Age- and gender-specific changes of hypocretin immunopositive neurons in C57Bl/6 mice. Neurosci Lett, 472: 29-32.

Burkley C, MacDonald EE, Tuiak SM, Volkoff H (2010). Molecular cloning and characterization of two putative appetite regulators in winter flounder (Pleuronectes americanus): Preprothyrotropin- releasing ormone (TRH) and preproorexin (OX). Peptides, 31: 1737-1747.

Butler AA (2012). More news about NUCB2/Nesfatin-1: a new factor in the hypothalamic control of glucose homeostasis? Diabetes, 6:1920-1922.

Caldwell LK, Pierce AL, Riley AG, Duncan CA, Nagler JJ (2014). Plasma nesfatin-1 is not affected by long-term food restriction and does not predict rematuration among iteroparous female rainbow trout (*Oncorhynchus mykiss*). PLoS ONE, 9: e85700-85709.

Campos VF, Collares T, Deschamps JC, Seixas FK, Dellagostin OA, Lanes CFC, Sandrini J, Marins LF, Okamoto M, Sampaio LA (2010). Identification tissue distribution and evaluation of brain neuropeptide Y gene expression in the Brazilian flounder *Paralichthys orbignyanus*. J Biosci, 35: 405-413.

Cellerino A, Valenzano DR, Reichard M (2015). From the bush to the bench: the annual *Nothobranchius* fishes as a new model system in biology. Biol Rev, doi: 10.1111/brv.12183.

Cerdá-Reverter J, Martinez-Rodriguez G, Zuny S, Carrillo M, Larhammar D (2000). Molecular evolution of neuropeptide Y (NPY) family peptides; Cloning of three NPY-related peptides from sea bass (*Dicentrarcus labrax*). Regu Pept, 95: 197-208.

Chen WB, Wang X, Zhou YL, Dong HY, Lin HR, Li WS (2011). Molecular cloning, tissue distribution and the expression in the regulation of food intake of prepro-orexin in Nile tilapia (*Oreochromis niloticus*). Zool Res, 32: 285-292.

Cooper EI, Zapata A, García Barrutia M, Ramírez JA (1983). Aging changes in lymphopoietic and myelopoietic organs of the annual cyprinodont fish, *Nothobranchius guentheri*. Exp. Gerontol, 18: 29-38.

Copeland DL, Duff RJ, Liu Q, Prokop J, Londraville RL (2011). Leptin in teleost fishes: an argument for comparative study. Front Physiol, 2: 26-36.

D'Angelo L (2013). Brain Atlas of an Emerging Teleostan Model: *Nothobranchius furzeri*. Anat Rec (Hoboken), 296: 681-691.

Danger JM, Tonon MC, Jenks BG, Saint-Pierre S, Martel JC, Fasolo A, Breton B, Quirion R, Pelletier G, Vaudry H (1990). Neuropeptide Y: localization in the central nervous system and neuroendocrine functions. Fundam Clin Pharmacol,4: 307-340.

Danger JM, Breton B, Vallarino M, Fournier A, Pelletier G, Vaudry H (1991). Neuropeptide Y in the trout brain and pituitary: localization, characterization and action on gonadotropin release. Endocrinology, 28: 2360-2368.

de Boer A, Ter Horst GJ, Lorist MM (2013). Physiological and psychosocial age-related changes associated with reduced food intake in older persons. Ageing Res Rev, 12: 316-328.

De la Fuente M, Medina S, Del Rio M, Ferrández MD, Hernanz A (2000). Effect of aging on the modulation of macrophage functions by neuropeptides. Life Sci, 67: 2125-2135.

Di Cicco E, Tozzini ET, Rossi G, Cellerino A (2011). The short-lived annual fish *Nothobranchius furzeri* shows a typical teleost aging process reinforced by high incidence of age-dependent neoplasias. Exp. Gerontol, 46: 249-256.

Drouot X, Moutereau S, Nguyen JP, Lefaucheur JP, Créange A, Remy P, Goldenberg F, d'Ortho MP (2003). Low levels of ventricular CSF orexin/hypocretin in advanced PD. Neurology, 61: 540-543.

Dyer CJ, Touchette KJ, Carroll JA, Allee GL, Matteri RL, (1999). Cloning of porcine prepro-orexin cDNA and effects of an intramuscular injection of synthetic porcine orexin-B on feed intake in young pigs, Domest Anim Endocrinol, 16: 145–148.

Fabrizio P, Pozza F, Pletcher SD, Gendron CM, Longo VD (2015). Regulation of longevity and stress resistance by Sch9 in yeast. Science, 292: 288-290.

Faraco JH, Appelbaum L, Marin W, Gaus SE, Mourrain P, Mignot E (2006). Regulation of hypocretin (orexin) expression in embryonic zebrafish. J Biol Chem, 281: 29753-29761.

Feijoo-Bandin S, Rodriguez-Penas D, Garcia-Rua V, Mosquera-Leal A, Otero MF, Pereira E, Rubio J, Martinez I, Seoane LM, Gualillo O, Calaza M, Garcia-Caballero T, Portoles M, Rosello-Lleti E, Dieguez D, Rivera M, Gonzalez-Juanatey JR, Lago F (2013). Nesfatin-1 in human and murine cardiomyocytes: Synthesis, secretion, and mobilization of GLUT-4. Endocrinology, 154: 4757-4767.

Fronczek R, Overeem S, Lee SY, Hegeman IM, van Pelt J, van Duinen SG, Lammers GJ, Swaab DF (2007). Hypocretin (orexin) loss in Alzheimer's disease. Neurobiol Aging, 33, 1642-1650.

Fuentes EN, Safian D, Einarsdottir IE, Valdés JA, Elorza AA, Molina A, Björnsson BT (2013). Nutritional status modulates plasma leptin, AMPK and TOR activation, and mitochondrial biogenesis: Implications for cell metabolism and growth in skeletal muscle of the fine flounder. Gen Comp Endocrinol, 186: 172-180.

Gao XB, Hermes G (2015). Neural plasticity in hypocretin neurons: the basis of hypocretinergic regulation of physiological and behavioural functions in animals. Front Syst Neurosci, 9: 142-155.

Genade T, Benedetti M, Terzibasi E, Roncaglia P, Valenzano DR, Cattaneo A, Cellerino A (2005). Annual fishes of the genus *Nothobranchius* as a model system for aging research. Aging Cell, 4: 223-233.

Gerhald GS, Kauffman EJ, Wang X, Stewart R, Moore JL, Kasales CJ, Demidenko E, Cheng KS (2002). Life spans and senscent phenotipes in two strains of Zebrafish (*Danio rerio*). Exp Gerontol, 37: 1055-1068.

Gerhald GS (2003). Comparative aspects of zebrafish (*Danio rerio*) as model for aging research. Exp. Gerontol, 38: 1333-1341.

Gonzalez R, Kerbel B, Chun A, Unniappan S (2010). Molecular, cellular and physiological evidences for the anorexigenic actions of nesfatin-1 in goldfish. PLoS One, 5: e15201-e15214.

Gonzalez R, Mohan H, Unniappan S (2012a). Nucleobindins: bioactive precursor proteins encoding putative endocrine factors? General Comp Endocrinol, 176: 341-346.

Gonzalez R, Shepperd E, Thiruppugazh V, Lohan S, Grey CL, Chang JP, Unniappan S (2012b). Nesfatin-1 regulates the hypothalamo-pituitary-ovarian axis of fish. Biol Reprod, 87: 84-95.

Hakansson ML, Hulting AL, Meister B (1996). Expression of leptin receptor mRNA in the hypothalamic arcuate nucleus- relationship with NPY neurons. Neuroreport, 7: 3087-3092.

Halford JC, Cooper GD, Dovey TM (2004). The pharmacology of human appetite expression. Curr Drug Targets, 5: 221-240.

Hansen M, Jovanovska V, Morris MJ (2004). Adaptive responses in hypothalamic neuropeptide Y in the face of prolonged high-fat feeding in the rat. J Neurochem, 88: 909-916.

Harel I, Benayoun BA, Machado B, Singh PP, Hu CK, Pech MF, Valenzano DR, Zhang E, Sharp SC, Artandi SE, Brunet A (2015). A platform for rapid exploration of aging and diseases in a naturally short-lived vertebrate. Cell 160: 1013-1026.

Hartmann N and Englert C (2012). A microinjection protocol for the generation of transgenic killifish (Species: *Nothobranchius furzeri*). Dev Dyn, 241: 1133-141.

Hartmann N, Reichwald K, Wittig I, Drose S, Schmeisser S, Luck C, Hahn C, Graf M, Gausmann U, Terzibasi E, Cellerino A, Ristow M, Brandt U, Platzer M, Englert C (2011). Mitochondrial DNA copy number and function decrease with age in the short-lived fish Nothobranchius furzeri. Aging Cell, 10: 824-831.

Hatef A, Shajan S, Unniappan S (2015). Nutrient status modulates the expression of nesfatin-1 encoding nucleobindin 2A and 2B mRNAs in zebrafish gut, liver and brain. General Comp Endocrinol, 215: 51-60.

Haynes AC, Jackson B, Chapman H, Tadayyon M, Johns A, Porter RA, Arch JR (2000). A selective orexin-1 receptor antagonist reduces food consumption in male and female rats, Regul Pept, 96: 45-51.

Hong SH, Lee KS, Kwak SJ, Kim AK, Bai H, Jung MS, Kwon OY, Song WJ, Tatar M, Yu K (2012). Minibrain/Dyrk1a regulates food intake through the Sir2-FOXO-sNPF/NPY pathway in Drosophila and mammals. PLoS Genet, 8: e1002857-e1002562.

Hoskins LJ, Xu, M, Volkoff H (2008). Interactions between gonadotropin-releasing hormone (GnRH) and orexin in the regulation of feeding and reproduction in goldfish (*Carassius auratus*), Hormones and Behavior, 54: 379-385.

Huesa G, van den Pol AN, Finger TE (2005). Differencial distribution of hypocretin (orexin) and melacortin-concentrating hormone in the goldfish brain. J Compar Neurol, 488: 476-491.

Hungs M, Fan J, Lin L, Lin X, Maki RA, Mignot E (2001). Identification and functional analysis of mutations in the hypocretin (orexin) genes of narcoleptic canines. Genome Res, 11: 531-539.

Goldstone AP, Unmehopa UA, Bloom SR, Swaab DF (2002). Hypothalamic NPY and agouti related protein are increased in human illness but not in Prader-Willi syndrome and other obese subjects. J. Clin. Endocrinol. Metab. 87, 927-937.

Gorrisen MHAG, Flik G, Huising MO (2006). Huising, Peptides and proteins regulating food intake: a comparative view. Ann Biol, 54: 447-473.

Ji W, Ping HC, Wei KJ, Zhang GR, Shi ZC, Yang RB, Zou GW, Wang WM (2015). Ghrelin, neuropeptide Y (NPY) and cholecystokinin (CCK) in blunt snout bream (*Megalobrama amblycephala*): cDNA cloning, tissue distribution and mRNA expression changes responding to fasting and refeeding. Gen Comp Endocrinol, 223: 108-119.

Kaipio K, Pesonen U (2009). The intracellular mobility of NPY and a putative mitochondrial form of NPY in neuronal cells. Neurosci Lett, 450: 181-185.

Kamijo M, Kojima K, Maruyama K, Konno N, Motohashi E, Ikegami T, Uchiyama M, Shioda S, Ando H, Matsuda K (2011). Neuropeptide Y in tiger puffer (Takifugu rubripes): distribution, cloning, characterization and mRNA expression responses to prandial condition. Zool Sci, 28: 882-890.

Kaphai P, Zid BM, Harper T, Koslover D, Sapin V, Benzer S (2004). Regulation of lifespan in Drosophila by modulation of genes in the TOR signalling pathway. Curr Biol,14: 885-890.

Kaslin J, Nystedt JM, Ostergard M, Peitsaro N, Panula P (2004). The orexin/ hypocretin system in zebrafish is connected to the aminergic and cholinergic system. J. Neurosci, 24: 2678-2689.

Kehoe AS and Volkoff H (2007). Cloning and characterization of neuropeptide Y (NPY) and cocaine and amphetamine regulated transcript (CART) in Atlantic cod (*Gadus morhua*). Comp Biochem Physiol A Mol Integr Physiol, 146: 451-461.

Kerbel B, Unniappan S (2012). Nesfatin-1 suppresses energy intake, co-localises ghrelin in the brain and gut, and alters ghrelin, cholecystokinin and orexin mRNA expression in goldfish. J Neuroendocrinol 24: 366-377.

Kessler BA, Stanley EM, Frederick-duus D, Fadel J (2011). Age-related loss of orexin/hypocretin neurons. Neuroscience, 178: 82-88.

Kir HM, Sahin D, Oztaş B, Musul M, Kuskay S (2014). Effects of single-dose neuropeptide Y on levels of hippocampal BDNF, MDA, GSH, and NO in a rat model of pentylenetetrazole-induced epileptic seizure. Bosn J Basic Med Sci, 13: 242-247.

Kiris G, Kumlu M, Dikel S (2007). Stimulatory effects of neuropeptide Y on food intake and growth of Oreochromis niloticus. Aquaculture, 264: 383-389.

Kmiec Z (2011). Aging and peptide control of food intake. J Physiol Pharmacol, 57: 7-16.

Knight ZA, Tan K, Birsoy K, Schmidth S, Garrison JL, Wysocki RW, Emiliano A, Ekstrand MI, Friedman JM (2012. Nolecular profiling of activated neurons by phosphorylated ribosome capture. Cell, 151: 1126-1137.

Kojima K, Amiya N, Kamijo M, Kageyama H, Uchiyama M, Shioda S, Matsuda K (2010). Relationship between alpha-melanocyte-stimulating hormone- and neuropeptide Y- containing neurons in the goldfish hypothalamus. Gen Comp Endocrinol, 167: 366-372.

Kotz CM, Mullett MA, Wang C (2005). Diminished feeding responsiveness to orexin A (hypocretin 1) in aged rats is accompanied by decreased neuronal activation. Am J Physiol Regul Integr Comp Physiol, 289: R359-R366.

Lakowski B and Hekimi S (1998). The genetics of caloric restriction in *Caenorhabditis elegans*. Proc Natl Acad Sci USA, 95: 13091-19096.

Landi F, Calvani R, Tosato M, Martone AM, Ortolani GS, Sisto A, Marzetti E (2015). Anorexia of Aging: Risk Factors, Consequences, and Potential Treatments. Nutrients, 8: 69-78.

Levitas-Djerbi T, Yelin-Bekerman L, Lerer-Goldshtein T, Appelbaum L (2015). Hypothalamic leptin-neurotensin-hypocretin neuronal networks in zebrafish. J Comp Neurol, 523: 831-48.

Levitsky DA (2005). The non-regulation of food intake in humans: hope for reversing the epidemic of obesity. Physiol Behav,86: 623-632.

Li Q, Dong C, Li W, Bu W, Wu J, Zhao W (2014). Neuropeptide Y protects cerebral cortical neurons by regulating microglial immune function. Neural Regen Res. 9: 959-957.

Librán-Pérez M, Geurden I, Dias K, Corraze G, Panserat S, Soengas JL (2015). Feeding rainbow trout with a lipid-enriched diet: effects on fatty acid sensing, regulation of food intake and cellular signalling pathways. J Exp Biol, 218: 2610-2619.

Lin F, Zhou C, Chen H, Wu H, Xin Z, Liu J, Gao Y, Yuan D, Wang T, Wei R, Chen D, Yang S, Wang Y, Pu Y, Li Z (2014). Molecular characterization, tissue distribution and feeding related changes of NUCB2A/nesfatin-1 in Ya-fish (*Schizothorax prenanti*). Gene, 536: 238-246.

Liu J, Merkle FT, Gandhi AV, Gagnon JA, Woods IG, Chiu CN, Shimogori T, Schier AF, Prober DA (2015). Evolutionarily conserved regulation of hypocretin neuron specification by Lhx9. Development, 142: 1113-1124.

Longo VD and Longo MP (2014). Fasting: molecular mechanism and clinical application. Cell Metabolism, 19: 181-192.

López-Patiño MA, Guijarro AI, Isorna E, Delgado MJ, Alonso-Bedate M, de Pedro N (1999). Neuropeptide Y has a stimulatory action on feeding behaviour in goldfish (*Carassius auratus*). Eur J Pharmacol, 377: 147-153.

Lu CY, Hsu CY (2015). Ambient temperature reduction extends lifespan via activating cellular degeneration activity in annual fish (*Nothobranchius rachovii*). Age (Dordr), 37: 33-44.

Lucas-Sánchez A, Almaida- Pagán PF, Madrid Pérez JA, de Costa Ruiz J, Mendiola López P (2011). Age-related makers in *Nothobranchius korthause*: fatty acid profile and locomotor activity rhythms. Exp Gerontol, 46: 970-978.

Lucas-Sánchez A, Almaida-Pagán PF, Tocher DR, Mendiola P, de Costa J (2014a). Age-related changes in mitochondrial membrane composition of *Nothobranchius rachovii*. J Gerontol A Biol Sci Med Sci, 69: 142-151.

Lucas-Sánchez A, Almaida- Pagán PF, Mendiola P, de Costa J (2014b). Nothobranchius as model for aging studies. A review. Aging and Disease, 5: 281-291.

Lucas-Sánchez A, Martínez. Nicolás A, Madrid JA, Almaida- Pagán PF, Mendiola López P, de Costa (2015) Circadian rhytms during the last days of *Nothobranchius rachovii*'s life: a descriptive model of circadian system breackdown. Chronobiol Int, 32: 395-404.

MacIntosh C, Morley JE, Chapman IM (2000). The anorexia of ageing. Nutrition, 16: 983-995.

MacDonald EE and Volkoff H (2009). Neuropeptide Y (NPY), cocaine-and amphetamine-regulated transcript (CART) and cholecystokinin (CCK) in winter skate (*Raja ocellata*): cDNA cloning, tissue distribution and mRNA expression responses to fasting. Gen Comp Endocrinol, 161: 252-261.

MacDonald EE and Volkoff H (2010). Molecular cloning and characterization of preproorexin in winter skate (*Laucoraja ocellata*) Gen of Compar Endocrinol, 169: 192-196.

Martone AM, Onder G, Vetrano DL, Ortolani E, Tosato M, Marzetti E, Landi F (2013). Anorexia of aging: a modificable risk factor for frailty. Nutrients, 5: 4126-4133.

Matsuda K (2009). Recent advances in the regulation of feeding behaviour by neuropeptides in fish. Ann N Y Acad Sci, 1163: 243-252.

Matsuda K, Sakashita A, Yokobori E, Azuma M (2012). Neuroendocrine control of feeding behavior and psychomotor activity by neuropeptideY in fish. Neuropeptides, 46: 275-283.

Mayer J and Thoma DJ (1967). Regulation of food intake and obesity. Science, 156: 328-337.

McDonald JK, Lumpkin MD, Samson WK, McCann SM (1985). Neuropeptide Y affects secretion of luteinizing hormone and growth hormone in ovariectomized rats. Proc Natl Acad Sci USA, 82: 561-564.

Meyer A, Van de Peer Y (2005). From 2r to 3r: evidence for a fish- specific genome duplication (fsgd). BioEsseys, 27: 937-945.

Minor RK, Chang JW, de Cabo R (2009). Hungry for life: How the arcuate nucleus and neuropeptide Y may play a critical role in mediating the benefits of calorie restriction. Mol Cell Endocrinol, 299: 79-88.

Mercer RE, Chee MJ, Colmers WF (2011). The role of NPY in hypothalamic mediated food intake. Front Neuroendocrinol, 32: 398-415.

Mohan H and Unniappan S (2012). Ontogenic pattern of nucleobindin-2/nesfatin-1 expression in the gastroenteropancreatic tissues and serum of Sprague Dawley rats. Regul Pept 175: 61-69.

Mohan H and Unniappan S (2013). Phylogenetic aspects of nucleobindin-2/nesfatin-1. Curr Pharm Des 19: 6929-6934.

Moore RY, Abrahamson EA, Van Den Po Al, (2001). The hypocretin neuron system: an arousal system in the human brain. Arch Ital Biol, 139: 195-205.

Morley JE and Silver AJ (1988). Anorexia in the elderly. Neurobiol Aging, 9: 9-16.

Mortazavi S, Gonzalez R, Ceddia R, Unniappan S (2015). Long-term infusion of nesfatin-1 causes a sustained regulation of whole-body energy homeostasis of male Fischer 344 rats. Front Cell Dev Biol, 3: 22-34.

Murashita K, Kurokawa T, Ebbesson LO, Stefansson SO, Rønnestad I (2009). Characterization, tissue distribution, and regulation of agouti-related protein (AgRP), cocaine-and amphetamine-regulated transcript (CART) and neuropeptide Y (NPY) in Atlantic salmon (Salmo salar). Gen Comp Endocrinol, 162: 160-171.

Nambu T, Sakura T, Mizukami K, Hosoya Y, Yanagisawa M, Goto K (1999). Distribution of orexin neurons in the adult rat brain, Brain Res. 827 243-260.

Narnaware YK, Peyon PP, Lin X, Peter RE (2000). Regulation of food intake by neuropeptide Y in goldfish. Am J Physiol Regul Integr Comp Physiol, 279: R1079-R1034.

Narnaware YK and Peter RE (2001). Effects of food deprivation and refeeding on neuropeptide Y (NPY) mRNA levels in goldfish. Comp Biochem Phys Biochem Mol Biol, 129: 633-637.

Nakamaki T, Matsuda K, Maruyama K, Miura T, Uchyama M, Funahashi H Sakurai T, Shioda S (2006). Regulation by orexin of feeding behaviour and locomotor activity in goldfish, J Neuroendocrinol, 18: 290-297.

Nisembaum LG, de Pedro N, Delgado MJ, Sánchez-Bretaño A, Isorna E (2014). Orexin as an input of circadian system in goldfish: Effects on clock gene expression and locomotor activity rhythms. Peptides, 52: 29-37.

Nixon JP and Smale L (2007). A comparative analysis of the distribution of immunoreactive orexin A and B in the brains of nocturnal and diurnal rodents, Behav. Brain Funct, 3: 28-55.

Novak CM, Jiang XL, Wang CF, Teske JA, Kotz CM, Levine JA (2005). Caloric restriction and physical activity in zebrafish (Danio rerio). Neurosci Lett, 383: 99-104.

Oh-I S, Shimizu H, Satoh T, Okada S, Adachi S, Inoue K, Eguchi H, Yamamoto M, Imaki T, Hashimoto K, Tsuchiya T, Monden T, Horiguchi K, Yamada M, Mori M (2006). Identification of nesfatin-1 as a satiety molecule in the hypothalamus. Nature, 443: 709-712.

Park MH, Jin HK, Min WK, Lee WW, Lee JE, Akiyama H, Herzog H, Enikolopov GN, Schuchman EH, Bae JS (2015). Neuropeptide Y regulates the hematopoietic stem cell microenvironment and prevents nerve injury in the bone marrow. EMBO J, 34: 1648-1660.

Paxton JR, Echmeyer WN, Kirshner D, editors. Encyclopedia of fish. New York: Academic Press; 1998.

Peter RE (1979). The brain and feeding behaviour. Fish Physiol, 52: 121-159.

Petzol A, Reichwald K, Groth M, Taudien S, Hartmann N, Priebe S, Shagin D, Englert C, Platzer M (2013). The transcript catalogue of short lived fish *Nothobranchius furzeri* provides insights into age-dependent changes of mRNA levels. BMC Genomics, 14: 185-200.

Pontet A, Danger JM, Dubourg P, Pelletrier G, Vaudry H, Calas A, Kah O (1989). Distribution and characterization of neuropeptide Y-like immunoreactivity in the brain and pituitary of the goldfish. Cell Tissue Res, 255: 528-538.

Porkka-Heiskanen T, Alanko L, Kalinchuk A, Heiskanen S, Stenberg D (2004). The effect of age on prepro-orexin gene expression and contents of orexin A and B in the rat brain. Neurobiol Aging, 25: 231-238.

Reichard M, Polačik M, Sedláček O (2009). Distribution, colour polymorphism and habitat use of the African killifish, *Nothobranchius furzeri*, the vertebrate with the shortest lifespan. Journal of Fish Biology, 74: 198-212.

Reichwald K, Lauber C, Nanda I, Kirschner J, Hartmann N, Schories S, Gausmann U, Taudien S, Schilhabel MB, Szafranski K, Glöckner G, Schmid M, Cellerino A, Schartl M, Englert C, Platzer M (2009). High tandem repeat content in the genome of the short-lived annual fish *Nothobranchius furzeri*: a new vertebrate model for aging research. Genome Biol, 10: R16-R33.

Reichard M, Polačik M, Blažek R, Vrtílek M (2014). Female bias in the adult sex ratio of African annual fishes: interspecific differences, seasonal trends and environmental predictors. Evolutionary Ecology, 28: 1105-1120.

Reichwald K, Petzold A, Koch P, Downie BR, Hartmann N, Pietsch S, Baumgart M, Chalopin D, Felder M, Bens M, Sahm A, Szafranski K, Taudien S, Groth M, Arisi I, Weise A, Bhatt AA, Sharma V, Kraus JM, Schmid F, Priebe S, Liehr T, Görlach M, Than ME, Hiller M, Kaesler HA, Volff J, Schetl M, Cellerino A, Englert C, Platzer M (2015). Insight into Sex Chromosome Evolution and Aging from the Genome of Short-Lived Fish. Cell, 163: 1527-1538.

Roa J and Herbison, AE (2012). Direct regulation of GnRH neuron excitability by arcuate nucleus POMC and NPY neuron neuropeptides in female mice. Endocrinology, 153: 5587-5599.

Roberts MG and Savage GE (1978). Effects of hypothalamic lesions on the food intake of the goldfish (*Carassius auratus*). Brain Behav Evol, 15: 150-164.

Rodgers RJ, Halford JC, R.L. Nunes de Souza RL, A.L. Canto de Souza AL, D.C. Piper DC, J.R. Arch JR, N. Upton N, R.A. Porter RA, A. Johns A, J.E. Blundell JE (2001). SB-334867, a selective orexin-1 receptor antagonist, enhances behavioural satiety and blocks the hyperphagic effect of orexin-A in rats, Eur J Neurosci, 13: 1444-1452.

Sakurai T, Amemiya A, Ishiim M, Matsuzaki I, Chemelli RM, Tanaka H, Williams SC, Richardson JS, Kozlowski GP, Wilson S, Arch JRS, Burckingham RE, Haynes AC, Carr SA, Annan RS, McNulty DE, Liu WS, Terrett JA, Elshourbagy NA, Bergsma DJ, Yanagisawa M (1998). Orexin and orexin receptor: a family of hypothalamic neuropeptides and G- protein coupled receptors that regulate feeding behaviour. Cell, 92: 573- 575.

Sawai N, Ueta Y, Nakazato M, Ozawa H (2010). Developmental and aging change of orexin-A and B immunoreactive neurons in the male rat hypothalamus. Neurosci Lett, 468: 51-55.

Sedbazar U, Ayush EA, Maejima Y, Yada T (2014). Neuropeptide Y and α-melanocyte-stimulating hormone reciprocally regulate nesfatin-1 neurons in the paraventricular nucleus of the hypothalamus. Neuroreport, 25:1453-1458.

Seiliez I Gabillard JC, Skiba-Cassy S, Garcia-Serrana D, Gutiérrez J, Kaushik S, Panserat S, Tesseraud S (2008). An *in vivo* and *in vitro* assessment of TOR signaling cascade in rainbow trout (*Oncorhynchus mykiss*). Am J Physiol Regul Intergr Comp Physiol, 295: R329-R335.

Sellayah, D and Sikder D (2014). Orexin restores aging-related brown adipose tissue dysfunction in male mice. Endocrinology, 155: 485-501.

Shahjahan M., Kitahashi T, Parhar IS (2014). Central pathways integrating metabolism and reproduction in teleost. Front Endocrinol (Lausanne), 5: 1-17.

Shwartz MW, Woods SC, Porte DJ, Seeley RJ, Baskin DG (2000). Central nervous system control of food intake. Nature, 404: 661-71

Silverstein, JT, Plisetskaya EM (2000). The effects of NPY and insulin on food intake regulation in fish. Am Zool 40: 296-308.

Sohn EH, Wolden- Hanson T, Matsumoto AM (2002). Testosterone (T)- induced changes in arcuate nucleus cocaine- amphetamine-regulated transcript and NPY mRNA are attenuated in old compared to young male Brown Norways rats: contribution of T to age-related changes in cocaine-amphetamine-regulated transcript and NPY gene expression. Endocrinology, 143: 954-963.

Son MY, Kim MJ, Yu K, Koo DB, Cho YS (2011). Involvement of neuropeptide Y and its Y1 and Y5 receptors in maintaining self-renewal and proliferation of human embryonic stem cells. J Cell Mol Med, 15: 152-165.

Stengel A, Goebel M, Yakubov I, Wang L, Witcher D, Coskun T, Taché Y, Sachs G, Lambrecht NW (2009). Identification and characterization of nesfatin-1 immunoreactivity in endocrine cell types of the rat gastric oxyntic mucosa. Endocrinology, 150:232-238.

Stengel A, Taché Y (2013). New developments on NUCB2/Nesfatin-1. Curr Pharm Des, 19: 6919-6920.

Stengel A (2015). Nesfatin-1- More than a food intake regulatory peptide. Peptides, 72:175-183.

Takemoto K (1982). Neuropeptide Y: complete amino acid sequence of the brain peptide. Proc Natl Acad Sci USA, 79: 548-549.

Terzibasi E, Valenzano DR, Benedetti M, Roncaglia P, Cattaneo A, Domenici L, Cellerino A (2008). Large differences in aging phenotype between strains of the short-lived annual fish *Nothobranchius furzeri*. PLoS ONE, 3: e3866-e3879.

Terzibasi E, Lefrançois C, Domenici P, Hartmann N, Graf M, Cellerino A (2009). Effect of dietary restriction on mortality and age-related phenotypes in the short- lived fish *Nothobranchius furzeri*. Aging Cell, 8: 88-99.

Terzibasi Tozzini E, Baumgart M, Battistoni G, Cellerino A (2012). Adult neurogenesis in the short-lived teleost *N. furzeri*: localization of neurogenic niches, molecular characterization and effect of aging. Aging Cell, 11: 241-251.

Terzibasi Tozzini E, Dorn A., Ng'oma E, Polačik M, Blažek R, Reichwald K, Petzold A, Watters B, Reichard M, Cellerino A (2013). Parallel evolution of senescence in annual fishes in response to extrinsic mortality. BMC Evolutionary Biology, 13: 77-89.

Topic Popovic N, Strunjak- Perovic I, Coz-Rakovac R, Barisic J, Jadan M, Persin Berakovic A, Sauerborn Klobucar R (2011). Tricaine methane- sulfonate (MS-222) application in fish anaesthesia. J Appl Ichthyol, 28: 553-564.

Travers S and Norgren R (1987). Gustatory neural processing in the hindbrain. Annu Rev Neurosci, 10: 595-632.

Valdesalici S, Cellerino A (2003) Extremely short lifespan in the annual fish *Nothobranchius furzeri*. Proc R Soc Lond Biol Sci, 270: 189-191.

Valenzano DR, Terzibasi E, Cattaneo A, Domenici L, Cellerino A (2006). Temperature affects longevity and age-related locomotor and cognitive decay in the short-lived fish *Nothobranchius furzeri*. Aging Cell, 5: 275-278.

Valenzano DR, Sharp S, Brunet A (2011). Transposon-Mediated Transgenesis in the Short-Lived African Killifish *Nothobranchius furzeri*, a Vertebrate Model for Aging. G3 (Bethesda), 1: 531-538.

Valenzano DR, Benayoun B, Singh PP, Zhang E, Etter PD, Hu C, Clément-Ziza M, Willemsen D, Cui R, Haral I, Machado BE, Yee M, Sharp SC, Bustamante CD, Beyer A, Johnson EA, Brunet A (2015). The African Turquoise Killifish Genome Provides Insights into Evolution and Genetic Architecture of Lifespan. Cell, 163: 1539-1554.

Volkoff H, Bjorklund JM, Peter RE (1999). Stimulation of feeding behaviour and food consumption in the goldfish, Carassius auratus, by orexin-A and orexin-B. Brain Res, 846: 204-209.

Volkoff H, Canosa LF, Unniappan S, Cerda-Reverter JM, Bernier NJ, Kelly SP (2005). Neuropeptides and the control of food intake in fish. Gen Comp Endorinol, 142: 3-19.

Volkoff H, Unniappan S, Kelly SP (2009). The endocrine regulation of food intake in: Bernier N, Kraak GVD, Farral A, Brauner C (Eds), Fish Physiology, vol. 28, Academy Press, Burlington, 2009: 421-465.

Volkoff H (2014a). In vitro assessment of interactions between appetite-regulating peptides in brain of goldfish (*Carassius auratus*). Peptides, 61: 61-68.

Volkoff H (2014b). Appetite regulating peptides in red-bellied piranha, *Pygocentrus nattereri*: cloning, tissue distribution and effect of fasting on mRNA expression levels. Peptides, 56:116- 124.

Wendler S, Hartmann N, Hoppe B, Englert C (2015). Age-dependent decline in fin regenerative capacity in the short-lived fish Nothobranchius furzeri. Aging Cell, 14: 857-866.

Wong KK, Ng SY, Lee LT, Ng HK, Chow BK (2011). Orexin and their receptors from fish to mammals: a comparative approach. Gen Compl Endocrinol, 171: 124-130.

Woodhead AD (1978). Fish in study of ageing. Exo Gerontol, 13: 125-140.

Wysokínski A, Sobóv T, Kloszewska I, Kostka T (2015). Mechanism of the anorexia of ageing- a review. Age, 37: 81-95.

Xu M and Volkoff H (2007). Molecular characterization of prepro- orexin in Atlantic cod (*Gadus morhua*): Cloning, localization, developmental profile and role in food intake regulation. Mol. Cell Endocrinol, 271: 28-37.

Yokobori E, Azuma M, Nishiguchi R, Kang KS, Kamijo M, Uchiyama M, Matsuda K (2012). Neuropeptide Y stimulates food intake in the Zebrafish, *Danio rerio*. J Neuroendocrinol 24: 766-773.

Yan A, Zhang L, Tang Z, Zhang Y, Qin C, Li B, Li W, Lin H (2011). Orange-spotted grouper (*Epinephelus coioides*) orexin: molecular cloning, tissue expression, ontogeny, daily rhythm and regulation of NPY gene expression. Peptides, 32: 1363-1370.

Yec CA and Curran SP (2016 *in press*). Gene-diet interactions and aging in *C. elegans*. Exp Gerontol, doi:10.1016/j.exger.2016.02.012.

Yu L, Tucci V, Kishi S, Zhdanadova IV (2006). Cognitive aging in zebrafish. PLoS One, 1: e14-e25.

Zhang JH, Sampogna S, Morales FR, Chase MH (2005a). Age-related changes of hypocretin in basal forebrain of guinea pig. Peptides, 26: 2590-2596.

Zhang JH, Sampogna S, Morales FR, Chase MH (2005b). Age-related ultrastructural changes in hypocretinergic terminals in the brainstem and spinal cord of cats. Neurosci Lett, 373: 171-174.

Zandbergen MA, Voormolen AHT, Peute J, Kah O, Goos HJ (1994). The immunohistochemical localization of neuropeptide Y positive cell bodies and fibers in forebrain and pituitary of the African catfish, *Clarias gariepinus*. Neth J Zool, 44: 44-54.

Zimanyi IA, Fathi Z, Poindexter GS (1998). Central regulation of feeding behaviour by neuropeptide Y. Curr Pharm Des, 4: 349-366.

Zimmerman S, Peters NC, Altare AE, Berg CE (2013). Optimized RNA ISH, RNA FISH and protein- RNA double labelling (IF/FISH) in *Drosophila ovaris.* Nature protocols, 8: 2158- 2179.